Bergische Universität Wuppertal

# The Spin Drude weight of the Heisenberg spin-1/2 XXZ model

Doctoral thesis

Svyatoslav Karabin

Thesis supervisor Prof. Dr. Andreas Klümper

Wuppertal 2025

# Danksagung

Mein herzlicher Dank gilt Prof. Dr. Andreas Klümper, der mich während der gesamten Entstehung dieser Arbeit begleitet und unterstützt hat. Seine wertvollen Anregungen und sein Vertrauen haben mir sowohl in den guten als auch in den schwierigen Momenten sehr geholfen.

Ganz besonders danke ich Chiara, die mich immer wieder ermutigt hat, an dieser Arbeit dranzubleiben. Während ich an der Dissertation geschrieben habe, hat sie mir das schönste Geschenk gemacht, das man sich vorstellen kann: unser Sohn. Ohne ihre Liebe und ihren Rückhalt wäre diese Arbeit nicht möglich gewesen.

Ein großes Dankeschön geht auch an meine Kollegen, die meine Zeit an der Universität zu etwas Besonderem gemacht haben. Aus der gemeinsamen Arbeit sind echte Freundschaften entstanden, die über das Studium hinaus bestehen werden.

# Contents


**1 Introduction** **1**

**2 Transport in one-dimensional integrable systems** **5**
2.1 XXZ Spin 1/2-Heisenberg spin chain . . . . . 6
2.2 Linear response theory . . . . . 7
2.3 Transport in the XXZ Spin 1/2-Heisenberg spin chain . . . . . 10
2.4 Spin conductivity . . . . . 11
2.5 Mazur's inequality . . . . . 16
2.6 Coordinate Bethe Ansatz and Zotos' Drude weight . . . . . 18

**3 Mazur bounds** **23**
3.1 Standard XXZ spin-1/2 thermodynamics . . . . . 23
3.2 Pseudo-local conserved quantities . . . . . 29
3.3 Mazur inequality at infinite and finite temperature . . . . . 35
3.4 Computation of $\mathfrak{A}_1\big|_{s=\bar{s}=0}$ . . . . . 37
3.5 Computation of $\mathfrak{A}_2\big|_{s=\bar{s}=0}$ . . . . . 41
3.6 $T$-, $Y$-systems . . . . . 43
3.7 Modified $T$-, $Y$-systems . . . . . 48
3.8 Calculations of $\langle \mathcal{J}_{\mathfrak{s}} Q(\varphi)\rangle$ . . . . . 51
3.9 High temperature limit: $T \to \infty$ . . . . . 55

**4 Spin Drude Weight** **57**
4.1 Introduction . . . . . 58
4.2 T- Y-system at the "simple root of unity" . . . . . 60
4.3 Thermodynamic properties of Y's zeros . . . . . 63
4.4 Calculation of the $g$-function from the zeros of $Y$-functions . . . . . 66
4.5 Drude weight analysis . . . . . 68
4.6 $T$- $Y$-system at root of unity . . . . . 74
4.7 NLIE derivation for $\nu_1 = 2$, $\nu_2 = 2$ . . . . . 75
4.8 Numerical analysis of NLIE for $\nu_1 = 2$, $\nu_2 = 2$ . . . . . 81

**5 Conclusions** **87**
5.1 Conclusion . . . . . 87
5.2 Future directions . . . . . 88

**Bibliography** **91**

# Chapter 1

# Introduction

Many-body quantum systems, combined with the principles of statistical mechanics, form a cornerstone of modern physics. They provide a robust structure for understanding the connection between microscopic behavior of particles with macroscopic observables. This powerful framework provides insights for understanding quantum materials, quantum devices, and exotic states of matter such as superconductors and quantum magnets. The methods of statistical mechanics are particularly valuable for many-body quantum systems, where interactions and quantum coherence lead to nontrivial phenomena. These include thermalization, phase transitions, and quantum transport properties. One-dimensional quantum systems are of great importance due to the significant role of quantum correlations and the limited phase space available for particle interactions. This leads to behaviors fundamentally distinct from their classical counterparts, especially due to quantum correlations and integrability. Quantum fluctuations dominate, leading to long-range correlations and non-standard transport regimes. One remarkable aspect of one-dimensional systems is their capacity to achieve exact solutions due to integrability. In this context, integrable models shed light on the underlying physics, allowing exact calculations of thermodynamic and dynamic properties.

Integrability is a fundamental aspect of certain quantum systems, characterized by the presence of an infinite number of conserved charges. These charges constrain the dynamics, preventing conventional thermalization and enabling exact solutions to problems that are otherwise difficult to solve. One of the most studied integrable models is the Heisenberg spin-1/2 XXZ chain, which describes interacting spins on a one-dimensional lattice with anisotropic coupling. This model is particularly important due to its ability to capture essential features of quantum magnetism in low dimensions. Its exact solvability arises from the Bethe Ansatz, a method that allows one to construct the exact eigenstates and eigenvalues of the system. The Thermodynamic Bethe Ansatz (TBA) extends these methods to finite temperatures, enabling the computation of thermodynamic quantities and certain correlation functions. Integrable systems, such as the XXZ chain, provide fertile ground for exploring non-equilibrium dynamics and transport, as they contain rich

structures even far from equilibrium.

Transport phenomena provide crucial insights into the dynamics of quantum systems. Properties such as thermal and spin conductivity reveal how conserved quantities, such as energy and spin, are transported within the system. In one-dimensional systems, the study of transport is particularly interesting due to the constraints imposed by the system's low dimensionality and integrability properties. Linear response theory serves as a powerful tool to study transport properties. By analyzing how a system responds to small external perturbations, one can derive key quantities like the Drude weight. The Drude weight measures the presence of a ballistic transport regime, where particles or conserved quantities propagate without scattering. In integrable systems, transport is often dominated by the conserved charges, leading to behaviours such as infinite conductivity at zero temperature.

The spin Drude weight is important for describing spin transport in quantum systems, including the XXZ chain. Unlike the thermal current, which is conserved in the XXZ model, the spin current is not generally conserved, making its behaviour more complex and interesting.

The foundational works by Zotos and by Fujimoto and Kawakami developed systematic methods for computing the spin Drude weight in the XXZ model. Their approach combined linear response theory with the Bethe Ansatz, utilizing the curvature of energy eigenvalues with respect to an applied magnetic flux. This method, a finite-temperature generalization of the Kohn formula, links transport properties to thermodynamic quantities. This results continue to serve as a critical reference point in the study of transport in integrable systems, encouraging additional studies on the influence of quasi-local conserved charges on transport phenomena.

The Mazur bound provides a lower limit for the Drude weight, connecting it to the overlap between the conserved charges and the current operator. In integrable systems, the existence of an infinite number of conserved charges strengthens the Mazur bound, thereby ensuring a finite Drude weight that persists at finite temperatures. Recent developments have identified quasi-local charges in the XXZ model, which extend the traditional notion of conserved quantities. These charges, though not strictly local, contribute significantly to transport properties, refining our understanding of the dynamics in integrable systems. The inclusion of quasi-local charges is essential for accurately describing the spin Drude weight, especially in regimes where traditional local conserved quantities fail to account for any transport contributions.

The XXZ model serves as a prototypical system for studying spin transport in one dimension. The complicated dependence of the spin Drude weight on temperature and anisotropy reflects the underlying integrable structure of the model. Using methods such as the generalized Gibbs ensemble and extended TBA equations, significant progress has been made in quantifying the spin Drude weight across different regimes. In the critical regime, where the system remains gapless, spin transport is ballistic, and the Drude weight

is finite. In contrast, in the massive regime or at the isotropic point, the system exhibits diffusive or insulating behaviour, with the Drude weight vanishing at finite temperatures. These results highlight the complexity of transport phenomena in integrable systems and the necessity of advanced mathematical tools to fully understand them.

This thesis aims to deepen the understanding of spin transport in the XXZ model by focusing on the spin Drude weight. The main objectives are to derive exact results for the spin Drude weight using the Bethe Ansatz and quasi-local charges and to explore the temperature and anisotropy dependence of the Drude weight in various regimes. Through these investigations, the thesis seeks to contribute to the broader understanding of integrable systems and their transport properties.

This thesis is organized in the following manner:

- Chapter 2
  This chapter introduces the foundational concepts necessary for understanding the rest of the thesis. It covers Zotos' approach for calculating the Drude weight, the derivation of the Mazur inequality, and Kohn's formula. These concepts address specific applications relevant to the analysis of spin transport in integrable systems.

- Chapter 3
  Here, we analyze the spin transport properties of the spin-1/2 XXZ Heisenberg model. Using the Mazur inequality, we compute the spin Drude weight and investigate the role of non-local conserved charges, focusing on their overlap with the spin current operator and their contribution to transport phenomena.

- Chapter 4
  This chapter addresses controversies in spin Drude weight calculations for the XXZ chain. We combine the thermodynamic Bethe Ansatz with Y-system relations to derive nonlinear integral equations for the Drude weight. These results are compared with Zotos' findings, with an additional focus on system size dependence and anisotropy effects.

# Chapter 2

# Transport in one-dimensional integrable systems

In this chapter, our goal is to establish the fundamental concepts that form the basis for the following chapters of this thesis. While the individual notions we present have been extensively discussed in the existing literature, our approach here is thought to address specific applications that are directly relevant to our research.

The one-dimensional spin-1/2 XXZ Heisenberg model will be the central model studied in this thesis. We will start by introducing it and its properties. We will then move on to linear response theory, which describes how a quantum system reacts to a small perturbation. The main result is given by the Kubo formula which establishes how physical quantites can be obtained from correlation functions of a system in equilibrium. Next, we will discuss the transport properties of the XXZ Heisenberg model, focusing on the spin and thermal currents. Finally, we will introduce the concept of spin conductivity and how it is determined from linear response theory. We will also derive Kohn's formula which will be employed for analyzing the Drude weight in Chapter 4.

An important tool for understanding transport properties is the Mazur bound. The Mazur inequality provides a lower bound on the long-time average of the time-dependent autocorrelation function of observables, in terms of equilibrium correlation functions involving conserved quantities. We will show the derivation of the Mazur inequality and its implications for the Drude weight. These results will then be used in Chapter 3.

Zotos' research on spin transport in the antiferromagnetic Heisenberg model offered important insights into the Drude weight using the Bethe ansatz method. He demonstrated that the Drude weight, which presents the ideal conductivity at zero frequency, decreases monotonically with temperature for $0 \leq \Delta \leq 1$, approaching its zero-temperature value following a power-law behavior. We will discuss the main results of Zotos' work and show its implications for the spin Drude weight in the XXZ model.

## 2.1 XXZ Spin 1/2-Heisenberg spin chain

As a starting point, we consider the one-dimensional spin-1/2 XXZ Heisenberg model [1, 2]. This is a strongly correlated model with nearest-neighbor interactions. The system is integrable by the Bethe ansatz means [3, 4, 5] and the properties of its ground state and elementary excitations have been extensively studied. The Hamiltonian is expressed as

$$H_{XXZ} = J\sum_{j=1}^{L}\Big(2\sigma_{j+1}^{+}\sigma_{j}^{-} + 2\sigma_{j+1}^{-}\sigma_{j}^{+} + \Delta(\sigma_{j+1}^{z}\sigma_{j}^{z} - 1) + \frac{h}{2}\sigma_{j}^{z}\Big), \tag{2.1}$$

where $L$ is the length of the chain, $J > 0$ represents the coupling constant, and $h$ represents an external magnetic field. We consider the case with periodic boundary conditions $\sigma_{L+1}^{a} \equiv \sigma_{1}^{a}$.

The raising and lowering operators are expressed in terms of Pauli matrices:

$$\sigma_{j}^{\pm} = \frac{1}{2}(\sigma_{j}^{x} \pm \mathrm{i}\sigma_{j}^{y}), \tag{2.2}$$

where

$$\sigma^{x} = \begin{pmatrix} 0 & 1 \\ 1 & 0 \end{pmatrix}, \quad \sigma^{y} = \begin{pmatrix} 0 & -\mathrm{i} \\ \mathrm{i} & 0 \end{pmatrix}, \quad \sigma^{z} = \begin{pmatrix} 1 & 0 \\ 0 & -1 \end{pmatrix}. \tag{2.3}$$

The Pauli matrices $\sigma_{j}^{a}$ with $a = x, y, z$ play the role of spin operators and act on individual sites denoted by $j$. They satisfy the following local commutation relations:

$$[\sigma_{i}^{a}, \sigma_{j}^{b}] = 2\mathrm{i}\delta_{ij}\epsilon^{abc}\sigma_{i}^{c} \quad i \neq j, \tag{2.4}$$

where $\epsilon^{abc}$ is the completely antisymmetric tensor.

The complete Hilbert space, in which a physical state resides, is given by $H = \bigotimes_{L} \mathbb{C}^2$. The dimension of the total Hilbert space grows exponentially with the system size, scaling as $2^L$.

The Hamiltonian in equation (2.1) consists of three main parts. The first two terms, involving $\sigma^+$ and $\sigma^-$, are known as hopping terms, responsible for transferring spin up or spin down to neighboring sites. The third term, proportional to $\Delta$, describes the anisotropic interaction between neighboring spins along the $z$-axis. The last term in equation (2.1) corresponds to the Zeeman term, which accounts for the interaction with an external magnetic field. Notably, it commutes with the Hamiltonian:

$$\left[H_{XXZ}, \sum_{j=1}^{L}\sigma_{j}^{z}\right] = 0. \tag{2.5}$$

This reveals that the Hamiltonian possesses $U(1)$ symmetry.

The parameter $\Delta$, referred to as anisotropy, defines the anisotropic Heisenberg model when $\Delta \neq 1$. Different values of $\Delta$ correspond to distinct physical scenarios:

- $\Delta = 0$ defines the free fermion or $XX$ model.
- $\Delta = 1$ defines the $XXX$ Hamiltonian.
- $\Delta = -1$ is the ferromagnetic isotropic point, marking the transition between the gapped ferromagnetic phase and the critical regime.
- $\Delta < -1$ describes the XXZ chain in a ferromagnetic phase, with the ground state characterized by spins aligned in either the $z$ or $-z$ direction. Excited states are separated by a gap.
- $\Delta > 1$ corresponds to an antiferromagnetic phase, characterized by long range order and degenerate ground states in the thermodynamic limit.
- $|\Delta| < 1$ corresponds to a critical regime where the model possesses a gapless spectrum for magnetic fields below saturation.
- $\Delta \to \infty$ corresponds to the antiferromagnetic Ising model.
- $\Delta \to -\infty$ corresponds to the ferromagnetic Ising model.

The parameter $J$ determines the energy scale of the system and the alignment of spins in the ground state. In this thesis, our primary focus will be on investigating the critical regime.

The exponential growth of the Hilbert space dimension with system size $2^L$ for the XXZ spin-1/2 chain renders direct diagonalization computationally intractable for even moderately sized systems. To overcome this limitation, alternative methods must be employed to compute the spectrum of the Hamiltonian. Integrability, combined with techniques such as the Bethe Ansatz, provides a means to circumvent numerical diagonalization in certain cases.

## 2.2 Linear response theory

Linear response theory [6] aims to investigate how a system reacts to external influences, often referred to as "sources", which could be, for example, electric or magnetic fields. We start by considering an equilibrium system described by the Hamiltonian $H_0(t)$ and introducing a small perturbation:

$$H(t) = H_0(t) + H'(t), \tag{2.6}$$

where the perturbative part is $H'(t) = \lambda(t)\mathcal{A}$, $\lambda(t)$ represents a real valued function of time, while $\mathcal{A}$ is a Hermitian operator. We can control the perturbation and turn it on or off at any time. Given the small magnitude of the perturbation, we expect the response

to be linear. This is why the theory is known as linear response theory. To first order in the perturbation, the expectation value of an operator takes on the following form:

$$\langle \mathcal{O} \rangle = \langle \mathcal{O} \rangle_{\lambda=0} + \delta \langle \mathcal{O}(t) \rangle . \tag{2.7}$$

Here, $\langle \mathcal{O} \rangle_{\lambda=0}$ represents the operator's behavior in the absence of any perturbation, and $\delta\langle \mathcal{O} \rangle$ denotes the macroscopic fluctuation. At equilibrium, the system is described by the density matrix $\rho_0$ satisfying $[H_0, \rho_0] = 0$, and the expectation value is given by $\langle A \rangle_{\lambda=0} = \mathrm{Tr}(\rho_0 A)$. For weak interaction, the fluctuation can be expressed by

$$\delta \langle \mathcal{O}(t) \rangle = \int_{-\infty}^{\infty} \mathrm{d}t' \chi(t - t') \lambda(t'), \tag{2.8}$$

where $\chi(t - t')$ is the response function. Now, let us examine an operator from different perspectives. We can express the expectation value of an operator in the Schrödinger, Heisenberg, and interaction pictures, as shown in Table 2.1.

| | |
|---|---|
| $\langle \mathcal{O} \rangle = \mathrm{Tr}(\mathcal{O}\rho_s(t))$ | Schrödinger picture |
| $\langle \mathcal{O} \rangle = \mathrm{Tr}(\mathcal{O}_H(t)\rho_0)$ | Heisenberg picture |
| $\langle \mathcal{O} \rangle = \mathrm{Tr}(\mathcal{O}(t)\rho(t))$ | Interaction picture |

Table 2.1: Expectation values in different pictures of quantum mechanics.

We can switch between these representations using appropriate relations. In the interaction picture, an operator is given by:

$$\mathcal{O}(t) = \mathrm{e}^{\mathrm{i}H_0 t} \mathcal{O} \mathrm{e}^{-\mathrm{i}H_0 t}. \tag{2.9}$$

To switch to the Heisenberg picture, we use the unitary operator $U(t)$:

$$\mathcal{O}_H(t) = U^\dagger(t) \mathcal{O}(t) U(t). \tag{2.10}$$

The density operator, after evolving for a time $t$, can be written as:

$$\rho(t) = U(t) \rho_0 U^\dagger(t). \tag{2.11}$$

The time evolution operator is defined as:

$$U(t) = \mathcal{T} \exp\left( -\mathrm{i} \int_{t_0}^{t} H'(t') \mathrm{d}t' \right) \tag{2.12}$$

where $\mathcal{T}$ is the time-ordering operator, which arranges operators with later times to the left. This operator satisfies the Schrödinger equation:

$$\mathrm{i}\partial_t U(t) = H'(t) U(t). \tag{2.13}$$

Since the perturbation is small, we can use the first-order approximation of the time evolution operator:

$$U(t) \approx 1 - \mathrm{i} \int_{t_0}^{t} \mathrm{d}t' H'(t'). \tag{2.14}$$

Let us compute the following expression:

$$\begin{aligned} U^\dagger(t)\mathcal{O}(t)U(t) &= \left(1 + \mathrm{i}\int_{t_0}^{t} \mathrm{d}t' H'(t')\right) \mathcal{O}(t) \left(1 - \mathrm{i}\int_{t_0}^{t} \mathrm{d}t' H'(t')\right) \\ &\approx \mathcal{O}(t) + \mathrm{i}\int_{t_0}^{t} \mathrm{d}t' [H'(t'), \mathcal{O}(t)] \\ &= \mathcal{O}(t) + \mathrm{i}\int_{t_0}^{t} \mathrm{d}t' [\mathcal{A}(t'), \mathcal{O}(t)]\lambda(t'). \end{aligned} \tag{2.15}$$

Now, we use this result to compute the expectation value:

$$\begin{aligned} \langle \mathcal{O} \rangle &= \mathrm{Tr}\left(U(t)\rho_0 U^\dagger(t)\mathcal{O}(t)\right) = \mathrm{Tr}\left(\rho_0 U^\dagger(t)\mathcal{O}(t)U(t)\right) \\ &= \langle \mathcal{O} \rangle_{\lambda=0} + \mathrm{i}\int_{t_0}^{t} \mathrm{d}t' \left\langle [\mathcal{A}(t'), \mathcal{O}(t)] \right\rangle_{\lambda=0} \lambda(t'). \end{aligned} \tag{2.16}$$

To connect with the general form of linear response theory, we take the limit $t_0 \to -\infty$, assuming the perturbation was turned on in the distant past. We also introduce the Heaviside step function $\theta(t - t')$ to enforce causality, which ensures that the response at time $t$ depends only on perturbations at earlier times $t' < t$. This allows us to extend the upper integration limit to infinity:

$$\langle \mathcal{O} \rangle = \langle \mathcal{O} \rangle_{\lambda=0} + \mathrm{i}\int_{-\infty}^{+\infty} \mathrm{d}t' \theta(t - t') \left\langle [\mathcal{A}(t'), \mathcal{O}(t)] \right\rangle_{\lambda=0} \lambda(t'). \tag{2.17}$$

Comparing this with (2.7) and (2.8), we identify the response function:

$$\chi(t - t') = -\mathrm{i}\theta(t - t') \left\langle [\mathcal{O}(t), \mathcal{A}(t')] \right\rangle. \tag{2.18}$$

This result shows that in the linear response regime, we can evaluate physical quantities from the equilibrium correlation functions. For simplicity, we will omit the subscript $\lambda = 0$ from now on in the expectation values. The key result is known in the literature as the Kubo formula. Taking the Fourier transform of both sides of (2.8) and applying the convolution theorem, we obtain:

$$\delta \left\langle \mathcal{O}(\omega) \right\rangle = \chi(\omega)\lambda(\omega). \tag{2.19}$$

The response function in the frequency domain is given by:

$$\chi(\omega) = -\mathrm{i}\int_{0}^{\infty} \mathrm{d}t\, \mathrm{e}^{\mathrm{i}\omega t} \left\langle [\mathcal{O}(t), \mathcal{A}(0)] \right\rangle. \tag{2.20}$$

Here, we have employed the following definitions of the Fourier transform:

$$f(\omega) = \int \mathrm{d}t\, \mathrm{e}^{\mathrm{i}\omega t} f(t), \quad f(t) = \int \frac{\mathrm{d}\omega}{2\pi} \mathrm{e}^{-\mathrm{i}\omega t} f(\omega). \tag{2.21}$$

## 2.3 Transport in the XXZ Spin 1/2-Heisenberg spin chain

Let us now study the transport properties of the XXZ Spin 1/2-Heisenberg model [7]. In this section, we apply the concepts of linear response theory introduced earlier. A key quantity of interest is the spin current, which can be derived from the discrete version of the continuity equation:

$$\dot{S}^z_k - (j^{\mathfrak{s}}_{k+1} - j^{\mathfrak{s}}_k) = 0. \tag{2.22}$$

This equation reflects the transport of spin magnetization from site $k$ to $k+1$. Additionally, we use Heisenberg's equation of motion:

$$\dot{S}^z_k = \mathrm{i}[H, \frac{1}{2}\sigma^z_k], \tag{2.23}$$

where we represent spin components as $S^a_j = \frac{1}{2}\sigma^a_j$, with $a = x, y, z$. For the local spin current, we have:

$$j^{\mathfrak{s}}_k = -2\mathrm{i}J(\sigma^+_{k+1}\sigma^-_k - \sigma^+_k\sigma^-_{k+1}) \tag{2.24}$$

and the total spin current is defined as $\mathcal{J}^0_{\mathfrak{s}} = \sum_{k=1}^{L} j^{\mathfrak{s}}_k$.
Another interesting quantity to analyze is the thermal current operator [8, 9], defined as $\mathcal{J}^0_{th} = \sum_{k=1}^{L} j^{th}_k$. The local thermal current can be derived similarly from the continuity equation:

$$\dot{h}_l = (j^{th}_{k+1} - j^{th}_k) = \mathrm{i}[h_l, H], \tag{2.25}$$

where $H = \sum_{k=1}^{L} h_l = h_0 + h\sum_{k=1}^{L} S^z_k$. The thermal current can be decomposed into two parts: the spin current and the energy current:

$$\mathcal{J}^0_{th} = \mathcal{J}^0_E + h\mathcal{J}^0_{\mathfrak{s}}. \tag{2.26}$$

The energy current can be calculated from (2.25) by setting the magnetic field to zero. In linear response theory, non zero expectation values of these currents arise due to temperature or magnetic field gradients. We can relate these currents to the gradients through the transport coefficients:

$$\begin{pmatrix} \mathcal{J}^0_{th} \\ \mathcal{J}^0_{\mathfrak{s}} \end{pmatrix} = \begin{pmatrix} \kappa_{th} & C^{th}_{\mathfrak{s}} \\ C^{\mathfrak{s}}_{th} & \sigma_{\mathfrak{s}} \end{pmatrix} \begin{pmatrix} -\Delta T \\ \Delta h \end{pmatrix}, \tag{2.27}$$

where $\kappa_{th}$ represents thermal conductivity, and $\sigma_s$ denotes spin conductivity. According to the Onsager relations [10], $C^{th}_{\mathfrak{s}} = TC^{\mathfrak{s}}_{th}$, where these coefficients link thermal current to a magnetic field gradient and the spin current to a thermal gradient. The transport coefficients, within the context of linear response theory, can be computed in terms of equilibrium correlation functions.

Now, let us shift our focus to spin conductivity, the central topic of this thesis. A convenient approach to introduce a spin current is by coupling the Hamiltonian to an external gauge field, as in Figure 2.1. This coupling can be achieved by making the substitutions of [11]:

$$\sigma_j^- \to \mathrm{e}^{\mathrm{i}\varphi_j(t)}\sigma_j^-, \quad \sigma_j^+ \to \mathrm{e}^{-\mathrm{i}\varphi_j(t)}\sigma_j^+ \tag{2.28}$$

into (2.1), we also take $h = 0$. Furthermore, we set:

$$\varphi_{j+1}(t) - \varphi_j(t) = \frac{\phi(t)}{L}. \tag{2.29}$$

This leads to:

$$H(t) = J\sum_{j=1}^{L}\left(2\sigma_{j+1}^+\sigma_j^-\mathrm{e}^{-\mathrm{i}\frac{\phi(t)}{L}} + 2\sigma_{j+1}^-\sigma_j^+\mathrm{e}^{\mathrm{i}\frac{\phi(t)}{L}} + \Delta(\sigma_{j+1}^z\sigma_j^z - 1)\right). \tag{2.30}$$

When we expand this expression for small $\phi(t)$, we obtain:

$$H(t) = H_0 + \frac{1}{L}\mathcal{J}_{\mathfrak{s}}^0\phi(t) + \mathcal{O}\left(\phi^2(t)\right). \tag{2.31}$$

This formula shows how we introduce a small, time-dependent perturbation within the framework of linear response theory, as in (2.6). Now, we substitute (2.28) into the total spin current:

$$\mathcal{J}_{\mathfrak{s}}(t) = -2\mathrm{i}J\sum_{k=1}^{L}\left(\mathrm{e}^{-\mathrm{i}\frac{\phi}{L}}\sigma_{k+1}^+\sigma_k^- - \mathrm{e}^{\mathrm{i}\frac{\phi}{L}}\sigma_k^+\sigma_{k+1}^-\right) \tag{2.32}$$

and expand it for small $\phi(t)$:

$$\mathcal{J}_{\mathfrak{s}}(t) = \mathcal{J}_{\mathfrak{s}}^0 - \frac{\phi(t)}{L}K + \mathcal{O}\left(\phi^2(t)\right), \tag{2.33}$$

where $K$ is the kinetic term of the (2.1). We want to measure $\mathcal{J}_{\mathfrak{s}}$, so we will calculate the expectation value of (2.33) in the presence of the perturbation caused by an external field.

## 2.4 Spin conductivity

In this section, we will analyze the spin conductivity of the Heisenberg spin-1/2 XXZ model using linear response theory. The conductivity relates the current to the electric field in Ohm's law:

$$J(\omega) \propto \sigma(\omega)E(\omega). \tag{2.34}$$

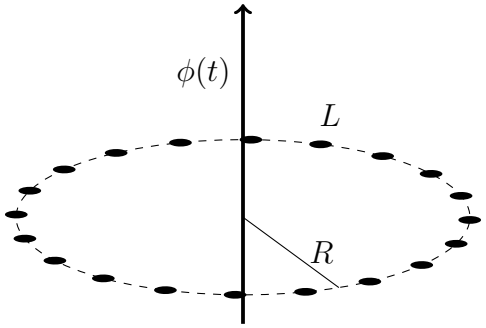



Figure 2.1: A ring of radius $R$ with $L$ lattice sites is considered, with periodic boundary conditions (PBCs) imposed to ensure translational invariance. An external gauge field generates an Aharonov–Bohm flux (twist) $\phi$, introducing phase shifts in the system.

Now, let us look at classical electromagnetism. The electric field is related to the scalar potential $A_0(\vec{x})$ and the vector potential $\vec{A}(\vec{x})$ by:

$$\vec{E} = -\vec{\nabla} A_0(\vec{x}) - \partial_t \vec{A}(\vec{x}), \tag{2.35}$$

where $A_0$ is the electric scalar potential, i.e. the time component of the four-potential $A_\mu = (A_0, \vec{A})$. It should not be confused with $\phi(t)$, the Aharonov-Bohm flux (or twist angle) threading the ring, i.e. the total Peierls phase of (2.28) rather than a genuine magnetic flux. In the gauge $A_0 = 0$, the flux $\phi(t) = e \oint \mathrm{d}\vec{x} \cdot \vec{A}(\vec{x})$ is related to the electric field through the following equations (for a more extensive treatment, see Chapter 1.3 of the book [12]):

$$\begin{aligned} L^{-1}\partial_t \phi(t) &= L^{-1} e \oint \mathrm{d}\vec{x} \cdot \partial_t \vec{A}(\vec{x}), \\ &= -L^{-1} e \oint \mathrm{d}\vec{x} \cdot \vec{E}(t) = -eaE(t), \end{aligned} \tag{2.36}$$

where the integral runs around the ring of circumference $2\pi R$. It is useful to consider the field $\phi(t)$ in Fourier space, after the integration we obtain:

$$\phi(\omega) = -\frac{\mathrm{i}ea}{\omega} E(\omega), \tag{2.37}$$

where $a = 2\pi R/L$. Now, let us calculate the expectation value of (2.33) in the presence of the external field $\phi(t)$:

$$\langle \mathcal{J}_{\mathfrak{s}}(t) \rangle - \langle \mathcal{J}_{\mathfrak{s}}(t) \rangle^0 = -\frac{\phi(t)}{L} \langle K(t) \rangle + \delta \langle \mathcal{J}^0_{\mathfrak{s}}(t) \rangle \,. \tag{2.38}$$

By applying the Fourier transform as in (2.21) and comparing with (2.34), we obtain an expression for the optical conductivity [6]:

$$\langle \sigma(\omega) \rangle = \frac{1}{(\omega + \mathrm{i}\epsilon)L} \Big( -\mathrm{i} \langle K \rangle + \int_0^\infty \mathrm{d}t \, \mathrm{e}^{\mathrm{i}\omega t} \langle [\mathcal{J}^0_{\mathfrak{s}}(t), \mathcal{J}^0_{\mathfrak{s}}(0)] \rangle \Big), \tag{2.39}$$

where the retarded prescription $\omega \to \omega + \mathrm{i}\epsilon$ (with $\epsilon \to 0^+$) has been introduced to ensure convergence. We also assumed that the second term on the left-hand side of (2.38) disappears because of the invariance of the XXZ Hamiltonian under parity transformation. Let us now focus on the integral in (2.39). Inserting a complete basis of energy states, we obtain:

$$\begin{aligned}
&\int_0^\infty \mathrm{d}t\, \mathrm{e}^{\mathrm{i}\omega t} \langle [\mathcal{J}_{\mathfrak{s}}^0(t), \mathcal{J}_{\mathfrak{s}}^0(0)] \rangle \\
&= \int_0^\infty \mathrm{d}t\, \mathrm{e}^{\mathrm{i}\omega t} \sum_{mn} \frac{\mathrm{e}^{-E_m\beta}}{Z} \Bigg( \langle m| \mathcal{J}_{\mathfrak{s}}^0 |n\rangle \langle n| \mathcal{J}_{\mathfrak{s}}^0 |m\rangle \, \mathrm{e}^{\mathrm{i}(E_m - E_n)t} \\
&- \langle m| \mathcal{J}_{\mathfrak{s}}^0 |n\rangle \langle n| \mathcal{J}_{\mathfrak{s}}^0 |m\rangle \, \mathrm{e}^{\mathrm{i}(E_n - E_m)t} \Bigg),
\end{aligned} \tag{2.40}$$

where, $E_m$ are eigenvalues of the Hamiltonian (2.1). We perform the time integral using the standard regularized result, where the same $\mathrm{i}\epsilon$ prescription enters the exponent as a convergence factor:

$$\int_0^\infty \mathrm{d}t\, \mathrm{e}^{\mathrm{i}(\Omega + \mathrm{i}\epsilon)t} = \frac{\mathrm{i}}{\Omega + \mathrm{i}\epsilon}. \tag{2.41}$$

For the first term in the commutator, we have $\Omega_1 = \omega + E_m - E_n$, while for the second term $\Omega_2 = \omega + E_n - E_m$. Note that for diagonal terms where $E_m = E_n$, both terms have the same denominator $\omega + \mathrm{i}\epsilon$ and thus cancel exactly. Only off-diagonal transitions with $E_m \neq E_n$ contribute. After relabeling the summation indices $m \leftrightarrow n$ in the second term and combining, we obtain:

$$\langle \sigma(\omega) \rangle = \frac{1}{(\omega + \mathrm{i}\epsilon)L} \left( -\mathrm{i} \langle K \rangle + \mathrm{i} \sum_{E_m \neq E_n} \frac{|\langle m| \mathcal{J}_{\mathfrak{s}}^0 |n\rangle|^2}{\omega - E_m + E_n + \mathrm{i}\epsilon} \left( \frac{\mathrm{e}^{-E_n\beta}}{Z} - \frac{\mathrm{e}^{-E_m\beta}}{Z} \right) \right). \tag{2.42}$$

The partition function is defined as

$$Z = \mathrm{Tr}\{\mathrm{e}^{-\beta H_{XXZ}}\}. \tag{2.43}$$

We make use of the following identity, which holds for $E_m \neq E_n$:

$$\frac{1}{\omega + \mathrm{i}\epsilon} \frac{1}{\omega - E_m + E_n + \mathrm{i}\epsilon} = \frac{1}{E_m - E_n} \left( \frac{1}{\omega - E_m + E_n + \mathrm{i}\epsilon} - \frac{1}{\omega + \mathrm{i}\epsilon} \right) \tag{2.44}$$

and of the Plemelj identity:

$$\frac{1}{\omega + \mathrm{i}\epsilon} = -\mathrm{i}\pi\delta(\omega) + \mathcal{P}\left(\frac{1}{\omega}\right). \tag{2.45}$$

Following the simplifications, the real part of the spin conductivity is given by

$$\begin{aligned}\mathrm{Re}\,\langle\sigma(\omega)\rangle = \frac{\pi\delta(\omega)}{L}\left(-\langle K\rangle + \sum_{E_m\neq E_n}\frac{|\,\langle m|\,\mathcal{J}_{\mathfrak{s}}^0\,|n\rangle\,|^2}{E_m-E_n}\left(\frac{\mathrm{e}^{-E_m\beta}}{Z}-\frac{\mathrm{e}^{-E_n\beta}}{Z}\right)\right)\\ -\sum_{E_m\neq E_n}\frac{\pi\delta(\omega-E_m+E_n)}{L}\frac{|\,\langle m|\,\mathcal{J}_{\mathfrak{s}}^0\,|n\rangle\,|^2}{E_m-E_n}\left(\frac{\mathrm{e}^{-E_m\beta}}{Z}-\frac{\mathrm{e}^{-E_n\beta}}{Z}\right).\end{aligned} \tag{2.46}$$

The real and imaginary components of the optical conductivity are not independent but are connected through the Kramers-Kronig relation. Therefore, our primary emphasis is placed on calculating the real part of conductivity. We can further simplify the equation (2.46) by taking into account the free energy per site

$$f(\phi) = -\frac{1}{\beta L}\log Z. \tag{2.47}$$

The second derivative with respect to the twist angle is called the Meissner fraction [13], and it is given by:

$$\begin{aligned}\partial_\phi^2 f(\phi)|_{\phi=0} =&\frac{1}{L}\Big[-\langle K\rangle + \sum_{E_m\neq E_n}\frac{|\,\langle m|\,\mathcal{J}_{\mathfrak{s}}^0\,|n\rangle\,|^2}{E_m-E_n}\left(\frac{\mathrm{e}^{-E_m\beta}}{Z}-\frac{\mathrm{e}^{-E_n\beta}}{Z}\right)\\ &-\beta\sum_{E_m=E_n}\frac{\mathrm{e}^{-E_n\beta}}{Z}|\,\langle m|\,\mathcal{J}_{\mathfrak{s}}^0\,|n\rangle\,|^2\Big].\end{aligned} \tag{2.48}$$

This expression is derived from the expansion in linear order in flux of the Hamiltonian and states. Inserting (2.48) into equation (2.46) and applying the Fourier transform, we obtain:

$$\mathrm{Re}\,\langle\sigma(\omega)\rangle = \pi\delta(\omega)\partial_\phi^2 f(\phi)|_{\phi=0} + \frac{1-\mathrm{e}^{-\omega\beta}}{2\omega L}\int_{-\infty}^{\infty}\mathrm{d}t\,\mathrm{e}^{\mathrm{i}\omega t}\,\langle\mathcal{J}_{\mathfrak{s}}^0(t)\mathcal{J}_{\mathfrak{s}}^0(0)\rangle\,. \tag{2.49}$$

In the thermodynamic limit the quantity in (2.48) vanishes. This occurs because the influence of the external field $\phi(t)$ is equivalent to a twist of the boundary conditions of the original Hamiltonian. In the thermodynamic limit, the real part of the spin conductivity reads

$$\lim_{L\to\infty}\mathrm{Re}\,\langle\sigma(\omega)\rangle = \lim_{L\to\infty}\frac{1-\mathrm{e}^{-\omega\beta}}{2\omega L}\int_{-\infty}^{\infty}\mathrm{d}t\,\mathrm{e}^{\mathrm{i}\omega t}\,\langle\mathcal{J}_{\mathfrak{s}}^0(t)\mathcal{J}_{\mathfrak{s}}^0(0)\rangle\,. \tag{2.50}$$

Now, let us take a closer look at the current-current correlation function. In the thermodynamic limit, it separates into two components: an asymptotic (non-decaying) part, which yields the Drude weight, and a regular part $C_{\mathfrak{s}}^{reg}(t)$:

$$\begin{aligned}C(t) &= \lim_{L\to\infty}\frac{\langle\mathcal{J}_{\mathfrak{s}}^0(t)\mathcal{J}_{\mathfrak{s}}^0(0)\rangle}{L}\\ &= \lim_{t\to\infty}\lim_{L\to\infty}\frac{\langle\mathcal{J}_{\mathfrak{s}}^0(t)\mathcal{J}_{\mathfrak{s}}^0(0)\rangle}{L} + C_{\mathfrak{s}}^{reg}(t).\end{aligned} \tag{2.51}$$

As anticipated $\lim_{t\to\infty} C^{reg}_{\mathfrak{s}}(t) = 0$. Finally, we can write the spin conductivity as

$$\begin{aligned}\lim_{L\to\infty} \operatorname{Re}\langle\sigma(\omega)\rangle =& \frac{1-\mathrm{e}^{-\omega\beta}}{2\omega}\int_{-\infty}^{\infty}\mathrm{d}t\,\mathrm{e}^{\mathrm{i}\omega t}\lim_{t\to\infty}\lim_{L\to\infty}\frac{\langle\mathcal{J}^0_{\mathfrak{s}}(t)\mathcal{J}^0_{\mathfrak{s}}(0)\rangle}{L}\\ &+\lim_{L\to\infty}\frac{1-\mathrm{e}^{-\omega\beta}}{2\omega L}\int_{-\infty}^{\infty}\mathrm{d}t\,\mathrm{e}^{\mathrm{i}\omega t}C^{reg}_{\mathfrak{s}}(t)\\ =& 2\pi D\delta(\omega)+\sigma_{reg}(\omega),\end{aligned} \tag{2.52}$$

where we define the Drude weight

$$D = \lim_{t\to\infty}\lim_{L\to\infty}\frac{\beta}{2L}\langle\mathcal{J}^0_{\mathfrak{s}}(t)\mathcal{J}^0_{\mathfrak{s}}(0)\rangle\,. \tag{2.53}$$

In the third line of (2.52), the singular part $2\pi D\delta(\omega)$ represents the ballistic, dissipationless contribution, while $\sigma_{reg}(\omega)$ characterizes the normal, dissipative transport. The Drude weight represents the weight of the singular component of conductivity at $\omega = 0$. When the Drude weight is finite ($D > 0$), it indicates infinite DC conductivity. Typically, the existence of a Drude weight is linked to conserved quantities, as we will see in the following section, these prevent the current from decaying. Now, we perturbatively expand the energy up to the order $\mathcal{O}(\phi^2(t))$ [14]

$$E_n(\phi) = E_n - \frac{\phi}{L}\langle n|\,\mathcal{J}^0_{\mathfrak{s}}\,|n\rangle - \left(\frac{\phi}{L}\right)^2\sum_{\substack{mn\\E_m\neq E_n}}\frac{|\,\langle m|\,\mathcal{J}^0_{\mathfrak{s}}\,|n\rangle\,|^2}{E_m-E_n} - \frac{1}{2}\left(\frac{\phi}{L}\right)^2\langle n|\,K\,|n\rangle\,. \tag{2.54}$$

Taking the second derivative with respect to $\phi$:

$$\frac{\mathrm{d}^2E_n}{\mathrm{d}\phi^2} = \frac{-2}{L^2}\sum_{\substack{mn\\E_m\neq E_n}}\frac{|\,\langle m|\,\mathcal{J}^0_{\mathfrak{s}}\,|n\rangle\,|^2}{E_m-E_n} - \frac{1}{L^2}\langle n|\,K\,|n\rangle\,. \tag{2.55}$$

The connection to the Drude weight becomes apparent by comparing this expression with the coefficient of the $\delta(\omega)$ term in (2.46). First, we perform a simplification involving the two exponential terms in (2.46). Splitting the sum:

$$\sum_{\substack{mn\\E_m\neq E_n}}\frac{|\,\langle m|\,\mathcal{J}^0_{\mathfrak{s}}\,|n\rangle\,|^2}{E_m-E_n}\left(\frac{\mathrm{e}^{-E_m\beta}}{Z}-\frac{\mathrm{e}^{-E_n\beta}}{Z}\right) = S_1 - S_2, \tag{2.56}$$

where $S_1$ contains $\mathrm{e}^{-E_m\beta}$ and $S_2$ contains $\mathrm{e}^{-E_n\beta}$. In $S_1$, we relabel $m \leftrightarrow n$. Since $|\,\langle n|\,\mathcal{J}^0_{\mathfrak{s}}\,|m\rangle\,|^2 = |\,\langle m|\,\mathcal{J}^0_{\mathfrak{s}}\,|n\rangle\,|^2$ and $\frac{1}{E_n-E_m} = -\frac{1}{E_m-E_n}$, we get $S_1 = -S_2$. Therefore:

$$S_1 - S_2 = -2S_2 = -2\sum_{\substack{mn\\E_m\neq E_n}}\frac{|\,\langle m|\,\mathcal{J}^0_{\mathfrak{s}}\,|n\rangle\,|^2}{E_m-E_n}\frac{\mathrm{e}^{-E_n\beta}}{Z}. \tag{2.57}$$

We now compute the thermal average of the energy curvature:

$$\begin{aligned}\frac{L}{2}\sum_n \frac{\mathrm{e}^{-E_n\beta}}{Z}\frac{\mathrm{d}^2E_n}{\mathrm{d}\phi^2} &= \frac{L}{2}\sum_n \frac{\mathrm{e}^{-E_n\beta}}{Z}\left(\frac{-2}{L^2}\sum_{\substack{m\\E_m\neq E_n}}\frac{|\langle m|\,\mathcal{J}_{\mathfrak{s}}^0\,|n\rangle\,|^2}{E_m-E_n}-\frac{1}{L^2}\langle n|\,K\,|n\rangle\right)\\ &= -\frac{1}{L}\sum_{\substack{mn\\E_m\neq E_n}}\frac{\mathrm{e}^{-E_n\beta}}{Z}\frac{|\langle m|\,\mathcal{J}_{\mathfrak{s}}^0\,|n\rangle\,|^2}{E_m-E_n}-\frac{1}{2L}\sum_n\frac{\mathrm{e}^{-E_n\beta}}{Z}\langle n|\,K\,|n\rangle \qquad (2.58)\\ &= -\frac{1}{2L}\left[\langle K\rangle+2\sum_{\substack{mn\\E_m\neq E_n}}\frac{\mathrm{e}^{-E_n\beta}}{Z}\frac{|\langle m|\,\mathcal{J}_{\mathfrak{s}}^0\,|n\rangle\,|^2}{E_m-E_n}\right].\end{aligned}$$

This yields Kohn's formula for the Drude weight:

$$D=\lim_{L\to\infty}\frac{L}{2}\sum_n\frac{\mathrm{e}^{-E_n\beta}}{Z}\frac{\mathrm{d}^2E_n}{\mathrm{d}\phi^2}\Big|_{\phi=0}=-\lim_{L\to\infty}\frac{1}{2L}\Big[\langle K\rangle+2\sum_{\substack{mn\\E_m\neq E_n}}\frac{\mathrm{e}^{-E_n\beta}}{Z}\frac{|\langle m|\,\mathcal{J}_{\mathfrak{s}}^0\,|n\rangle\,|^2}{E_m-E_n}\Big]. \qquad (2.59)$$

We observe that the Drude weight is equivalent to the thermal average of the energy level curvatures with respect to $\phi$. This expression generalizes Kohn's formula [15] to the finite-temperature case.

## 2.5 Mazur's inequality

In their papers [16, 17], Mazur and Suzuki highlighted the connection between conserved charges and the Drude weight. Our approach will follow the lines presented in [7], additional related notions can be found in [9, 18, 19, 20]. The spin current in the XXZ model is protected in the critical regime due to the presence of conserved charges and the structure of the Drude weight. At zero magnetization, a finite spin Drude weight, indicating dissipationless conductive behaviour at finite temperatures, is only observed when $|\Delta|<1$. In contrast, for $|\Delta|\geq 1$, the spin Drude weight vanishes and spin transport is no longer ballistic. For magnetization different from zero, a finite Drude weight is present for any $T$ and $\Delta$. We will begin by analyzing the time average of the current-current correlator, which is given by:

$$I_C=\lim_{\tau\to\infty}\frac{1}{\tau}\int_0^\tau \mathrm{d}t\,\langle\mathcal{J}_{\mathfrak{s}}^0(t)\mathcal{J}_{\mathfrak{s}}^0(0)\rangle=\lim_{\tau\to\infty}\frac{1}{\tau}\int_0^\tau \mathrm{d}t\,C_{JJ}. \qquad (2.60)$$

Now, let us consider the limit of the following integral:

$$\lim_{\tau\to\infty}\frac{1}{\tau}\int_0^\tau \mathrm{d}t\,\mathrm{e}^{\mathrm{i}(E_m-E_n)t}=\lim_{\tau\to\infty}\frac{\mathrm{e}^{\mathrm{i}(E_m-E_n)\tau}-1}{\mathrm{i}\tau(E_m-E_n)}=\begin{cases}0, & \text{if } (E_m-E_n)\neq 0\\ 1, & \text{if } (E_m-E_n)=0\end{cases}. \qquad (2.61)$$

Using this result in (2.60), we get

$$I_C = \sum_{\substack{mn \\ E_m=E_n}} \left|\langle m|\, \mathcal{J}_{\mathfrak{s}}^0\, |n\rangle\right|^2 \frac{\mathrm{e}^{-\beta E_m}}{Z}. \tag{2.62}$$

We consider all the conserved quantities of the system. Let $\{Q_i\}$ be a set of operators forming a basis for the vector space of conserved charges, satisfying $[Q_i, Q_j] = 0$ and $[H, Q_i] = 0$. We define a scalar product by:

$$\langle AB\rangle = \frac{1}{Z}\mathrm{Tr}\big[\mathrm{e}^{-\beta H}AB\big]. \tag{2.63}$$

We also choose $Q_i$ such that they are orthogonal:

$$\langle Q_i Q_j\rangle = \delta_{ij}\,\langle Q_i^2\rangle\,. \tag{2.64}$$

With these conditions, we can expand any conserved charge as:

$$A = \sum_i \frac{\langle AQ_i\rangle}{\langle Q_i^2\rangle} Q_i. \tag{2.65}$$

This implies that we can decompose the current operator into two parts in the energy eigenbasis: a diagonal part and a part with off-diagonal entries:

$$\mathcal{J}_{\mathfrak{s}}^0 = \sum_i a_i Q_i + \hat{\mathcal{J}}. \tag{2.66}$$

Due to the orthogonal basis, we have that $\langle m|\, \hat{\mathcal{J}}\, |n\rangle = 0$ if $E_m = E_n$. Now, let us reconsider equation (2.62)

$$\begin{aligned} I_C &= \sum_{\substack{mn \\ E_m=E_n}} \langle m|\, \mathcal{J}_{\mathfrak{s}}^0\, |n\rangle\, \langle n|\, \mathcal{J}_{\mathfrak{s}}^0\, |m\rangle\, \frac{\mathrm{e}^{-\beta E_m}}{Z} \\ &= \sum_{ij} \sum_{\substack{mn \\ E_m=E_n}} \frac{\langle \mathcal{J}_{\mathfrak{s}}^0 Q_i\rangle}{\langle Q_i^2\rangle} \frac{\langle \mathcal{J}_{\mathfrak{s}}^0 Q_j\rangle}{\langle Q_j^2\rangle}\, \langle m|\, Q_i\, |n\rangle\, \langle n|\, Q_j\, |m\rangle\, \frac{\mathrm{e}^{-\beta E_m}}{Z} \\ &= \sum_{ij} \sum_m \frac{\langle \mathcal{J}_{\mathfrak{s}}^0 Q_i\rangle}{\langle Q_i^2\rangle} \frac{\langle \mathcal{J}_{\mathfrak{s}}^0 Q_j\rangle}{\langle Q_j^2\rangle}\, \langle m|\, Q_i Q_j\, |m\rangle\, \frac{\mathrm{e}^{-\beta E_m}}{Z} \\ &= \sum_{ij} \frac{\langle \mathcal{J}_{\mathfrak{s}}^0 Q_i\rangle}{\langle Q_i^2\rangle} \frac{\langle \mathcal{J}_{\mathfrak{s}}^0 Q_j\rangle}{\langle Q_j^2\rangle} \delta_{ij}\, \langle Q_j^2\rangle = \sum_i \frac{|\,\langle \mathcal{J}_{\mathfrak{s}}^0 Q_i\rangle\,|^2}{\langle Q_i^2\rangle}. \end{aligned} \tag{2.67}$$

In the thermodynamic limit, the time average reduces to the long-time limit. Comparing (2.60) with (2.53), we obtain:

$$D = \lim_{t\to\infty}\lim_{L\to\infty} \frac{\beta}{2L}\,\langle \mathcal{J}_{\mathfrak{s}}^0(t)\mathcal{J}_{\mathfrak{s}}^0(0)\rangle = \lim_{L\to\infty} \frac{\beta}{2L} \sum_{i=1}^{\infty} \frac{|\,\langle \mathcal{J}_{\mathfrak{s}}^0 Q_i\rangle\,|^2}{\langle Q_i^2\rangle}. \tag{2.68}$$

Here, we assume that in the thermodynamic limit, the system equilibrates, and the integral average is substituted by a constant. Sometimes, it is more advantageous to work with a restricted set of conserved quantities, as it may simplify the numerical or analytical evaluation of scalar products. This leads to the substitution of the equality with an inequality, and this procedure is often referred to as the derivation of the lower bounds for the Drude weight

$$D = \lim_{L\to\infty} \frac{\beta}{2L} \sum_{i=1}^{\infty} \frac{|\langle \mathcal{J}_{\mathfrak{s}}^0 Q_i\rangle|^2}{\langle Q_i^2\rangle} \geq \lim_{L\to\infty} \frac{\beta}{2L} \sum_{i=1}^{K} \frac{|\langle \mathcal{J}_{\mathfrak{s}}^0 Q_i\rangle|^2}{\langle Q_i^2\rangle}. \tag{2.69}$$

It can be demonstrated that at zero magnetic field all local conserved charges $Q_i$ exhibit even behaviour under spin inversion, whereas the spin current is odd under spin inversion: $C^{-1}\mathcal{J}_{\mathfrak{s}}^0 C = -\mathcal{J}_{\mathfrak{s}}^0$. As a result, the scalar product, as seen in (2.69), satisfies $\langle \mathcal{J}_{\mathfrak{s}}^0 Q_i\rangle = 0$ for all $i$, leading to a vanishing Mazur bound. The justification for the existence of a finite Drude weight comes from the presence of quasi-local conserved charges, which are odd under the spin transformation, thus preserving the Drude weight from decay.

## 2.6 Coordinate Bethe Ansatz and Zotos' Drude weight

One method employed to investigate the spectrum of the XXZ model is the Coordinate Bethe Ansatz (CBA) [2, 21, 22]. The CBA has also been applied by Zotos [23] to calculate the spin Drude weight. This computation is achieved by expressing the Drude weight as the thermal average of energy level curvatures within a Hamiltonian subjected to a fictitious flux, as illustrated in Equation (2.59). We define the reference state as the fully polarized state with all spins up, characterized by $S_j^+ |0\rangle = 0$ for $j = 1, \ldots, L$. This results in a state with all spins up. A generic state with $M$ flipped (down) spins is then given by

$$\Psi = \sum_{\{n_l\}} f(n_1, \ldots, n_M) |n_1, \ldots, n_M\rangle . \tag{2.70}$$

Here, the sum is over $\binom{L}{M}$ choices of spin configurations, and $n_l$ represents the position on the lattice. Additionally, we use the lowering operator to construct the basis vector state, denoted as $|n_1, \ldots, n_M\rangle = S_{n_1}^- \ldots S_{n_M}^- |0\rangle$. The Bethe Ansatz consists in assuming that the coordinate wave function has the following form:

$$f(n_1, \ldots, n_M) = \sum_{\mathcal{P}}^{M!} A_{\mathcal{P}} \exp\left[\mathrm{i} \sum_{j=1}^{M} k_{\mathcal{P}_j n_j}\right], \tag{2.71}$$

where $\mathcal{P}$ represents the permutation of indices of $M$ momenta $k$. Now, we insert 2.70 and 2.71 into the Schrödinger equation:

$$H|\Psi\rangle - E|\Psi\rangle = 0 \tag{2.72}$$

with $E = JL\Delta$. The following condition for the wave function arises from 2.72:

$$\begin{aligned} &f(n_1, \ldots, n_j + 1, n_j + 1, \ldots, n_M) + f(n_1, \ldots, n_j, n_j, \ldots, n_M) \\ &= 2\Delta f(n_1, \ldots, n_j + 1, n_j, \ldots, n_M). \end{aligned} \tag{2.73}$$

After some algebra, we obtain the following expression for the amplitude:

$$A_{\mathcal{P}} = \exp\left[\frac{\mathrm{i}}{\pi}\sum_{j<l}^{M}\tilde{\theta}(k_{\mathcal{P}_j}, k_{\mathcal{P}_l})\right], \tag{2.74}$$

where $\tilde{\theta}(k, k')$ is the scattering phase of two magnons which is related to $k_j$. By using the periodicity condition, where $f(n_1, \ldots, n_M) = f(n_2, \ldots, n_1 + L)$, we obtain the quantization equation:

$$\mathrm{e}^{\mathrm{i}k_j L} = \prod_{l\neq j}\mathrm{e}^{\mathrm{i}\tilde{\theta}(k_j,k_l)}. \tag{2.75}$$

The logarithmic form of this equation is given by:

$$k_j N = 2\pi\tilde{I}_j - \sum_{l=1}^{M}\theta(k_j, k_l), \quad j = 1, \ldots, M, \tag{2.76}$$

where

$$\begin{aligned} \theta(k, k') &= \tilde{\theta}(k, k') - \pi \\ &= 2\arctan\frac{\Delta\sin\frac{1}{2}(k - k')}{\cos\frac{1}{2}(k - k') - \Delta\cos\frac{1}{2}(k - k')}. \end{aligned} \tag{2.77}$$

$\tilde{I}_j$ takes integer or half-integer values if $M$ is even or odd. In the critical regime $|\Delta| < 1$, we use the parametrization:

$$\mathrm{e}^{\mathrm{i}k} = \frac{\sinh(\lambda + \mathrm{i}\frac{\gamma}{2})}{\sinh(\lambda - \mathrm{i}\frac{\gamma}{2})}. \tag{2.78}$$

The parameter $\gamma$ is chosen such that $\Delta = \cos(\gamma)$. Finally, from the quantization condition, we get the Bethe equations:

$$\Big(\frac{\sinh(\lambda_j + \mathrm{i}\frac{\gamma}{2})}{\sinh(\lambda_j - \mathrm{i}\frac{\gamma}{2})}\Big)^L = \mathrm{e}^{\mathrm{i}\phi}\prod_{l\neq j}^{M}\frac{\sinh(\lambda_j - \lambda_l + \mathrm{i}\gamma)}{\sinh(\lambda_j - \lambda_l - \mathrm{i}\gamma)}, \quad j = 1, \ldots, M. \tag{2.79}$$

The factor $\mathrm{e}^{\mathrm{i}\phi}$ appears due to the coupling to an external field, as in Equation (2.30). The solutions to this equation are arranged into strings of positive parity:

$$\lambda_{\alpha,+}^{n_k,k} = \lambda_\alpha^k + \mathrm{i}\frac{\gamma}{2}(n_k + 1 - 2k) + \mathcal{O}(\mathrm{e}^{-\delta L}) \tag{2.80}$$

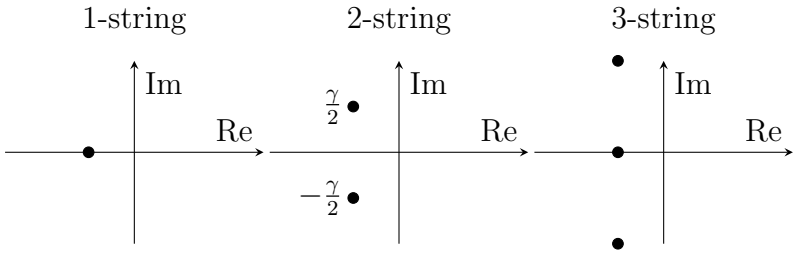



Figure 2.2: Example of strings.

or negative parity:

$$\lambda_{\alpha,-} = \mathrm{i}\frac{\gamma}{2}\nu + \mathcal{O}(\mathrm{e}^{-\delta L}). \tag{2.81}$$

The string solution was used by Takahashi, Suzuki and Gaudin [24, 25, 26] to classify the complex solutions for the momenta of quasi-particles. Despite numerous studies on these solutions and their deviations, this topic remains an area of ongoing discussion and debate. The parameter $n_k$ denotes the type of the string and in the case of the simple root of unity $\gamma = \pi/\nu$ is $n_k = k$, $k = 1 \dots \nu - 1$. The deviations $\mathcal{O}(\mathrm{e}^{-\delta L})$ decay exponentially with the system size and the strings in the thermodynamic limit tend to become perfect strings with zero deviation. Only the centres of strings, denoted as $\lambda_\alpha^k$, characterize a given state of the system. They satisfy the Bethe-Gaudin-Takahashi equations:

$$L t_{n_j}^{v_j}(\lambda_\alpha^j) = 2\pi I_\alpha^j + \sum_{k=1}^{\nu}\sum_{\beta=1}^{M_k}\Theta_{jk}(\lambda_\alpha^j - \lambda_\beta^k) - n_j\phi L \quad \alpha = 1, \dots, M_k. \tag{2.82}$$

$I_\alpha^j$ is an integer if $M_k$ is odd and a half-integer if $M_k$ is even. Here, $M_k$ denotes the number of strings of type $k$ and parity $v_j$, and it satisfies the equation

$$\sum_{k=1}^{\nu} k M_k = M. \tag{2.83}$$

Additionally,

$$t_{n_j}^{v_j}(\lambda) = 2v_j \arctan\left(\left(\cot n_j\frac{\gamma}{2}\right)^{v_j}\tanh\lambda\right) \tag{2.84}$$

and

$$\Theta_{jk}(\lambda) = t_{|n_j-n_k|}^{v_j v_k}(\lambda) + t_{n_j+n_k}^{v_j v_k}(\lambda) + 2\sum_{i=1}^{Min(n_j,n_k)-1} t_{|n_j-n_k|+2i}^{v_j v_k}(\lambda). \tag{2.85}$$

To proceed, we introduce the counting function:

$$Z_j(\lambda) = \frac{1}{2\pi}t_j(\lambda) + \frac{1}{2\pi L}\sum_{k=1}^{\nu}\sum_{\beta=1}^{M_k}\Theta_{jk}(\lambda_\alpha^j - \lambda_\beta^k) - \frac{n_j\phi}{2\pi}. \tag{2.86}$$

Now, let us consider our system in the thermodynamic limit, where ($L \gg 1$). In this limit, the strings $\lambda_\alpha^j$ form a continuum, and they can be described by the densities of string particles $\rho_j(\lambda)$ and hole densities $\rho_j^p(\lambda)$. The total number of particles and holes in an interval is determined through the counting function:

$$Z_j(\lambda + \mathrm{d}\lambda) - Z_j(\lambda) = \big(\rho_j(\lambda) + \rho_j^h(\lambda)\big)\,\mathrm{d}\lambda. \tag{2.87}$$

Now, if we consider $\mathrm{d}\lambda$ as an infinitesimal interval, we can derive the following equation from (2.86) and (2.87):

$$\rho_j(\lambda) + \rho_j^h(\lambda) = a_j(\lambda) + \sum_k T_{jk} * \rho_k(\lambda), \tag{2.88}$$

where

$$a_j(\lambda) = \frac{1}{2\pi}\frac{\mathrm{d}t_j(\lambda)}{\mathrm{d}\lambda}, \qquad T_{jk}(\lambda) = \frac{1}{2\pi}\frac{\mathrm{d}\Theta_{jk}(\lambda)}{\mathrm{d}\lambda}. \tag{2.89}$$

The equilibrium state is obtained by minimizing the free energy:

$$\begin{aligned} f &= e - Ts \\ &= \sum_j \int_{-\infty}^{\infty} \mathrm{d}\lambda \Big( \epsilon_j \rho_j(\lambda) - T\left(\rho_j(\lambda) + \rho_j^h(\lambda)\right) \log\left(\rho_j(\lambda) + \rho_j^h(\lambda)\right) \\ &\quad - T\rho_j(\lambda)\log\rho_j(\lambda) - T\rho_j^h(\lambda)\log\rho_j^h(\lambda)\Big) \end{aligned} \tag{2.90}$$

subject to the constraint in (2.89). This results in the non-linear integral equations for $\eta_j(\lambda) = \rho_j^h(\lambda)/\rho_j(\lambda)$, commonly referred to as the TBA (thermodynamic Bethe ansatz) equations:

$$\log\eta_j(\lambda) = \beta\epsilon_j(\lambda) - \sum_k T_{jk} * \log(1 + \eta_k^{-1}(\lambda)). \tag{2.91}$$

The bare energy is given by:

$$\epsilon_j(\lambda) = -2J\eta\sin(\frac{\pi}{\eta})a_j(\lambda). \tag{2.92}$$

The Drude weight is determined through a finite-size correction analysis, as described in [23] and [27]. We introduce the following expansion for the rapidities:

$$\lambda_\alpha^j = \lambda_{j\alpha}^\infty + \frac{g_{j\alpha}^{(1)}}{L} + \frac{g_{j\alpha}^{(2)}}{L^2}, \tag{2.93}$$

where $\lambda_{j\alpha}^{\infty}$ are the rapidities for a system with system size $L$. The finite size coefficients $g_{j\alpha}^{(1)}$ and $g_{j\alpha}^{(2)}$, when inserted into the counting function (2.86), yield the following equations:

$$\begin{aligned} g_j^{(1)}\rho_j(\lambda)(1+\eta_j(\lambda)) &= \frac{n_j\phi}{2\pi} - \sum_k T_{jk} * g_k^{(1)}\rho_k(\lambda), \\ g_j^{(2)}\rho_j(\lambda)(1+\eta_j(\lambda)) &= \frac{\mathrm{d}}{\mathrm{d}\lambda} f_j(\lambda) - \sum_k T_{jk} * g_k^{(2)}\rho_k(\lambda), \\ f_j(\lambda) &= \frac{1}{2}(g_j^{(1)})^2\rho_j(\lambda)(1+\eta_j(\lambda)) + \frac{1}{2}\sum_k T_{jk} * (g_k^{(1)})^2\rho_k(\lambda). \end{aligned} \tag{2.94}$$

The expression for the Drude weight in terms of the finite-size coefficients is given in [27]:

$$D = \frac{1}{2}\sum_j \int_{-\infty}^{\infty} \left( \frac{\mathrm{d}^2\epsilon_j(\lambda)}{\mathrm{d}\lambda^2} \left( \frac{\partial g_j^{(1)}}{\partial\phi} \right)^2 \rho_j(\lambda) + \frac{\mathrm{d}\epsilon_j(\lambda)}{\mathrm{d}\lambda} \frac{\partial^2 g_j^{(2)}}{\partial\phi^2} \rho_j(\lambda) \right). \tag{2.95}$$

Finally, by applying the Dressing formalism and using (2.94), we find Zotos' formula

$$D = \frac{J\sin\gamma}{4\pi\beta\gamma} \sum_j \int_{-\infty}^{\infty} \frac{\eta_j(\lambda) \left( \frac{\partial}{\partial\beta h} \log\eta_j(\lambda) \right)^2 \left( \frac{\partial}{\partial\lambda} \log\eta_j(\lambda) \right)^2}{(1+\eta_j(\lambda))^2 \frac{\partial}{\partial\beta} \log\eta_j}. \tag{2.96}$$

A numerical analysis of Zotos' formula indicates that the Drude weight exhibits discontinuities as a function of $\Delta$ for $T > 0$. This phenomenon becomes particularly evident when we expand the equation (2.96) for $T \to \infty$.

# Chapter 3

# Mazur bounds

In this chapter, we explore the spin transport properties of the spin-1/2 XXZ Heisenberg model. Specifically, we employ the Mazur inequality [16] to calculate the Drude weight. In an integrable one-dimensional quantum system, an infinite set of local conserved quantities can prevent a current from fully decaying. To deepen our understanding, we examine one such set of non-local conserved charges, as identified by Pereira et al. [28], which exhibit a non-trivial overlap with the current operator.

## 3.1 Standard XXZ spin-1/2 thermodynamics

In this section, we will provide a summary of the quantum transfer matrix approach applied to the XXZ spin-1/2 model. The quantities introduced here are fundamental to address the Drude weight problem. The free energy and various other thermodynamic properties of the system can be computed from the leading or largest eigenvalue of the quantum transfer matrix. To calculate the Drude weight, we will introduce analogous operators whose largest eigenvalue will be connected to the dynamic properties of the system. A detailed treatment of the quantum transfer matrix approach can be found in references [29, 30, 31].

The Hamiltonian for the anisotropic Heisenberg anti-ferromagnet is given by

$$H_{XXZ} = J\sum_{j=1}^{L}\Big(\sigma_{j-1}^{x}\sigma_{j}^{x} + \sigma_{j-1}^{y}\sigma_{j}^{y} + \Delta(\sigma_{j-1}^{z}\sigma_{j}^{z} - 1)\Big), \tag{3.1}$$

where $J > 0$, $\Delta = \cosh(\eta)$ with $\eta = \frac{l}{m}\pi\mathrm{i}$, $l, m \in \mathbb{Z}^{+}$, $l < m$ (ensuring $|\Delta| < 1$), and $\sigma^{\alpha}$ with $\alpha = x, y, z$ are Pauli matrices. We impose periodic boundary conditions, namely $\sigma_{N+1}^{\alpha} = \sigma_{1}^{\alpha}$ for all $\alpha = x, y, z$. The Hamiltonian operator acts on the Vector space $V = V_1 \otimes V_2 \otimes \cdots \otimes V_L$, where $V_i \in \mathbb{C}^2$ represents the local Hilbert space at the $i$-th point of the chain.

The associated $R$-matrix, defined as

$$R(\lambda,\mu) = \begin{pmatrix} 1 & 0 & 0 & 0 \\ 0 & b(\lambda,\mu) & c(\lambda,\mu) & 0 \\ 0 & c(\lambda,\mu) & b(\lambda,\mu) & 0 \\ 0 & 0 & 0 & 1 \end{pmatrix}, \tag{3.2}$$

with

$$b(\lambda,\mu) = \frac{\sinh(\lambda-\mu)}{\sinh(\lambda-\mu+\eta)}, \qquad c(\lambda,\mu) = \frac{\sinh(\eta)}{\sinh(\lambda-\mu+\eta)} \tag{3.3}$$

satisfies the Yang-Baxter equation [32] in $\mathbb{C}^2 \otimes \mathbb{C}^2 \otimes \mathbb{C}^2$

$$R_{jk}(\lambda,\mu)R_{jl}(\lambda,\nu)R_{kl}(\mu,\nu) = R_{kl}(\mu,\nu)R_{jl}(\lambda,\nu)R_{jk}(\lambda,\mu). \tag{3.4}$$

The following properties are also satisfied:

$$\begin{aligned} R(\lambda,\lambda) &= P, \\ R_{12}(\lambda,\mu)R_{21}(\mu,\lambda) &= \mathrm{id}. \end{aligned} \tag{3.5}$$

The $R$-matrix function takes spectral parameters $\lambda, \mu \in \mathbb{C}$ as its arguments. The Hamiltonian can be generated from the $R$-matrix through the relation

$$\sum_{j=1}^{L} \partial_\lambda PR(\lambda,0)|_{\lambda=0} = \frac{1}{2J\sinh(\eta)} H_{XXZ}, \tag{3.6}$$

where $P$ represents the permutation operator that acts on the tensor product space $\mathbb{C}^2 \otimes \mathbb{C}^2$.

To proceed, we explicitly define the $R$-matrix in terms of basis matrices

$$R_{jk}(\lambda,\mu) = R^{\alpha\gamma}_{\beta\delta}(e_j)^{\beta}_{\alpha}(e_k)^{\delta}_{\gamma}, \tag{3.7}$$

where the indices $j$ and $k$ correspond to the quantum space ($j = 1 \dots L$) and auxiliary space ($k = \overline{1} \dots \overline{N}$), respectively. The $R$-matrix acts on the tensor product space $\mathbb{C}^2 \otimes \mathbb{C}^2$ and is represented in the basis $\{e_1^1, e_1^2, e_2^1, e_2^2\}$, where $e_\alpha^a$ are the basis matrices of the local Hilbert space at site $j$. The matrix element $R^{\alpha\gamma}_{\beta\delta}$ encodes the interaction between basis states. The basis vectors are defined as follows:

$$e_1^1 = \begin{pmatrix} 1 & 0 \\ 0 & 0 \end{pmatrix}, \quad e_1^2 = \begin{pmatrix} 0 & 1 \\ 0 & 0 \end{pmatrix}, \quad e_2^1 = \begin{pmatrix} 0 & 0 \\ 1 & 0 \end{pmatrix}, \quad e_2^2 = \begin{pmatrix} 0 & 0 \\ 0 & 1 \end{pmatrix}. \tag{3.8}$$

The monodromy matrix is constructed using $L$-operators. Specifically,

$$T(\lambda) = L_L(\lambda,\nu)\dots L_1(\lambda,\nu), \tag{3.9}$$

where the $L$-operator at site $j$ has matrix elements:

$$(L_j)^{\alpha}_{\beta}(\lambda,\mu) = R^{\alpha\gamma}_{\beta\delta}(\lambda,\mu)(e_j)^{\delta}_{\gamma}. \tag{3.10}$$

The transfer matrix is defined as the trace over the auxiliary space:

$$t(\lambda) = \mathrm{tr}T(\lambda). \tag{3.11}$$

It generates conserved quantities and it can be diagonalized by using the algebraic Bethe ansatz. From equations (3.4), (3.9), and (3.10), the following RTT-relation follows:

$$R_{jk}(\lambda,\mu)T_j(\lambda)T_k(\mu) = T_k(\mu)T_j(\lambda)R_{jk}(\lambda,\mu). \tag{3.12}$$

The Yang-Baxter equation can then be written as

$$\breve{R}(\lambda,\mu)(L_j(\lambda,\nu)) \otimes (L_j(\mu,\nu)) = (L_j(\mu,\nu)) \otimes (L_j(\lambda,\nu))\breve{R}(\lambda,\mu), \tag{3.13}$$

where

$$\breve{R}^{\alpha\gamma}_{\beta\delta} = R^{\gamma\alpha}_{\beta\delta}. \tag{3.14}$$

The Trotter formula allows us to express the density matrix in terms of monodromy matrices

$$\lim_{N\to\infty} \rho_{N,L} = \mathrm{e}^{-\beta H}, \tag{3.15}$$

where

$$\begin{aligned}
\rho_{N,L} &:= \left(\overline{t}(\tau)t(-\tau)\right)^{\frac{N}{2}} \\
&= \mathrm{Tr}_{\overline{1}\ldots\overline{N}}\left[\overline{T}_{\overline{N}}(\tau)T_{\overline{N-1}}(-\tau)\ldots\overline{T}_{\overline{2}}(\tau)T_{\overline{1}}(-\tau)\right] \\
&= \mathrm{Tr}_{\overline{1}\ldots\overline{N}}\left[T_1^{QTM}(0)\ldots T_L^{QTM}(0)\right]
\end{aligned} \tag{3.16}$$

and $\tau = \frac{\beta}{N}$. The parameter $N$ is referred to as "the Trotter number". We define two types of monodromy matrices

$$\begin{aligned}
T_{\overline{j}}(\lambda) &= R_{\overline{j}L}(\lambda,\mu)\ldots R_{\overline{j}1}(\lambda,\mu), \\
\overline{T}_{\overline{j}}(\lambda) &= R_{1\overline{j}}(\mu,\lambda)\ldots R_{L\overline{j}}(\mu,\lambda)
\end{aligned} \tag{3.17}$$

with corresponding transfer matrices:

$$\overline{t}(\tau) = \mathrm{tr}_{\overline{j}}\overline{T}_{\overline{j}}(\tau), \quad t(\tau) = \mathrm{tr}_{\overline{j}}T_{\overline{j}}(\tau). \tag{3.18}$$

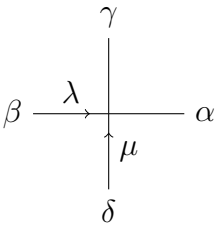
In the last line of the equation (3.16) we introduced the quantum monodromy matrix

$$T_j^{QTM}(\lambda) = R_{j\overline{N}}(\lambda,\tau)R^{t1}_{\overline{N-1}j}(-\tau,\lambda)\ldots R_{j\overline{2}}(\lambda,\tau)R^{t_1}_{\overline{1}j}(-\tau,\lambda), \tag{3.19}$$

The transposition $t^1$ is performed with respect to the first space in which $R(\lambda,\mu)$ is embedded. The quantum transfer matrix $t^{QTM}(\lambda)$ is then the partial trace over the auxiliary space:

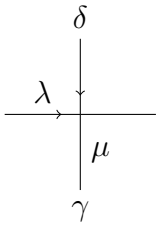
$$t^{QTM}(\lambda) = \mathrm{Tr}_j T_j^{QTM}(\lambda). \tag{3.20}$$

To better understand the quantum transfer matrix, it is helpful to introduce the graphical representation of integrability objects. We identify an $R$-matrix element with

$R^{\alpha\gamma}_{\beta\delta}(\lambda,\mu) =$ 

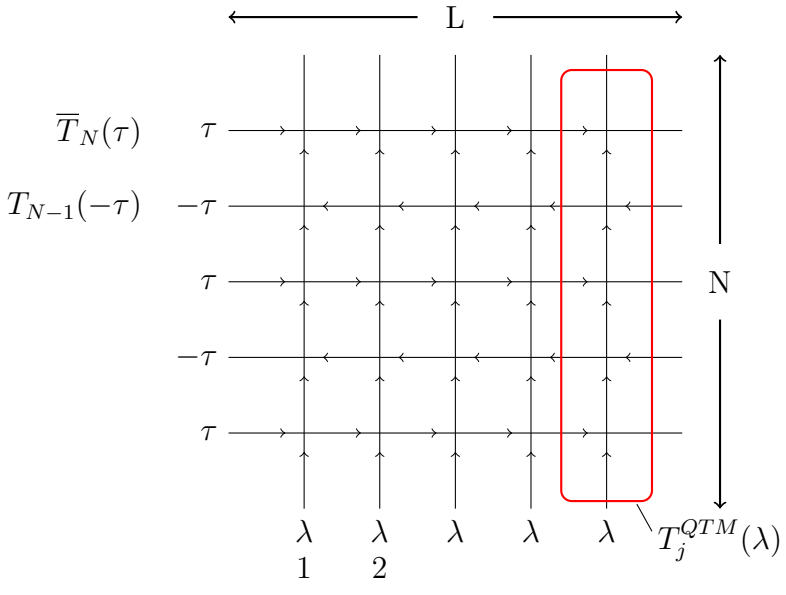
(3.21)

and its partial transposition with respect to the first space

$(R^{t_1})^{\gamma\alpha}_{\delta\beta}(\mu,\lambda) = R^{\delta\alpha}_{\gamma\beta}(\mu,\lambda) =$ 

. (3.22)

Each arrangement of vertices translates into a product of $R$-matrices, and a connection is represented by a summation over indices. The density matrix is represented with



. (3.23)

The graphical representation of the quantum transfer matrix is illustrated as follows:




. (3.24)

This diagram shows the configuration on the right-hand side of equation (3.19). Note that this corresponds to the arrangement of vertices in the density matrix in the vertical direction.

The quantum transfer matrix can be represented using $L$-matrices. To achieve this, we introduce two types of $L$-matrices:

$$(e_a)^{\beta}_{\alpha}(L_j)^{\alpha}_{\beta}(\lambda,\mu) = R_{aj}(\lambda,\mu), \quad (e_a)^{\beta}_{\alpha}(\tilde{L}_j)^{\alpha}_{\beta}(-\mu,\lambda) = R^{t_1}_{ja}(-\mu,\lambda), \tag{3.25}$$

or explicitly,

$$\begin{aligned} L_j(\lambda,\mu) &= \begin{pmatrix} (e_j)^1_1 + b(\lambda,\mu)(e_j)^2_2 & c(\lambda,\mu)(e_j)^1_2 \\ c(\lambda,\mu)(e_j)^2_1 & b(\lambda,\mu)(e_j)^1_1 + (e_j)^2_2 \end{pmatrix}, \\ \tilde{L}_j(-\mu,\lambda) &= \begin{pmatrix} (e_j)^1_1 + b(-\mu,\lambda)(e_j)^2_2 & c(-\mu,\lambda)(e_j)^2_1 \\ c(-\mu,\lambda)(e_j)^1_2 & b(-\mu,\lambda)(e_j)^1_1 + (e_j)^2_2 \end{pmatrix}, \end{aligned} \tag{3.26}$$

where $b(\lambda,\mu)$ and $c(\lambda,\mu)$ are defined in (3.3). It is easy to see that the quantum transfer matrix in terms of L-matrices is given by

$$T^{QTM}(\lambda) = L_N(\lambda,\tau)\tilde{L}_{N-1}(-\tau,\lambda)\dots L_2(\lambda,\tau)\tilde{L}_1(-\tau,\lambda) \tag{3.27}$$

and it acts as a lower triangular matrix on the ground state

$$|0\rangle = \begin{pmatrix} 1 \\ 0 \end{pmatrix} \otimes \begin{pmatrix} 0 \\ 1 \end{pmatrix} \otimes \cdots \otimes \begin{pmatrix} 0 \\ 1 \end{pmatrix}. \tag{3.28}$$

The thermodynamic properties of a quantum spin model can be extracted from the partition function

$$Z_L = \lim_{N\to\infty} Z_{N,L} = \mathrm{tr}\rho_L. \tag{3.29}$$

Let $\Lambda_n(\lambda)$, where $n = 0, 1, \dots, 2^N - 1$, represent the eigenvalues of $t^{QTM}(\lambda)$, arranged in the following order:

$$|\Lambda_0(\lambda)| \geq |\Lambda_1(\lambda)| \geq |\Lambda_2(\lambda)| \geq \cdots \geq |\Lambda_{2^N-1}(\lambda)|. \tag{3.30}$$

We can compute the free energy per lattice site as

$$\begin{aligned} -\beta f &= \lim_{L\to\infty}\lim_{N\to\infty}\frac{\log Z_L}{L} = \frac{1}{L}\log \operatorname{tr}(t^{QTM}(0))^L \\ &= \lim_{L\to\infty}\lim_{N\to\infty}\frac{1}{L}\log\left[\Lambda_0^L(0)\left(1+\sum_{n=1}^{2^N-1}\left(\frac{\Lambda_n(0)}{\Lambda_0(0)}\right)^L\right)\right] \approx \lim_{N\to\infty}\log\Lambda_0(0). \end{aligned} \tag{3.31}$$

The relations in (3.31) remain valid under the following conditions:

- Assuming the interchangeability of the Trotter limit ($N \to \infty$) and the thermodynamic limit ($L \to \infty$), a belief supported for most fundamental models at temperatures above zero.
- As long as the condition $|\Lambda_0(0)/\Lambda_n(0)| < 1$ holds, there is a gap between the largest eigenvalue and the subsequent ones.

This significant result suggests that thermodynamic properties can be calculated from the leading eigenvalue of the quantum transfer matrix.

To compute the largest eigenvalue of the quantum transfer matrix, we employ the algebraic Bethe ansatz. We interpret the quantum transfer matrix $T_a^{QTM}(\lambda)$ as a $2 \times 2$ matrix with operator-valued entries:

$$T_a^{QTM}(\lambda) = \begin{pmatrix} A(\lambda) & B(\lambda) \\ C(\lambda) & D(\lambda) \end{pmatrix}_a . \tag{3.32}$$

The Yang-Baxter equations provide a set of quadratic relations for the entries of $T_a^{QTM}(\lambda)$, enabling us to compute the eigenvalue of the quantum transfer matrix

$$t^{QTM}(\lambda) = A(\lambda) + D(\lambda) \tag{3.33}$$

evaluated on the pseudo vacuum state $|0\rangle_{GS}$. Applying the ground state transforms the monodromy matrix into a lower triangular form

$$T_a^{QTM}(\lambda)\,|0\rangle_{GS} = \begin{pmatrix} a(\lambda) & B(\lambda) \\ 0 & d(\lambda) \end{pmatrix}_a |0\rangle_{GS}\,, \tag{3.34}$$

where $a(\lambda)$ and $d(\lambda)$ are some complex functions dependent on the spectral parameter $\lambda$. For a generic set of $\{\lambda_j\}_{j=0}^K \in \mathbb{C}$, we define

$$|\{\lambda\}_{j=0}^K\rangle = \prod_{j=1}^K B(\lambda_j)\,|0\rangle_{GS}\,. \tag{3.35}$$

To diagonalize the transfer matrix, we commute all the $B(\lambda_j)$ operators with the $A(\lambda)$ and $D(\lambda)$ operators:

$$\begin{aligned} t^{QTM}(\lambda)\,|\{\lambda_j\}_{j=0}^{K}\rangle &= \big[A(\lambda)+D(\lambda)\big]B(\lambda_1)\dots B(\lambda_k)\,|0\rangle_{GS} \\ &= \big[\Lambda_0(\lambda)\big]B(\lambda_1)\dots B(\lambda_k)\,|0\rangle_{GS}\,, \end{aligned} \tag{3.36}$$

where $\Lambda_0(\lambda)$ is determined from commutation relations and takes the form:

$$\Lambda_0(\lambda) = a(\lambda)\frac{Q(\lambda-\eta)}{Q(\lambda)} + d(\lambda)\frac{Q(\lambda+\eta)}{Q(\lambda)} \tag{3.37}$$

and

$$Q(\lambda) = \prod_{j=1}^{K}\sinh(\lambda-\lambda_j). \tag{3.38}$$

The parameters $\{\lambda_k\}$ must satisfy the Bethe Ansatz equations:

$$\frac{a(\lambda_j)Q(\lambda_j-\eta)}{d(\lambda_j)Q(\lambda_j+\eta)} = -1, \tag{3.39}$$

for $j = 1,\dots,K$. Here, $a(\lambda)$ and $d(\lambda)$ denote the eigenvalues of the diagonal monodromy matrix entries acting on the pseudo vacuum state $|0\rangle_{GS}$.

## 3.2 Pseudo-local conserved quantities

In this section, we will develop quasilocal conserved quantities for the spin-1/2 XXZ model with periodic boundary conditions. Unlike strictly local charges, quasilocal charges have operator densities that decay exponentially with distance rather than having compact support. These conserved quantities are expected to have an overlap with the spin current operator, thereby providing a non-zero Mazur bound for the spin Drude weight. See also, [33], [28]. At first, we will construct a generator function for the quasilocal conserved quantities using a two-parameter transfer matrix. Then, we will proceed to extract the conserved quantities from this operator.

We define the two parameter Lax operator acting in $V_j \otimes \mathcal{A}$, where $\mathcal{A}$ is an auxiliary space with dimension $d_{\mathcal{A}}$. The Lax operator is expressed as:

$$L_j(\varphi,s) = \begin{pmatrix} \sinh\left(\varphi+\eta S^z_{\mathcal{A}}(s)\right) & \sinh(\eta)S^-_{\mathcal{A}}(s) \\ \sinh(\eta)S^+_{\mathcal{A}}(s) & \sinh\left(\varphi-\eta S^z_{\mathcal{A}}(s)\right) \end{pmatrix}_j, \tag{3.40}$$

where $S^\alpha_{\mathcal{A}}$, $\alpha = \pm, z$ are the spin operators, $s \in \mathbb{C}$, and we focus on the case $\varphi = \lambda - \mu$. We will work with the cyclic representation of $U_q[SU(2)]$, and we specialize to the root

of unity case, *i.e.* $q = \mathrm{e}^{\mathrm{i}\frac{l\pi}{m}}$ with $l, m \in \mathbb{Z}$. At the root of unity, the auxiliary space $\mathcal{A}$ becomes finite dimensional with $d_{\mathcal{A}} = m$. The spin operators take the form:

$$\begin{aligned} S^z_{\mathcal{A}}(s)\,|k\rangle &= \frac{1}{\eta}\sum_{k=0}^{\infty}(s+\eta k)\,|k\rangle\,, \\ S^+_{\mathcal{A}}(s)\,|k\rangle &= -\sum_{k=0}^{\infty}\frac{\sinh(2s+\eta k)}{\sinh(\eta)}\,|k+1\rangle\,, \\ S^-_{\mathcal{A}}(s)\,|k\rangle &= \sum_{k=1}^{\infty}\frac{\sinh(\eta k)}{\sinh(\eta)}\,|k-1\rangle\,, \end{aligned} \tag{3.41}$$

where the auxiliary space index $k$ can be restricted to $0 \le k \le m-1$ and they satisfy the algebra

$$\begin{aligned} [S^z, S^\pm] &= \pm S^\pm, \\ [S^+, S^-] &= \frac{\sinh(2\eta S^z)}{\sinh(\eta)}. \end{aligned} \tag{3.42}$$

The definition of the monodromy matrix is given by

$$T_{\mathcal{A}}(\varphi, s) = \mathcal{L}_L(\varphi, s)\mathcal{L}_{L-1}(\varphi, s)\ldots\mathcal{L}_1(\varphi, s) \tag{3.43}$$

and by tracing over the auxiliary space, the transfer matrix

$$t_{\mathcal{A}}(\varphi, s) = \mathrm{tr}_{\mathcal{A}}[T_{\mathcal{A}}(\varphi, s)]. \tag{3.44}$$

It can be shown that the transfer matrix $t_j(\theta)$, which generates the XXZ Hamiltonian, commutes with the two-parameter transfer matrix

$$[t_{\mathcal{A}}(\varphi, s), t_j(\theta)] = 0 \qquad \forall\varphi, \theta \in \mathbb{C}. \tag{3.45}$$

This implies that $t_{\mathcal{A}}(\varphi, s)$ enriches the set of conserved charges associated with the XXZ Hamiltonian, generating additional conserved quantities beyond the well-known local charges (such as the Hamiltonian and momentum). These quantities will later be shown to exhibit quasi-local structure.

Consider the two parameter Lax operator

$$\mathcal{L}_j(\varphi, s) = \mathrm{i}\sum_{\alpha\in J}\sigma^\alpha_j A^\alpha_{\mathcal{A}}(\varphi, s) \tag{3.46}$$

in terms of operators

$$\begin{aligned} A^0(\varphi, s) &= -\mathrm{i}\sinh(\varphi)\cosh(\eta S^z(s)), \\ A^z(\varphi, s) &= -\mathrm{i}\cosh(\varphi)\sinh(\eta S^z(s)), \\ A^\pm(\varphi, s) &= -\mathrm{i}\sinh(\eta)S^\mp(s), \end{aligned} \tag{3.47}$$

where $J = \{0, z, \pm\}$ and $\sigma^0 = \mathbb{1}$. The transfer matrix, in this notation is given by

$$\begin{aligned} t_{\mathcal{A}}(\varphi, s) &= \mathrm{i}^L \sum_{\{\alpha_j\}} \mathrm{tr}\{A_{\alpha_L} \dots A_{\alpha_2} A_{\alpha_1}\} \prod_{j=1}^{N} \sigma_j^{\alpha_j}, \\ &= \mathrm{i}^L \sum_{\{\alpha_j\}} \mathrm{tr}\{A^t_{\alpha_1} A^t_{\alpha_2} \dots A^t_{\alpha_L}\} \prod_{j=1}^{N} \sigma_j^{\alpha_j}. \end{aligned} \tag{3.48}$$

Now we apply the parity operator $\mathcal{P}^{-1}\sigma_j^{\alpha_j}\mathcal{P} = \sigma_{L+1-j}^{\alpha_j}$

$$\begin{aligned} \mathcal{P}^{-1} t_{\mathcal{A}}(\varphi, s)\mathcal{P} &= \mathrm{i}^L \sum_{\{\alpha_j\}} \mathrm{tr}\{A_{\alpha_L} \dots A_{\alpha_2} A_{\alpha_1}\} \prod_{j=1}^{L} \sigma_{L+1-j}^{\alpha_j}, \\ &= \mathrm{i}^L \sum_{\{\alpha_j\}} \mathrm{tr}\{A_{\alpha_1} A_{\alpha_2} \dots A_{\alpha_L}\} \prod_{j=1}^{L} \sigma_j^{\alpha_j}, \end{aligned} \tag{3.49}$$

where $A^t_{\alpha_j}$ is the transpose of $A_{\alpha_j}$. Finally we define a two parameter conserved quantity which is odd under under parity transformation

$$\begin{aligned} I(\varphi, s) &= (-\mathrm{i})^L \big[\hat{P} t_{\mathcal{A}}(\varphi, s)\hat{P} - t_{\mathcal{A}}(\varphi, s)\big] \\ &= \sum_{\{\alpha_j\}} \mathrm{tr}\{A_{\alpha_1} \dots A_{\alpha_L} - A^t_{\alpha_1} \dots A^t_{\alpha_L}\} \prod_{j=1}^{L} \sigma_j^{\alpha_j}. \end{aligned} \tag{3.50}$$

In order to study the "quasi locality" at $T \to \infty$, we calculate the inner product

$$\langle I^\dagger(\varphi, s) I(\varphi, s)\rangle = 2\mathrm{tr}_{\mathcal{A}\otimes\mathcal{A}}\big\{\big[T_1(\varphi, s, \overline{s})\big]^L - \big[T_2(\varphi, s, \overline{s})\big]^L\big\}, \tag{3.51}$$

where $T_1(\varphi, s, s)$ and $T_2(\varphi, s, s)$ are transfer matrices in $\mathcal{A} \otimes \mathcal{A}$

$$\begin{aligned} T_1(\varphi, s, \overline{s}) &= \sum_{\alpha=0,z,\pm} C_\alpha A^*_\alpha(\varphi, s) \otimes A_\alpha(\varphi, \overline{s}), \\ T_2(\varphi, s, \overline{s}) &= \sum_{\alpha=0,z,\pm} C_\alpha A^*_\alpha(\varphi, s) \otimes A^t_\alpha(\varphi, \overline{s}) \end{aligned} \tag{3.52}$$

and

$$C_\alpha = \frac{1}{2}\mathrm{tr}\{\sigma^\alpha(\sigma^\alpha)^\dagger\}. \tag{3.53}$$

The inner product is defined as $\langle AB^\dagger\rangle = 2^{-N}\mathrm{tr}\{AB^\dagger\}$. The substitution of (3.47) into

(3.52) leads to

$$
\begin{aligned}
T_1(\varphi,0,0) = &\sum_{k,r=0}^{m-1} \Big( |\sinh(\varphi)|^2 \cosh(\eta k)\cosh(\eta r) \\
&- |\cosh(\varphi)|^2 \sinh(\eta k)\sinh(\eta r) \Big) |k,r\rangle \langle k,r| \,, \\
&- \frac{1}{2} \sum_{k,r=0}^{m-2} \Big( \sinh(\eta(k+1))\sinh(\eta(r+1)) |k,r\rangle \langle k+1,r+1| \\
&+ \sinh(\eta k)\sinh(\eta r) |k+1,r+1\rangle \langle k,r| \Big) \\
T_2(\varphi,0,0) = &\sum_{k,r=0}^{m-1} \Big( |\sinh(\varphi)|^2 \cosh(\eta k)\cosh(\eta r) \\
&- |\cosh(\varphi)|^2 \sinh(\eta k)\sinh(\eta r) \Big) |k,r\rangle \langle k,r| \,, \\
&- \frac{1}{2} \sum_{k,r=0}^{m-2} \Big( \sinh(\eta(k+1))\sinh(\eta(r+1)) |k,r+1\rangle \langle k+1,r| \\
&+ \sinh(\eta k)\sinh(\eta r) |k+1,r\rangle \langle k,r+1| \Big).
\end{aligned}
\tag{3.54}
$$

The transfer matrices exhibit block diagonal structure in subspaces of the tensor-product basis. When considering $T_1(\varphi,0,0)$, the subspaces correspond to fixed values of $k = 0,...,m-1$, with states given by $|r,(r+k)(\mathrm{mod}\, m)\rangle$. For $T_2(\varphi,0,0)$, the Kronecker states are $|r,(-r+k)(\mathrm{mod}\, m)\rangle$. The states $|r,(r+k)\ (\mathrm{mod}\ m)\rangle$ and $|r,(-r+k)\ (\mathrm{mod}\ m)\rangle$ arise from symmetry constraints in the block diagonal structure of the transfer matrices $T_1$ and $T_2$.

To analyze the scaling behavior in (3.51) as $N$ approaches infinity, we focus on the subspace where the transfer matrices have their largest eigenvalue. This corresponds to the $k = 0$ subspace for both $T_1(\varphi,0,0)$ and $T_2(\varphi,0,0)$, since this sector contains the ground state $|0\rangle$ and yields the dominant contribution in the thermodynamic limit. Within this

subspace, we denote $|r, \pm r\rangle$ as $|r\rangle$ and reduce the transfer matrices accordingly

$$\begin{aligned}
\mathcal{T}_1(\varphi) &= \sum_{r=0}^{m-1} \left( |\sinh(\varphi)|^2 \cosh^2(\eta r) - |\cosh(\varphi)|^2 \sinh^2(\eta r) \right) |r\rangle \langle r| \,, \\
&\quad - \frac{1}{2} \sum_{r=0}^{m-2} \left( \sinh^2(\eta(r+1)) \, |r\rangle \langle r+1| + \sinh^2(\eta r) \, |r+1\rangle \langle r| \right) \\
\mathcal{T}_2(\varphi) &= |\sinh(\varphi)|^2 \, |0\rangle \langle 0| \\
&\quad + (-1)^l \sum_{r=0}^{m-1} \left( |\sinh(\varphi)|^2 \cosh^2(\eta r) - |\cosh(\varphi)|^2 \sinh^2(\eta r) \right) |r\rangle \langle r| \,, \\
&\quad - \frac{(-1)^l}{2} \sum_{r=1}^{m-2} \left( \sinh(\eta r) \sinh(\eta(r+1)) (|r+1\rangle \langle r| + |r\rangle \langle r+1|) \right).
\end{aligned} \tag{3.55}$$

The solution to the eigenvalue equation $\langle 0_L| \, \mathcal{T}_i(\varphi) = |\sinh(\varphi)|^2 \langle 0_L|$ is given by

$$\langle 0_L| = \sum_{r=0}^{m-1} (-1)^r \frac{\sin(2(m-2)\mathrm{Im}\varphi)}{2m\mathrm{Im}\varphi} \tag{3.56}$$

and it is normalized such that $\langle 0_L|0\rangle = 1$. By considering a large number of transfer matrices, we perform a projection of the auxiliary space onto the eigenvectors of $\mathcal{T}_1$ and $\mathcal{T}_2$ having an eigenvalue of 1

$$\begin{aligned}
\lim_{L\to\infty} \mathcal{T}_1^N(\varphi) &= |\sinh\varphi|^{2L} \, |0\rangle \langle 0_L| \,, \\
\lim_{L\to\infty} \mathcal{T}_2^N(\varphi) &= |\sinh\varphi|^{2L} \, |0\rangle \langle 0| \,.
\end{aligned} \tag{3.57}$$

Through a further analysis, we find that the transfer matrices $\mathcal{T}_1$ and $\mathcal{T}_2$ are related by a similarity transformation. As a result of this connection, we deduce that $||I(\varphi, s)||^2 = 0$. This means that $I(\varphi, 0)$ is not a quasilocal conserved charge. We seek to prove that the conserved quantities, defined as

$$Q(\varphi) := \frac{\partial I(\varphi, s)}{\partial s}\Big|_{s=0} \tag{3.58}$$

exhibit quasilocal characteristics. The norm of the (3.58) can be written as

$$\begin{aligned}\|Q(\varphi)\|^2 &= 2\mathrm{tr}_{\mathcal{A}\otimes\mathcal{A}}\Big\{\frac{\partial^2}{\partial s\partial\overline{s}}\mathcal{T}_1^L(\varphi)\Big\}\Big|_{s=0} - 2\mathrm{tr}_{\mathcal{A}\otimes\mathcal{A}}\Big\{\frac{\partial^2}{\partial s\partial\overline{s}}\mathcal{T}_2^L(\varphi)\Big\}\Big|_{s=0}\\ &= 2L\mathrm{tr}_{\mathcal{A}\otimes\mathcal{A}}\Big\{\mathcal{T}_1^{L-1}(\varphi)\mathcal{T}_1^{(1,1)}(\varphi) - \mathcal{T}_2^{L-1}(\varphi)\mathcal{T}_2^{(1,1)}(\varphi)\Big\}\\ &+ 2L\sum_{n=0}^{L-2}\mathrm{tr}_{\mathcal{A}\otimes\mathcal{A}}\Big\{\mathcal{T}_1^{(1,0)}(\varphi)\mathcal{T}_1^{n}(\varphi)\mathcal{T}_1^{(0,1)}(\varphi)\mathcal{T}_1^{L-2-n}(\varphi)\Big\}\\ &- 2L\sum_{n=0}^{L-2}\mathrm{tr}_{\mathcal{A}\otimes\mathcal{A}}\Big\{\mathcal{T}_2^{(1,0)}(\varphi)\mathcal{T}_2^{n}(\varphi)\mathcal{T}_2^{(0,1)}(\varphi)\mathcal{T}_2^{L-2-n}(\varphi)\Big\},\end{aligned} \tag{3.59}$$

where

$$\mathcal{T}_j^{(n,m)}(\varphi) := \frac{\partial^n}{\partial^n s}\frac{\partial^m}{\partial^m\overline{s}}\mathcal{T}_j(\varphi)\Big|_{s=0}. \tag{3.60}$$

We observe that

$$\begin{aligned}\mathcal{T}_1^{(1,0)}|0\rangle &= \mathcal{T}_1^{(0,1)}|0\rangle,\\ \mathcal{T}_2^{(1,0)}|0\rangle &= \mathcal{T}_2^{(0,1)}|0\rangle.\end{aligned} \tag{3.61}$$

These equations imply that for large $N$, the last two terms of (3.59) vanish. The other two contributions are evaluated as follows:

$$\begin{aligned}\langle 0_L|\mathcal{T}_1^{(1,1)}|0\rangle &= |\cosh\varphi|^2 - 2\frac{\sin(2(m-1)\mathrm{Im}\varphi)}{\sin(2m\mathrm{Im}\varphi)},\\ \langle 0|\mathcal{T}_2^{(1,1)}|0\rangle &= |\cosh\varphi|^2.\end{aligned} \tag{3.62}$$

Substituting these into (3.59), we obtain:

$$\frac{\|Q(\varphi)\|^2}{L} = -4|\sinh\varphi|^{2L-2}\frac{\sin(2(m-1)\mathrm{Im}\varphi)}{\sin(2m\mathrm{Im}\varphi)}. \tag{3.63}$$

Then we can conclude that $Q$ is quasilocal for $m > 1$. Upon further investigation, it is possible to show that $\langle I_p^\dagger(\varphi,s)I_p(\varphi,s)\rangle \propto L^2$, where $I_p = \frac{\partial^p}{\partial s^p}I(\varphi,s)$. Consequently, quantities with $p > 1$ do not hold significant relevance for the analysis of the spin Drude weight. The result (3.59) provides the denominator in the Mazur bound (2.69). In the following section, we compute the numerator.

## 3.3 Mazur inequality at infinite and finite temperature

Let us now investigate the quantity $|\langle \mathcal{J}_{\mathfrak{s}} Q(\varphi)\rangle|^2$, which appears as the numerator in the Mazur bound (2.69). We begin with the following calculations:

$$\begin{aligned}\langle \mathcal{J}_{\mathfrak{s}} Q(\varphi)\rangle &= 2^{-L}\mathrm{Tr}\{\mathcal{J}_{\mathfrak{s}} Q(\varphi)\}\\ &= L\mathrm{i}\sum_{\{\alpha_i\}}\frac{\partial}{\partial s}\mathrm{tr}\{A_{\alpha_1}\dots A_{\alpha_L} - A^\dagger_{\alpha_1}\dots A^\dagger_{\alpha_L}\}\big|_{s=0}\\ &\times 2^{-L}\mathrm{Tr}\{\prod_{j=1}^{L}\sigma_j^{\alpha_j}(\sigma_1^+\sigma_2^- - \sigma_1^-\sigma_2^+)\}\\ &= \frac{L\mathrm{i}}{2}\frac{\partial}{\partial s}\mathrm{tr}\{[A_-(s), A_+(s)](A_0(s))^{L-2}\}\big|_{s=0}\\ &= L\mathrm{i}(\sinh\varphi)^{L-2}\sinh(\eta).\end{aligned} \tag{3.64}$$

In the last step, the factors of $(A_0)^L$ project the auxiliary space onto $|0\rangle$.

The identification of a quantity that ensures $\langle \mathcal{J}_{\mathfrak{s}} Q(\varphi)\rangle$ is non-zero implies, based on Mazur's inequality, that the Drude weight remains finite for temperatures above zero. Now, we have all the necessary ingredients to study the spin Drude weight at $T \to \infty$. We begin by considering the following definition of the Drude weight:

$$D(T) = \lim_{t\to\infty}\lim_{N\to\infty}\frac{1}{2LT}\langle \mathcal{J}_{\mathfrak{s}}(t)\mathcal{J}_{\mathfrak{s}}(0)\rangle \geq \frac{1}{4T}\sum_n D_{Q_n}, \tag{3.65}$$

where the Mazur bound contribution from the conserved quantity $Q_n$ is

$$D_{Q_n} := \frac{2}{L}\frac{|\langle \mathcal{J}_{\mathfrak{s}} Q_n\rangle|^2}{||Q_n||^2}. \tag{3.66}$$

Note that the inequality becomes an equality when we include a complete basis of pseudo-local conserved quantities. We can use the equations (3.63) and (3.64) to obtain a lower bound for the Drude weight:

$$D_Q = \frac{1}{2}\frac{\sinh^2\eta}{\sinh^2\varphi}\frac{\sin(2m\mathrm{Im}\varphi)}{\sin(2(m-1)\mathrm{Im}\varphi)}. \tag{3.67}$$

For the special choice of $\varphi \to \frac{\pi\mathrm{i}}{2}$, this lower bound becomes

$$D_Q = \frac{\sin^2\gamma}{2}\frac{m}{m-1}, \tag{3.68}$$

which has been reported in the works of Pereira et al. [28] and Prosen [33]. Additionally, we observe that this lower bound exhibits discontinuous behavior as a function of $\Delta$.

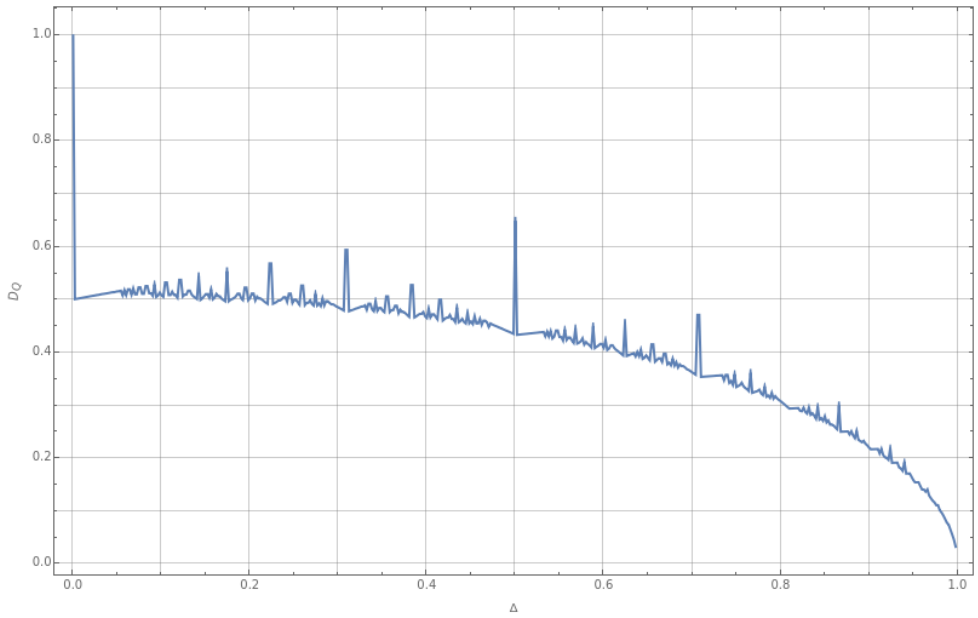



Figure 3.1: The behavior of the lower bound $D_Q(\Delta)$ for $\varphi \to \frac{\pi \mathrm{i}}{2}$ exhibits a discontinuous nature, which arises from the term $\frac{m}{m-1}$ in (3.68).

**Finite temperature.** To extend this analysis, we use the definition (3.51)

$$Q(\varphi) = (-\mathrm{i})^L \frac{\partial}{\partial s}\left[\hat{P} t_{\mathcal{A}}(\varphi, s)\hat{P} - t_{\mathcal{A}}(\varphi, s)\right] \tag{3.69}$$

and the scalar product is given by

$$\langle Q^\dagger(\varphi) Q(\varphi)\rangle = \mathfrak{A}_1\big|_{s=\bar{s}=0} + \mathfrak{A}_2\big|_{s=\bar{s}=0}, \tag{3.70}$$

where

$$\begin{aligned} \mathfrak{A}_1 &= 2\frac{\partial^2}{\partial \bar{s}\partial s}\left\langle t^\dagger_{\mathcal{A}}(\varphi, s) t_{\mathcal{A}}(\varphi, s)\right\rangle, \\ \mathfrak{A}_2 &= -2\frac{\partial^2}{\partial \bar{s}\partial s}\left\langle t^\dagger_{\mathcal{A}}(\varphi, s)\mathcal{P} t_{\mathcal{A}}(\varphi, s)\mathcal{P}\right\rangle. \end{aligned} \tag{3.71}$$

In the following sections, we present a finite-temperature formulation for calculating the Drude weight using the functions $\mathfrak{A}_1$, $\mathfrak{A}_2$, and $\langle \mathcal{J}_s Q_n\rangle$, all of which become temperature-dependent. Finally, we analyze the high-temperature limit to recover the previously obtained results.

## 3.4 Computation of $\mathfrak{A}_1\Big|_{s=\overline{s}=0}$

The calculation of the function $\mathfrak{A}_1$ can be carried out by adapting the theory presented in Section 3.1. Using the definition of the inner product, it can be expressed as:

$$\mathfrak{A}_1(\lambda) = \frac{2}{Z_L}\frac{\partial^2}{\partial\overline{s}\partial s}\mathrm{tr}_{1\dots L}\left[\mathrm{e}^{-\beta H}t^{\dagger}_{\mathcal{A}}(\varphi,s)t_{\mathcal{A}}(\varphi,s)\right]. \tag{3.72}$$

This is graphically represented in Figure 3.2. For simplicity, we will omit the lines over the indices that denote the space $1\dots N$. We are only interested in the value of $\mathfrak{A}_1(\lambda)$ in the point $\lambda \to 0$ and $s \to 0$. In the transfer quantum matrix formalism, the eigenvalue $\mathfrak{A}_1$ is given by

$$\mathfrak{A}_1(0)|_{s=\overline{s}=0} = \frac{2}{Z_L}\lim_{N\to\infty}\frac{\partial^2}{\partial\overline{s}\partial s}\mathrm{tr}_{a_1,\dots,a_N,\mathcal{A}_1,\mathcal{A}_2}\left\{(t^{1QTM}(0))^L\right\}\Big|_{s=\overline{s}=0}, \tag{3.73}$$

where the quantum transfer matrix include two additional auxiliary spaces

$$t^{1QTM}(\lambda) = \mathrm{tr}_{V_j}\left\{T_j^{1QTM}(\lambda)\right\}. \tag{3.74}$$

The quantum monodromy matrix is given by

$$\begin{aligned} T_j^{1QTM}(\lambda) &= R_{j,a_1}(\lambda-\tau)R^{t_1}_{a_2,j}(-\tau-\lambda)\dots \\ &R_{j,a_{N-1}}(\lambda-\tau)R^{t_1}_{a_N,j}(-\tau-\lambda)R_{j,a_{N+1}}(\lambda+\varphi,s)R^{\dagger_1}_{j,a_{N+2}}(\overline{\lambda}+\varphi,s), \end{aligned} \tag{3.75}$$

where $a_{N+1} = \mathcal{A}_1$ and $a_{N+2} = \mathcal{A}_2$. We seek a state that can transform the monodromy matrix $T^{1QTM}(\lambda)$ into a lower triangular form. Such a state is given by:

$$\langle 0|^1_{GS} = \left(\langle +|\otimes\langle -|\right)^{\frac{N}{2}}\otimes\langle 0|\otimes\langle m-1| \tag{3.76}$$

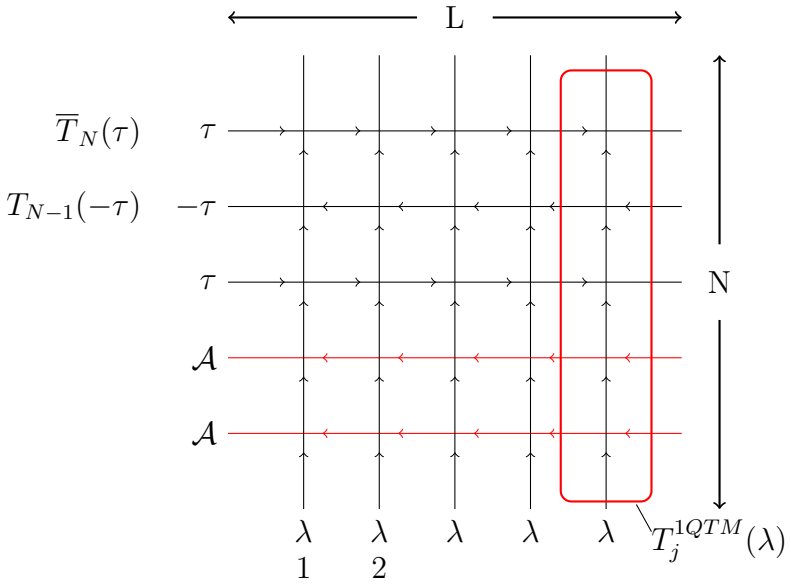



Figure 3.2: The two red lines represent the insertions of $t^\dagger_{\mathcal{A}}(\varphi,s)t_{\mathcal{A}}(\varphi,s)$.

with $\langle+| = (1,0)$ and $\langle-| = (0,1)$. Let us now examine the effect of these states on the corresponding $R$-matrices:

$$
\begin{aligned}
&\langle+|\, L(\lambda-\tau) = \langle+| \begin{pmatrix} 1 & * \\ 0 & \frac{\sinh(\lambda-\tau)}{\sinh(\lambda-\tau+\eta)} \end{pmatrix}, \\
&\langle-|\, L^{t_1}(-\tau-\lambda) = \langle-| \begin{pmatrix} \frac{\sinh(\lambda+\tau)}{\sinh(\lambda+\tau-\eta)} & * \\ 0 & 1 \end{pmatrix}, \\
&\langle 0|\, L^{\dagger_1}(\overline{\lambda}+\varphi,s) \\
&= \langle 0| \begin{pmatrix} \sinh(\lambda+\overline{\varphi}+\eta S^z_{\mathcal{A}}(\overline{s})) & -\sinh(\eta) S^+_{\mathcal{A}}(-\overline{s}) \\ -\sinh(\eta) S^-_{\mathcal{A}}(-\overline{s}) & \sinh(\lambda+\overline{\varphi}-\eta S^z_{\mathcal{A}}(s)) \end{pmatrix} \\
&= \langle 0| \begin{pmatrix} \sinh(\lambda+\overline{\varphi}+\overline{s}) & * \\ 0 & \sinh(\lambda+\overline{\varphi}-\overline{s}) \end{pmatrix}, \\
&\langle m-1|\, L(\lambda+\varphi,s) \\
&= \langle m-1| \begin{pmatrix} \sinh(\lambda+\varphi+\eta S^z_{\mathcal{A}}(s)) & \sinh(\eta) S^-_{\mathcal{A}}(s) \\ \sinh(\eta) S^+_{\mathcal{A}}(s) & \sinh(\lambda+\varphi-\eta S^z_{\mathcal{A}}(s)) \end{pmatrix} \\
&= \langle m-1|\, (-1)^l \begin{pmatrix} \sinh(\lambda+\varphi+s-\eta) & * \\ 0 & \sinh(\lambda+\varphi-s+\eta) \end{pmatrix}.
\end{aligned}
\tag{3.77}
$$

With the symbol "*", we denote values that are not relevant for our calculations. We apply the ground state to the entries of the monodromy matrix:

$$\langle 0|^1_{GS}\, A(\lambda) = a(\lambda)\, \langle 0|^1_{GS}\,, \quad \langle 0|^1_{GS}\, D(\lambda) = d(\lambda)\, \langle 0|^1_{GS}\,, \quad \langle 0|^1_{GS}\, B(\lambda) = 0 \tag{3.78}$$

furthermore, with the use of (3.77), we obtain

$$\begin{aligned} a(\lambda) &= (-1)^l \Big(\frac{\sinh(\lambda+\tau)}{\sinh(\lambda+\tau-\eta)}\Big)^{\frac{N}{2}} \sinh(\lambda+\varphi+s-\eta)\sinh(\lambda+\overline{\varphi}+\overline{s}), \\ d(\lambda) &= (-1)^l \Big(\frac{\sinh(\lambda-\tau)}{\sinh(\lambda-\tau+\eta)}\Big)^{\frac{N}{2}} \sinh(\lambda+\varphi-s+\eta)\sinh(\lambda+\overline{\varphi}-\overline{s}). \end{aligned} \tag{3.79}$$

From the $RTT$-equations, we derive the following relations for the entries of the monodromy matrix:

$$\begin{aligned} C(\mu)A(\lambda) &= \frac{1}{b(\mu-\lambda)} A(\lambda)C(\mu) - \frac{c(\mu-\lambda)}{b(\mu-\lambda)} A(\mu)C(\lambda), \\ C(\mu)D(\lambda) &= \frac{1}{b(\mu-\lambda)} D(\lambda)C(\mu) - \frac{c(\mu-\lambda)}{b(\mu-\lambda)} D(\mu)C(\lambda), \\ [C(\lambda), C(\mu)] &= 0. \end{aligned} \tag{3.80}$$

Now we apply the reference state to the quantum transfer matrix:

$$\begin{aligned} &\langle\{\lambda\}^K_{j=0}|\, t^{1QTM}(\lambda) = \langle 0|_{GS} \prod_{j=1}^{K} C(\lambda_j)\big[A(\lambda)+D(\lambda)\big] \\ &= \langle 0|_{GS} \Big\{ \big[a(\lambda)\prod_{j=1}^{K}\frac{1}{b(\lambda_j-\lambda)} + d(\lambda)\prod_{j=1}^{K}\frac{1}{b(\lambda-\lambda_j)}\big]\prod_{j=1}^{K} C(\lambda_j) \\ &- \sum_{j=1}^{K}\Big(a(\lambda_j)\frac{c(\lambda_j-\lambda)}{b(\lambda_j-\lambda)}\prod_{\substack{k=1\\k\neq j}}^{K}\frac{1}{b(\lambda_k-\lambda_j)} \\ &+ d(\lambda_j)\frac{c(\lambda-\lambda_j)}{b(\lambda-\lambda_j)}\prod_{\substack{k=1\\k\neq j}}^{K}\frac{1}{b(\lambda_j-\lambda_k)}\Big) C(\lambda)\prod_{\substack{k=1\\k\neq j}}^{K} C(\lambda_k)\Big\}. \end{aligned} \tag{3.81}$$

The second line in this expression corresponds to the desired eigenvalue contribution, while the third and the fourth lines, involving the sum over $j$, must vanish for the state to be an eigenstate.

By imposing that the coefficients of the unwanted terms vanish, i.e., by setting the third and fourth lines of (3.81) to zero, we obtain the Bethe Ansatz equations for the

rapidities $\{\lambda_j\}$:

$$\frac{d(\lambda_j)}{a(\lambda_j)} = \prod_{\substack{k=1 \\ k\neq j}}^{K} \frac{\sinh(\lambda_j - \lambda_k - \eta)}{\sinh(\lambda_j - \lambda_k + \eta)}, \qquad j = 1 \dots K. \tag{3.82}$$

The largest eigenvalue $\Lambda_1(\lambda)$ of $t^{1QTM}(\lambda)$ is given by:

$$\Lambda_1(\lambda) = a(\lambda)\frac{Q(\lambda-\eta)}{Q(\lambda)} + d(\lambda)\frac{Q(\lambda+\eta)}{Q(\lambda)}. \tag{3.83}$$

To determine the parameter $K$, we analyze (3.83) at $T \to \infty$ and for $s = 0$. The analyticity requirement of the eigenvalue enforces its structure to be:

$$\Lambda_1(\lambda) = (-1)^l c \sinh(\lambda - a)\sinh(\lambda - b). \tag{3.84}$$

Moreover, according to Pereira, et al., we obtain:

$$\Lambda_1(0) = 2\sinh(\varphi)\sinh(\overline{\varphi}). \tag{3.85}$$

As a result, we conclude that $a = -\varphi$, $b = -\overline{\varphi}$, and $c = 2(-1)^l$. We now put (3.83) into the following form:

$$\Lambda_1(\lambda) = (-1)^l \frac{\sinh(\lambda+\overline{\varphi})}{Q(\lambda)}\big(q(\lambda-\eta) + q(\lambda+\eta)\big), \tag{3.86}$$

where

$$q(\lambda) = \sinh(\lambda+\varphi)\prod_{j=1}^{K}\sinh(\lambda-\lambda_j). \tag{3.87}$$

By requiring (3.85) to satisfy (3.86), we find that the following equation must hold:

$$2(-1)^l q(\lambda) = q(\lambda+\eta) + q(\lambda-\eta). \tag{3.88}$$

The solution to this equation is given by:

$$q(\lambda) = \sinh(m(\lambda+\varphi)). \tag{3.89}$$

From this, we can deduce that the system contains $K = N/2 + m - 1$ Bethe Ansatz roots $\lambda_j$. We define $Q(\lambda) = Q_T(\lambda)Q_s(\lambda)$ where

$$Q_T(\lambda) = \prod_{j=1}^{N/2}\sinh(\lambda-\lambda_k), \qquad Q_s(\lambda) = \prod_{j=1}^{m-1}\sinh(\lambda-\mu_k) \tag{3.90}$$

and $\mu_k|_{s=0,\lambda=0} = \mu_k^0 = -\varphi + k\eta$ with $k = 1 \dots m-1$. From this, we can obtain Bethe Ansatz equations for calculating $\mathfrak{A}_1$. These equations will be used to derive nonlinear integral equations in the form of TBA equations in Sections 3.6 and 3.7.

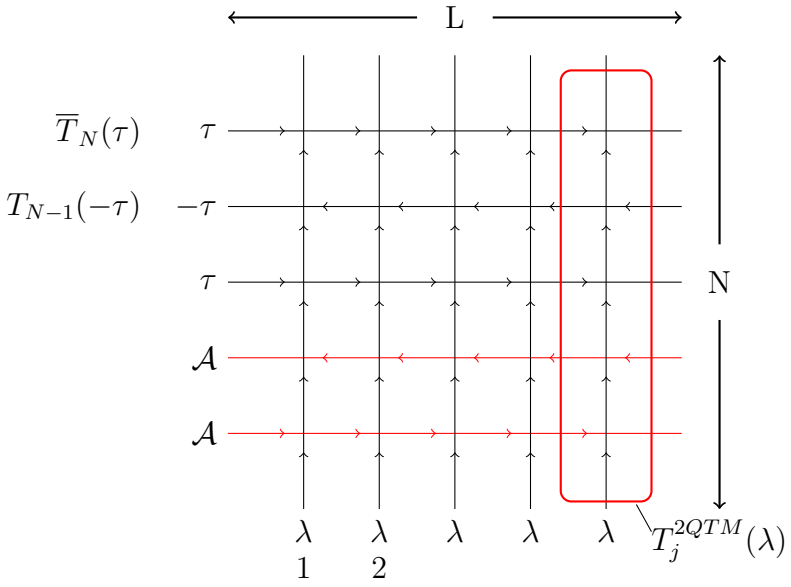



Figure 3.3: The two red lines represent the insertions of $t^\dagger_{\mathcal{A}}(\varphi,s)\mathcal{P}t_{\mathcal{A}}(\varphi,s)\mathcal{P}$.

## 3.5 Computation of $\mathfrak{A}_2\big|_{s=\overline{s}=0}$

To compute the function $\mathfrak{A}_2$, we employ a similar approach as for $\mathfrak{A}_1$. We begin our calculation by introducing the following definition:

$$\mathfrak{A}_2(\lambda) = -\frac{2}{Z_L}\frac{\partial^2}{\partial\overline{s}\partial s}\mathrm{tr}_{1\dots L}\left[\mathrm{e}^{-\beta H}t^\dagger_{\mathcal{A}}(\varphi,s)\mathcal{P}t_{\mathcal{A}}(\varphi,s)\mathcal{P}\right]. \tag{3.91}$$

Within the framework of the quantum matrix formalism, the operator $\mathfrak{A}_2$ at $\lambda = 0$ is given by the following expression:

$$\mathfrak{A}_2(0)|_{s=\overline{s}=0} = -\frac{2}{Z_L}\lim_{N\to\infty}\frac{\partial^2}{\partial\overline{s}\partial s}\mathrm{tr}_{a_1,\dots,a_N,\mathcal{A}_1,\mathcal{A}_2}\left\{(t^{2QTM}(0))^L\right\}\Big|_{s=\overline{s}=0}. \tag{3.92}$$

Similar to before, the transfer matrix is defined through a trace:

$$t^{2QTM}(\lambda) = \mathrm{tr}_{V_j}\{T_j^{2QTM}(\lambda)\}. \tag{3.93}$$

Then we consider the quantum monodromy matrix, expressed in terms of $R$-matrices, defined as

$$\begin{aligned} T_j^{2QTM}(\lambda) = {} & R_{j,a_1}(\lambda-\tau)R^{t_1}_{a_2,j}(-\tau-\lambda)\dots \\ & R_{j,a_{M-1}}(\lambda-\tau)R^{t_1}_{a_M,j}(-\tau-\lambda)R_{j,a_{M+1}}(\lambda+\varphi,s)R^\dagger_{j,a_{M+2}}(-\overline{\lambda}+\varphi,s), \end{aligned} \tag{3.94}$$

where the last two $R-$matrices correspond to the insertions visible in the Figure 3.3. The ground state

$$|0\rangle_{GS}^2 = (|-\rangle \otimes |+\rangle)^{\frac{N}{2}} \otimes |0\rangle \otimes |0\rangle \tag{3.95}$$

makes the monodromy matrix lower triangular matrix. We apply it on the $L$-matrices

$$\begin{aligned}
L(\lambda-\tau)\,|-\rangle &= \begin{pmatrix} \frac{\sinh(\lambda-\tau)}{\sinh(\lambda-\tau+\eta)} & 0 \\ * & 1 \end{pmatrix} |-\rangle\,, \\
L(-\tau-\lambda)\,|+\rangle &= \begin{pmatrix} 1 & 0 \\ * & \frac{\sinh(\lambda+\tau)}{\sinh(\lambda+\tau-\eta)} \end{pmatrix} |+\rangle\,, \\
L(\lambda+\varphi,s)\,|0\rangle &= \begin{pmatrix} \sinh(\lambda+\varphi+s) & 0 \\ * & \sinh(\lambda+\varphi-s) \end{pmatrix} |0\rangle\,, \\
L^{\dagger}(-\overline{\lambda}+\varphi,s)\,|0\rangle &= \begin{pmatrix} -\sinh(\lambda-\overline{\varphi}-\overline{s}) & 0 \\ * & -\sinh(\lambda-\overline{\varphi}+\overline{s}) \end{pmatrix} |0\rangle\,.
\end{aligned} \tag{3.96}$$

Now, we can use these results to compute $A(\lambda)\,|0\rangle_{GS}^2 = a(\lambda)\,|0\rangle_{GS}^2$ and $D(\lambda)\,|0\rangle_{GS}^2 = d(\lambda)\,|0\rangle_{GS}^2$. Thus, we obtain:

$$\begin{aligned}
a(\lambda) &= \Big(\frac{\sinh(\lambda-\tau)}{\sinh(\lambda-\tau+\eta)}\Big)^{\frac{N}{2}} \sinh(\lambda+\varphi+s)\sinh(-\lambda+\overline{\varphi}+\overline{s}), \\
d(\lambda) &= \Big(\frac{\sinh(\lambda+\tau)}{\sinh(\lambda+\tau-\eta)}\Big)^{\frac{N}{2}} \sinh(\lambda+\varphi-s)\sinh(-\lambda+\overline{\varphi}-\overline{s}).
\end{aligned} \tag{3.97}$$

Using the $RTT$-relations:

$$\begin{aligned}
A(\lambda)C(\mu) &= \frac{1}{b(\lambda-\mu)}C(\mu)A(\lambda) - \frac{c(\lambda-\mu)}{b(\lambda-\mu)}C(\lambda)A(\mu), \\
D(\lambda)C(\mu) &= \frac{1}{b(\mu-\lambda)}C(\mu)D(\lambda) - \frac{c(\mu-\lambda)}{b(\mu-\lambda)}C(\lambda)D(\mu)
\end{aligned} \tag{3.98}$$

and the eigenvalue problem:

$$t^{2QTM}(\lambda)\,|\{\lambda\}_{j=1}^K\rangle = \Lambda_2(\lambda,\lambda_j)\,|\{\lambda\}_{j=1}^K\rangle \tag{3.99}$$

we can find the largest eigenvalue of $t^{2QTM}(\lambda)$

$$\Lambda_2(\lambda) = a(\lambda)\frac{Q(\lambda+\eta)}{Q(\lambda)} + d(\lambda)\frac{Q(\lambda-\eta)}{Q(\lambda)}, \tag{3.100}$$

where

$$Q(\lambda) = \prod_{j=1}^{K} \sinh(\lambda-\lambda_j). \tag{3.101}$$

The roots $\lambda_j$ satisfy the Bethe ansatz equations

$$\frac{d(\lambda_j)}{a(\lambda_j)} = \prod_{\substack{k=1 \\ k\neq j}}^{K} \frac{\sinh(\lambda_j - \lambda_k - \eta)}{\sinh(\lambda_j - \lambda_k + \eta)}, \qquad j = 1 \dots K. \tag{3.102}$$

To determine the number of Bethe roots $K$, we consider the largest eigenvalue (3.100) in the limit as $T \to \infty$ and $s = 0$:

$$\Lambda_2(\lambda) = \sinh(\lambda + \varphi)\sinh(-\lambda + \overline{\varphi})\frac{Q(\lambda + \eta)}{Q(\lambda)} + \sinh(\lambda + \varphi)\sinh(-\lambda + \overline{\varphi})\frac{Q(\lambda - \eta)}{Q(\lambda)} \tag{3.103}$$

and compare it with the expression provided by Pereira et al. $\Lambda_2(0) = -2|\sinh\varphi|^2$. We then obtain the following result:

$$2\prod_{j=1}^{K}\sinh(\lambda - \lambda_j) = \prod_{j=1}^{K}\sinh(\lambda - \lambda_j - \eta) + \prod_{j=1}^{K}\sinh(\lambda - \lambda_j + \eta). \tag{3.104}$$

This equation is satisfied for $K = 0$. For finite temperature and $s$, we find that $K = \frac{N}{2}$. To compute the largest eigenvalues as given by (3.83) and (3.100), we need to solve the Bethe-Ansatz equations (3.82) and (3.102). Solving these equations is feasible by use of the NLIEs for two auxiliary functions and root distribution close to the real axis, we derive alternative nonlinear integral equations in the form of TBA equations in Sections 3.6 and 3.7.

## 3.6 $T$-, $Y$-systems

In order to avoid the formidable challenge of directly solving the Bethe-Ansatz equations, especially when dealing with larger system sizes, we employ the concept of $T$- and $Y$-systems [34]. These systems provide functional relations for the transfer matrices $T_n(\lambda)$ and certain combinations thereof $Y_n(\lambda)$. These $T$- and $Y$-systems can be manipulated and transformed into non-linear integral equations, which can be solved numerically. The advantage of the non-linear equations lies in their independence from the Bethe ansatz roots, and their computational complexity does not increase with the system size.

The function $T_1(\lambda)$ corresponds to the previously introduced transfer matrix, while $T_n(\lambda)$, where $n > 1$, represents higher spin transfer matrices. Let us begin by presenting the standard description of $T$- and $Y$-systems, and in the subsequent sections, we will adapt this description to compute the largest eigenvalues as given in equations (3.83) and (3.100). The expressions for the $T_n(\lambda)$ functions are given as:

$$T_n(\lambda) := \sum_{k=1}^{n+1}\psi(\lambda + \frac{\eta}{2}(2k - n - 2))\frac{Q(\lambda + \frac{\eta}{2}(n+1))Q(\lambda - \frac{\eta}{2}(n+1))}{Q(\lambda + \frac{\eta}{2}(2k - n - 3))Q(\lambda + \frac{\eta}{2}(2k - n - 1))}. \tag{3.105}$$

The functions $Q(\lambda)$ and $\psi(\lambda)$ are defined as:

$$\begin{aligned} Q(\lambda) &= \prod_{j=1}^{\frac{N}{2}} \sinh(\lambda - \lambda_j), \\ \psi(\lambda) &= \big(\sinh(\lambda - \tau + \frac{\eta}{2}) \sinh(\lambda + \tau - \frac{\eta}{2})\big)^{\frac{N}{2}}. \end{aligned} \tag{3.106}$$

The values of $\lambda_j$ satisfy the Bethe-Ansatz equations, or equivalently, $T_1(\lambda_j) = 0$. Notably, the function $Q(\lambda)$ exhibits the periodicity property $Q(\lambda + \eta\nu) = (-1)^m Q(\lambda)$. Note that $T_0(\lambda) = \psi(\lambda)$.

Now, let us return to the definition of the anisotropy $\Delta$:

$$\Delta = \cos\theta, \quad \theta = \frac{\nu}{\pi}. \tag{3.107}$$

The functional relations for the $T$- and $Y$-systems hold only for rational values of $\nu$. To express $\nu$ in terms of its continued fraction expansion, we write:

$$\nu = \nu_1 + \cfrac{1}{\nu_2 + \cfrac{1}{\ddots \cfrac{}{\nu_{\alpha-1} + \cfrac{1}{\nu_\alpha}}}}, \tag{3.108}$$

where $\nu_i$ are positive integers. In this chapter, we focus on the "simple root of unity", i.e., we set $\nu = \nu_1$.

The $T$-system satisfies

$$T_n(\lambda + \frac{\eta}{2}) T_n(\lambda - \frac{\eta}{2}) = T_{n+1}(\lambda) T_{n-1}(\lambda) + T_0(\lambda + \frac{\eta}{2}(n+1)) T_0(\lambda - \frac{\eta}{2}(n+1)) \tag{3.109}$$

for any $\lambda \in \mathbb{C}$ and

$$T_\nu(\lambda) = T_{\nu-2}(\lambda) + 2(-1)^{-\frac{N}{2}} T_0(\lambda + \frac{\eta}{2}\nu). \tag{3.110}$$

For $1 \le j \le \nu - 2$, we define the $Y$-functions:

$$\begin{aligned} Y_j(\lambda) &= \frac{T_{j+1}(\lambda) T_{j-1}(\lambda)}{T_0(\lambda + \frac{\eta}{2}(j+1)) T_0(\lambda - \frac{\eta}{2}(j+1))}, \\ 1 + Y_j(\lambda) &= \frac{T_j(\lambda + \frac{\eta}{2}) T_j(\lambda - \frac{\eta}{2})}{T_0(\lambda + \frac{\eta}{2}(j+1)) T_0(\lambda - \frac{\eta}{2}(j+1))}, \\ K(\lambda) &= (-1)^m \frac{T_{\nu-2}(\lambda)}{T_0(\lambda + \frac{\eta}{2}\nu)}, \end{aligned} \tag{3.111}$$

which satisfy the $Y$-system

$$\begin{aligned} &Y_j(\lambda+\frac{\eta}{2})Y_j(\lambda-\frac{\eta}{2}) = (1+Y_{j-1}(\lambda))(1+Y_{j+1}(\lambda)),\\ &1+Y_{\nu-1}(\lambda) = (1+K(\lambda))^2,\\ &K(\lambda+\frac{\eta}{2})K(\lambda-\frac{\eta}{2}) = 1+Y_{\nu-2}(\lambda) \end{aligned} \tag{3.112}$$

for $1 \leq j \leq \nu-2$. For convenience, we set $T_{-1}(\lambda)=0$ and $Y_0(\lambda)=0$.

To compute the $Y$-functions, we transform the function equations (3.112) into non-linear integral equations. To begin, we examine the presence of singularities in the (3.112) for $j=1$. From the left-hand side, we observe that we need to consider the singularities of $Y_1(\lambda)$ within the interval $[-\frac{\eta}{2},\frac{\eta}{2}]$, which is referred to as the "physical strip". To address this, we analyze (3.111) for $j=1$ and obtain the following expression:

$$\begin{aligned} Y_1(v) = &\left(\frac{\sinh(\lambda-\tau+\frac{\eta}{2})\sinh(\lambda+\tau-\frac{\eta}{2})}{\sinh(\lambda+\tau+\frac{\eta}{2})\sinh(\lambda-\tau-\frac{\eta}{2})}\right)^{\frac{N}{2}}\\ &\times\frac{T_2(v)}{\left(\sinh(\lambda-\tau+\frac{3}{2}\eta)\sinh(\lambda+\tau-\frac{3}{2}\eta)\right)^{\frac{N}{2}}}. \end{aligned} \tag{3.113}$$

The singularities within the physical strip are found within the first parentheses on the right-hand side, and they can be summarized as follows:

- $\lambda_z = \pm\tau \mp \frac{\eta}{2}$ zeros of order $\frac{N}{2}$,
- $\lambda_p = \pm\tau \pm \frac{\eta}{2}$ poles of order $\frac{N}{2}$.

We call the positions of zeroes $\lambda_z$ and the positions of poles $\lambda_p$. Let us proceed by defining Y-functions that are free of singularities:

$$\overline{Y}_1(\lambda) = \left(\frac{\tanh\frac{\pi\mathrm{i}}{2\eta}(\lambda+\tau+\frac{\eta}{2})}{\tanh\frac{\pi\mathrm{i}}{2\eta}(\lambda-\tau+\frac{\eta}{2})}\right)^{\frac{N}{2}} Y_1(\lambda), \tag{3.114}$$

which satisfy:

$$\overline{Y}_1(\lambda+\frac{\eta}{2})\overline{Y}_1(\lambda-\frac{\eta}{2}) = Y_1(\lambda+\frac{\eta}{2})Y_1(\lambda-\frac{\eta}{2}). \tag{3.115}$$

Here, we used the property of the hyperbolic tangent $\tanh(\lambda+\frac{\pi}{4}\mathrm{i})\tanh(\lambda-\frac{\pi}{4}\mathrm{i})=1$.

Now, keeping in mind the following definition of the Fourier transform:

$$\begin{aligned} \mathcal{F}[f(x)](k) &= \int_{-\infty}^{\infty} f(x)\mathrm{e}^{-\mathrm{i}kx}\mathrm{d}x,\\ \mathcal{F}^{-1}[f(k)](x) &= \frac{1}{2\pi}\int_{-\infty}^{\infty} f(k)\mathrm{e}^{\mathrm{i}kx}\mathrm{d}k \end{aligned} \tag{3.116}$$

and the property:

$$\mathcal{F}\left[f(x+\frac{\eta}{2})\right](k) = \mathrm{e}^{\mathrm{i}k\frac{\eta}{2}}\mathcal{F}\left[f(x)\right](k) \tag{3.117}$$

which holds for functions with a physical strip free of singularities, we apply the logarithm to (3.112) and the Fourier transform, and we get:

$$\log\mathcal{F}\left[\overline{Y}_1(\lambda+\frac{\eta}{2})\overline{Y}_1(\lambda-\frac{\eta}{2})\right] = 2\cosh(k)\mathcal{F}\left[\log\overline{Y}_1(\lambda)\right] = \mathcal{F}\left[\log(1+Y_2(\lambda))\right]. \tag{3.118}$$

After using (3.114) and performing the inverse Fourier transformation, we obtain the non-linear equation for $Y_1(\lambda)$. The same procedure is employed to find $Y_j(\lambda)$ with $j>1$ and for $K(\lambda)$. Here, we notice that there are no singularities that produce a driving term.

Finally, we obtain the non-linear integral equations for the $Y$'s:

$$\begin{aligned}
&\log Y_j(\lambda) = p_j(\lambda) + \sum_{l=1}^{\nu-1} s_{jl} * \log(1+Y_l)[\lambda] \quad \text{for } j=1,\dots,\nu-2,\\
&\log(1+Y_{\nu-1}(\lambda)) = 2\log(1+K(\lambda)),\\
&\log K(\lambda) = s*\log(1+Y_{\nu-2})[\lambda]
\end{aligned} \tag{3.119}$$

with the driving term:

$$p_j(\lambda) = \delta_{j,1}\frac{N}{2}\log\frac{\tanh\frac{\pi\mathrm{i}}{2\eta}(\lambda-\tau+\frac{\eta}{2})}{\tanh\frac{\pi\mathrm{i}}{2\eta}(\lambda+\tau+\frac{\eta}{2})} \tag{3.120}$$

and the kernel:

$$s_{jl}(\lambda) = (\delta_{j-1,l}+\delta_{j+1,l})s(\lambda). \tag{3.121}$$

If we assume the Trotter limit $N\to\infty$ to hold, and $\tau=\beta/N$, we get

$$p_j(\lambda) = -\delta_{j,1}\frac{\beta\pi\mathrm{i}}{\eta\sinh(\frac{\pi\mathrm{i}}{\eta}(\lambda+\frac{\eta}{2}))}. \tag{3.122}$$

The symbol $*$ denotes convolution, and the function $s(\lambda)$ is defined as:

$$s(\lambda) = \frac{\nu}{2\pi\cosh(\nu\lambda)}. \tag{3.123}$$

To calculate the largest eigenvalue, we consider the functional relation:

$$T_1(\lambda+\frac{\eta}{2})T_1(\lambda-\frac{\eta}{2}) = T_0(\lambda+\eta)T_0(\lambda-\eta)(1+Y_1(\lambda)). \tag{3.124}$$

This relation is free of singularities in the physical strip, allowing us to safely take the logarithm and apply Fourier transforms. As a result, we obtain the following formula:

$$\begin{aligned}
\log T_1(\lambda) =& s*\frac{\eta}{2}\log\Big(\sinh(\lambda+\tau+\frac{\eta}{2})\sinh(\lambda-\tau-\frac{\eta}{2})\\
&\times\sinh(\lambda+\tau-\frac{3}{2}\eta)\sinh(\lambda-\tau+\frac{3}{2}\eta)\Big) + s*\log(1+Y_1)[\lambda].
\end{aligned} \tag{3.125}$$

The non-linear integral equations (3.119) can be solved by numerical means, often using an iterative approach. Then we can inserte the $Y_1(\lambda)$ into (3.125) to compute $T_1(\lambda)$.

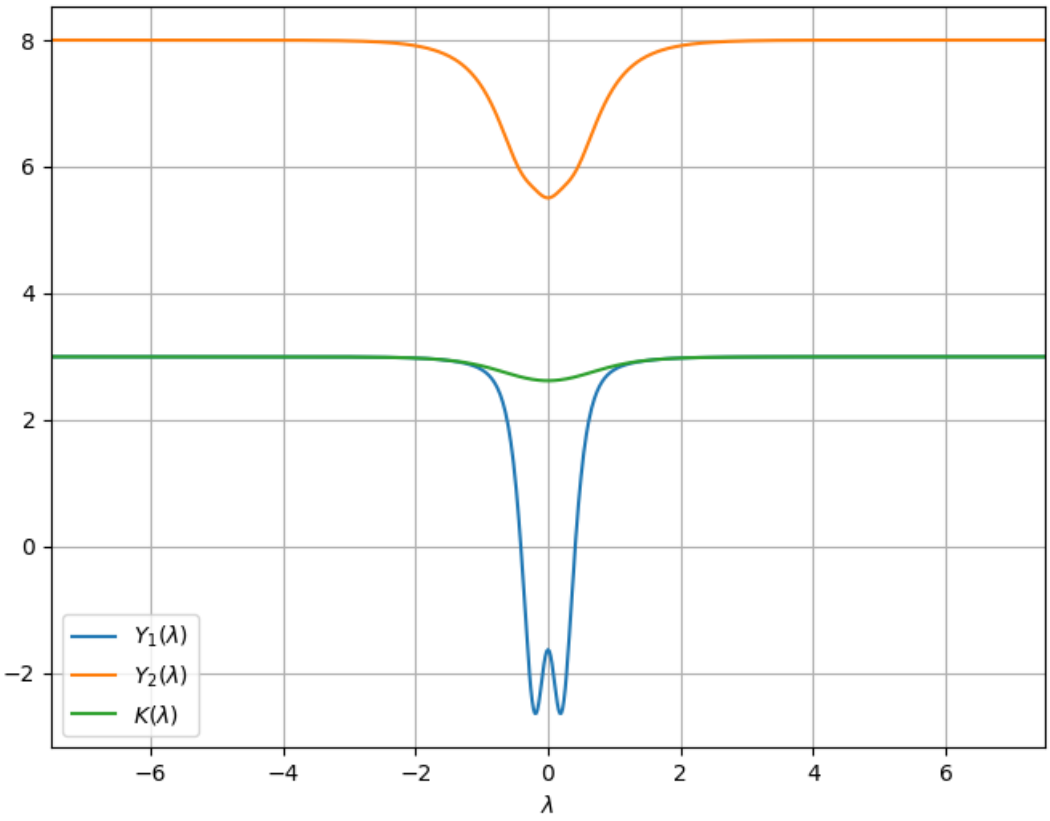



Figure 3.4: The behavior of $Y_1(\lambda)$, $Y_2(\lambda)$, and $K(\lambda)$ in the case of $\nu = 4$ and $\beta = 1$. In general, the $Y$-functions exhibit asymptotic behavior, where $Y_j(\pm\infty) = j(j+2)$ for $j = \nu - 2$, and $K(\pm\infty) = \nu - 1$.

## 3.7 Modified $T$-, $Y$-systems

In order to use the $T$- and $Y$-system formalism for the calculation of the eigenvalues $\Lambda_1(\lambda)$ and $\Lambda_2(\lambda)$, certain modifications are necessary. Specifically, we introduce modified $T$-functions denoted with a tilde on top, as follows:

$$\widetilde{T}_j(\lambda) = \prod_{\gamma=1}^{j} \frac{l(\lambda - \frac{\eta}{2}(2\gamma - j))}{\psi(\lambda - \frac{\eta}{2} j)} T_j(\lambda). \tag{3.126}$$

Here, it is important to note that $\psi(\lambda)$ is not the same function as the one in (3.106), but rather an unknown function defined by the relation:

$$\frac{\psi(\lambda + \frac{\eta}{2})}{\psi(\lambda - \frac{\eta}{2})} = \frac{r(\lambda + \frac{\eta}{2})}{l(\lambda - \frac{\eta}{2})}. \tag{3.127}$$

On the other hand, the functions $l(\lambda)$ and $r(\lambda)$ are known functions that vary from $\Lambda_1(\lambda)$ to $\Lambda_2(\lambda)$. It is worth mentioning that from (3.126), we can see that $\widetilde{T}_0(\lambda) = 1$.

The equations (3.126) can also be expressed as:

$$\begin{aligned} \widetilde{T}_n(\lambda) = &\prod_{\gamma=1}^{n+1} \prod_{i=1}^{n-\gamma+1} \prod_{j=1}^{\gamma-1} l(\lambda - \frac{\eta}{2}(2i - n)) r(\lambda + \frac{\eta}{2}(2j - n)) \\ &\times \frac{Q\left(\lambda + \frac{\eta}{2}(n+1)\right) Q\left(\lambda - \frac{\eta}{2}(n+1)\right)}{Q\left(\lambda + \frac{\eta}{2}(2\gamma - n - 3)\right) Q\left(\lambda + \frac{\eta}{2}(2\gamma - n - 1)\right)}. \end{aligned} \tag{3.128}$$

This formula can be easily verified using the chain rule for (3.127). For instance:

$$\frac{\psi(\lambda + \frac{\eta}{2})}{\psi(\lambda - \frac{3}{2}\eta)} = \frac{\psi(\lambda + \frac{\eta}{2})}{\psi(\lambda - \frac{\eta}{2})} \frac{\psi(\lambda - \frac{\eta}{2})}{\psi(\lambda - \frac{3}{2}\eta)} = \frac{r(\lambda + \frac{\eta}{2})}{l(\lambda - \frac{\eta}{2})} \frac{r(\lambda - \frac{\eta}{2})}{l(\lambda - \frac{3}{2}\eta)}. \tag{3.129}$$

The functions $T_n(\lambda)$ satisfy the relations (3.109) and (3.110). Now, we want to define $Y_j(\lambda)$ and $K(\lambda)$ starting from $\widetilde{T}_j(\lambda)$. To create a consistent $Y$-system instead of $K(\lambda)$, we introduce two functions called $K^+(\lambda)$ and $K^-(\lambda)$. This is defined as follows:

$$\begin{aligned} Y_j(\lambda) &= \frac{\widetilde{T}_{j+1}(\lambda)\widetilde{T}_{j-1}(\lambda)}{\prod_{\gamma=1}^{j} r(\lambda + \frac{\eta}{2}(2\gamma - j + 1)) l(\lambda - \frac{\eta}{2}(2\gamma - j + 1))}, \\ 1 + Y_j(\lambda) &= \frac{\widetilde{T}_j(\lambda + \frac{\eta}{2})\widetilde{T}_j(\lambda - \frac{\eta}{2})}{\prod_{\gamma=1}^{j} r(\lambda + \frac{\eta}{2}(2\gamma - j + 1)) l(\lambda - \frac{\eta}{2}(2\gamma - j + 1))}, \\ K^+(\lambda) &= (-1)^t \frac{T_{\nu-2}(\lambda)}{\prod_{\gamma=1}^{\nu-2} r(\lambda + \frac{\eta}{2}(\nu - 2\gamma))}, \\ K^-(\lambda) &= (-1)^t \frac{T_{\nu-2}(\lambda)}{\prod_{\gamma=1}^{\nu-2} l(\lambda - \frac{\eta}{2}(\nu - 2\gamma))}, \end{aligned} \tag{3.130}$$

where $t = \frac{N}{2} + m - 1$ for $\Lambda_1(\lambda)$ and $t = \frac{N}{2}$ for $\Lambda_2(\lambda)$.

The modified $T$-functions satisfy the following relation:

$$\begin{aligned}
&\widetilde{T}_j(\lambda + \frac{\eta}{2})\widetilde{T}_j(\lambda - \frac{\eta}{2}) = \\
&= \prod_{\gamma=1}^{j} r(\lambda + \frac{\eta}{2}(2\gamma - j + 1))l(\lambda - \frac{\eta}{2}(2\gamma - j + 1)) + \widetilde{T}_{j+1}(\lambda)\widetilde{T}_{j-1}(\lambda) \\
&= \prod_{\gamma=1}^{j} r(\lambda + \frac{\eta}{2}(2\gamma - j + 1))l(\lambda - \frac{\eta}{2}(2\gamma - j + 1))\big(1 + Y_j(\lambda)\big)
\end{aligned} \tag{3.131}$$

and

$$\begin{aligned}
T_\nu(\lambda) &= r(\lambda - \frac{\eta}{2}(\nu - 2))l(\lambda + \frac{\eta}{2}(\nu - 2))T_{\nu-2}(\lambda) \\
&\quad + (-1)^t \prod_{\gamma=1}^{\nu} r(\lambda - \frac{\eta}{2}(\nu - 2\gamma)) + (-1)^t \prod_{\gamma=1}^{\nu} l(\lambda + \frac{\eta}{2}(\nu - 2\gamma)).
\end{aligned} \tag{3.132}$$

The $Y$-system for $1 \le j \le \nu - 2$, is given by

$$\begin{aligned}
&Y_j(\lambda + \frac{\eta}{2})Y_j(\lambda - \frac{\eta}{2}) = (1 + Y_{j-1}(\lambda))(1 + Y_{j+1}(\lambda)), \\
&1 + Y_{\nu-1}(\lambda) = 1 + \alpha^+(\lambda)K^+(\lambda) + \alpha^-(\lambda)K^-(\lambda) + \beta(\lambda)K^+(\lambda)K^-(\lambda), \\
&K^+(\lambda + \frac{\eta}{2})K^-(\lambda - \frac{\eta}{2}) = 1 + Y_{\nu-2}(\lambda),
\end{aligned} \tag{3.133}$$

where

$$\begin{aligned}
&\alpha^+(\lambda) = \frac{l(\lambda + \frac{\eta}{2}(\nu - 2))}{r(\lambda + \frac{\eta}{2}\nu)}, \qquad \alpha^-(\lambda) = \frac{r(\lambda - \frac{\eta}{2}(\nu - 2))}{l(\lambda - \frac{\eta}{2}\nu)}, \\
&\beta(\lambda) = \alpha^+(\lambda)\alpha^-(\lambda).
\end{aligned} \tag{3.134}$$

The functions $K^+(\lambda)$ and $K^-(\lambda)$ are related as follows:

$$K^+(\lambda) = \prod_{\gamma=1}^{\nu-2} \frac{l(\lambda - \frac{\eta}{2}(\nu - 2\gamma))}{r(\lambda + \frac{\eta}{2}(\nu - 2\gamma))} K^-(\lambda). \tag{3.135}$$

This relationship allows us to obtain:

$$\begin{aligned}
K^+(\lambda + \frac{\eta}{2})K^+(\lambda - \frac{\eta}{2}) &= \prod_{\gamma=1}^{\nu-2} \frac{l(\lambda - \frac{\eta}{2}(\nu - 2\gamma + 1))}{r(\lambda + \frac{\eta}{2}(\nu - 2\gamma - 1))}(1 + Y_{\nu-2}(\lambda)), \\
K^-(\lambda + \frac{\eta}{2})K^-(\lambda - \frac{\eta}{2}) &= \prod_{\gamma=1}^{\nu-2} \frac{r(\lambda + \frac{\eta}{2}(\nu - 2\gamma + 1))}{l(\lambda - \frac{\eta}{2}(\nu - 2\gamma - 1))}(1 + Y_{\nu-2}(\lambda)).
\end{aligned} \tag{3.136}$$

Now, we have all the ingredients to formulate the non-linear integral equations. After applying the procedure explained in the previous section, we obtain the following set of equations:

$$\begin{aligned}
&\log Y_j(\lambda) = p_j(\lambda) + d_j(\lambda) + \sum_{l=1}^{\nu-1} s_{jl} * \log(1+Y_l)[\lambda] \quad \text{for } j = 1, \dots, \nu-2, \\
&\log(1+Y_{\nu-1}(\lambda)) = \log(1+\alpha^+(\lambda))K^+(\lambda) + \alpha^-(\lambda))K^-(\lambda) + \beta(\lambda)K^+(\lambda)K^-(\lambda), \\
&\log K^+(\lambda) = d_k^+(\lambda) + \sum_{\gamma=1}^{\nu-2} \log\left(\frac{l(\lambda - \frac{\eta}{2}(\nu-2\gamma+1))}{r(\lambda+\frac{\eta}{2}(\nu-2\gamma-1))}\right) + s * \log(1+Y_{\nu-2}(\lambda)), \\
&\log K^-(\lambda) = d_k^-(\lambda) + \sum_{\gamma=1}^{\nu-2} \log\left(\frac{r(\lambda + \frac{\eta}{2}(\nu-2\gamma+1))}{l(\lambda-\frac{\eta}{2}(\nu-2\gamma-1))}\right) + s * \log(1+Y_{\nu-2}(\lambda)).
\end{aligned} \tag{3.137}$$

Here, the driving term $p_j(\lambda)$ and the kernel $s_{jl}$ remain the same as in the standard case. The modifications introduce new driving terms $d_j(\lambda)$, $d_k^+(\lambda)$, and $d_k^-(\lambda)$, which must be carefully determined.

As the next step, we will relate the eigenvalues $\Lambda_1(\lambda)$ and $\Lambda_2(\lambda)$ to the function $\widetilde{T}_1(\lambda)$. To do this, let us provide the explicit expression of $\widetilde{T}_1(\lambda)$:

$$\widetilde{T}_1(\lambda) = l(\lambda - \frac{\eta}{2})\frac{Q(\lambda+\eta)}{Q(\lambda)} + r(\lambda+\frac{\eta}{2})\frac{Q(\lambda-\eta)}{Q(\lambda)}. \tag{3.138}$$

We observe that the following relation is satisfied:

$$\Lambda_1(\lambda) = \frac{(-1)^l}{(\sinh(\lambda+\tau-\eta)\sinh(\lambda-\tau+\eta))^{\frac{N}{2}}}\widetilde{T}_1(\lambda), \tag{3.139}$$

where:

$$\begin{aligned}
&l(\lambda - \frac{\eta}{2}) \\
&= \Big(\sinh(\lambda-\tau)\sinh(\lambda+\tau-\eta)\Big)^{\frac{N}{2}} \sinh(\lambda+\varphi-s+\eta)\sinh(\lambda+\overline{\varphi}-\overline{s}), \\
&r(\lambda+\frac{\eta}{2}) \\
&= \Big(\sinh(\lambda+\tau)\sinh(\lambda-\tau+\eta)\Big)^{\frac{N}{2}} \sinh(\lambda+\varphi+s-\eta)\sinh(\lambda+\overline{\varphi}+\overline{s}).
\end{aligned} \tag{3.140}$$

For $\Lambda_2(\lambda)$, the following relation holds:

$$\Lambda_2(\lambda) = \frac{-1}{(\sinh(\lambda+\tau-\eta)\sinh(\lambda-\tau+\eta))^{\frac{N}{2}}}\widetilde{T}_1(\lambda) \tag{3.141}$$

and the functions $l(\lambda)$ and $r(\lambda)$ are given by

$$\begin{aligned} l(\lambda-\frac{\eta}{2}) &= \Big(\sinh(\lambda-\tau)\sinh(\lambda+\tau-\eta)\Big)^{\frac{N}{2}}\sinh(\lambda+\varphi+s)\sinh(\lambda-\overline{\varphi}-\overline{s}),\\ r(\lambda+\frac{\eta}{2}) &= \Big(\sinh(\lambda+\tau)\sinh(\lambda-\tau+\eta)\Big)^{\frac{N}{2}}\sinh(\lambda+\varphi-s)\sinh(\lambda-\overline{\varphi}+\overline{s}). \end{aligned} \tag{3.142}$$

By using this definition, the analytical structure of the standard $T$- and $Y$-functions is preserved, but in addition, new poles and zeroes, arising from terms containing $\varphi$ and $s$, need to be considered.

The $\widetilde{T}_1(\lambda)$ can be calculated from $Y_1(\lambda)$ by using:

$$\log\widetilde{T}_1(\lambda) = s * \Big(\log(l(\lambda-\eta)r(\lambda+\eta)) + \log(1+Y_1(\lambda))\Big). \tag{3.143}$$

## 3.8 Calculations of $\langle \mathcal{J}_{\mathfrak{s}} Q(\varphi)\rangle$

The last piece to compute in order to evaluate a lower bound of the spin Drude weight is the numerator of the equation (3.66). We insert the definition of $Q(\varphi)$ as in (3.69) to obtain:

$$\begin{aligned} \langle J_{\mathfrak{s}} Q(\varphi)\rangle\,|_{s=0} &= (-1)^L\partial_s\Big(\langle \mathcal{J}_{\mathfrak{s}}\hat{P}t_{\mathcal{A}}(\varphi,s)\hat{P}\rangle\,|_{s=0} - \langle \mathcal{J}_{\mathfrak{s}} t_{\mathcal{A}}(\varphi,s)\rangle\,|_{s=0}\Big)\\ &= -2(-1)^L\partial_s\langle \mathcal{J}_{\mathfrak{s}} t_{\mathcal{A}}(\varphi,s)\rangle\,|_{s=0}. \end{aligned} \tag{3.144}$$

The simplification in the second line occurs because the spin operator under a parity transformation changes sign: $\hat{P}\mathcal{J}_{\mathfrak{s}}\hat{P} = -\mathcal{J}_{\mathfrak{s}}$.

The operators $A_j$ contained in the transfer matrix $t_{\mathcal{A}}(\varphi,s)$ are translation-invariant, so $\hat{A}^{-1}A_j\hat{A} = A_{j-1}$. Then we can write:

$$\langle \mathcal{J}_{\mathfrak{s}} t_{\mathcal{A}}(\varphi,s)\rangle = -2\mathrm{i}LJ\,\langle(\sigma_2^+\sigma_1^- - \sigma_1^-\sigma_2^+)t_{\mathcal{A}}(\varphi,s)\rangle\,. \tag{3.145}$$

We introduce a modified partition function:

$$Z(\varphi,s) = \mathrm{tr}_V[\rho(\varphi,s)], \tag{3.146}$$

where the density function $\rho(\varphi,s)$ is defined as

$$\rho(\varphi,s) = \mathrm{e}^{-\beta H_L}t_{\mathcal{A}}(\varphi,s). \tag{3.147}$$

Then we can recast equation (3.145) as:

$$\langle \mathcal{J}_{\mathfrak{s}} t_{\mathcal{A}}(\varphi,s)\rangle\,|_{s=0} = -2\mathrm{i}LJ\Big(\langle(e_2)_1^1(e_1)_2^2\rangle_s - \langle(e_1)_2^1(e_2)_1^2\rangle_s\Big)\frac{Z(\varphi,s)}{Z}\bigg|_{s=0}, \tag{3.148}$$

where $\langle A \rangle_s = \mathrm{tr}_V\{\rho(\varphi, s)A\}/Z(\varphi, s)$.

To address our problem, we define the following quantum monodromy matrix:

$$\begin{aligned} T_j^{QTM}(\lambda) =& R_{j,a_1}(\lambda-\tau)R^{t_1}_{a_2,j}(-\tau-\lambda)\dots \\ & R_{j,a_{N-1}}(\lambda-\tau)R^{t_1}_{a_N,j}(-\tau-\lambda)R_{j,\mathcal{A}}(\lambda+\varphi,s) \end{aligned} \tag{3.149}$$

which acts on the reference state

$$|0\rangle_{GS} = (|+\rangle \otimes |-\rangle)^{\frac{N}{2}} \otimes |0\rangle\,. \tag{3.150}$$

Similar calculations, as performed for the eigenvalues $\Lambda_1(\lambda)$ and $\Lambda_2(\lambda)$, lead to the result for the largest eigenvalue of $\langle \mathcal{J}_{\mathfrak{s}} Q(\varphi)\rangle$, which is given by

$$\Lambda(\lambda) = a(\lambda)\prod_{j=1}^{\frac{N}{2}} \frac{\sinh(\lambda-\lambda_j+\eta)}{\sinh(\lambda-\lambda_j)} + d(\lambda)\prod_{j=1}^{\frac{N}{2}} \frac{\sinh(\lambda-\lambda_j-\eta)}{\sinh(\lambda-\lambda_j)}, \tag{3.151}$$

where

$$\begin{aligned} a(\lambda) &= \left(\frac{\sinh(\lambda-\tau)}{\sinh(\lambda-\tau+\eta)}\right)^{\frac{N}{2}} \sinh(\lambda+\varphi+s), \\ d(\lambda) &= \left(\frac{\sinh(\lambda+\tau)}{\sinh(\lambda+\tau-\eta)}\right)^{\frac{N}{2}} \sinh(\lambda+\varphi-s) \end{aligned} \tag{3.152}$$

and $\lambda_j$ satisfy the Bethe Ansatz equations.

Let us introduce an external magnetic field, denoted as $h$, in the $z$ direction. This can be achieved by applying a twist to the monodromy matrix:

$$T(\lambda) \to T(\lambda) \begin{bmatrix} \mathrm{e}^{\frac{h}{2T}} & 0 \\ 0 & \mathrm{e}^{-\frac{h}{2T}}, \end{bmatrix}. \tag{3.153}$$

Alternatively, this transformation can be expressed as $a(\lambda) \mapsto \mathrm{e}^{\frac{h}{2T}} a(\lambda)$ and $d(\lambda) \mapsto \mathrm{e}^{-\frac{h}{2T}} d(\lambda)$.

In the computation of the leading eigenvalue $\Lambda(\lambda)$, usually a different approach is employed when compared to the eigenvalues $\Lambda_1(\lambda)$ and $\Lambda_2(\lambda)$. Initially, we define an auxiliary function, and then we formulate non-linear integral equations for this function. This approach enables us to work with a single meromorphic function in the complex plane instead of dealing directly with the Bethe roots. Subsequently, all quantities of interest can be expressed in terms of this auxiliary function, denoted as $\mathfrak{a}(\lambda)$. For a detailed discussion, please refer to [31, 35] and [36, 37].

We define the auxiliary function as follows:

$$\mathfrak{a}(\lambda) = \left(\frac{\sinh(\lambda-\tau)\sinh(\lambda+\tau-\eta)}{\sinh(\lambda+\tau)\sinh(\lambda-\tau+\eta)}\right)^{\frac{N}{2}} \frac{\sinh(\lambda+\varphi-\eta)}{\sinh(\lambda+\varphi+\eta)} \frac{Q(\lambda+\eta)}{Q(\lambda-\eta)} \mathrm{e}^{\frac{h}{T}}. \tag{3.154}$$

It satisfies $1+\mathfrak{a}(\lambda_j)=0$.

The largest eigenvalue can be recast in the following form:

$$\Lambda(\lambda)=d(\lambda)\frac{Q(\lambda-\eta)}{Q(\lambda)}\Big(1+\mathfrak{a}(\lambda)\Big). \tag{3.155}$$

From the analytic properties of $\mathfrak{a}(\lambda)$ and $1+\mathfrak{a}(\lambda)$, it is possible to demonstrate that $\Lambda(\lambda)$ can be derived from (the integration contour $\mathcal{C}$ is depicted in Figure 3.5):

$$\begin{aligned}\log\Lambda(\lambda)&=\log(\sinh(\lambda+\varphi-s))-\frac{h}{2T}+\int_{\mathcal{C}}\frac{\mathrm{d}w}{2\pi i}e(w-\lambda)\log(1+\mathfrak{a}(w))\\&=\log(\sinh(\lambda+\varphi+s))+\frac{h}{2T}-\int_{\mathcal{C}}\frac{\mathrm{d}w}{2\pi i}e(w-\lambda)\log(1+\overline{\mathfrak{a}}(w)).\end{aligned} \tag{3.156}$$

The dual auxiliary function is defined as $\overline{\mathfrak{a}}(\lambda)=\frac{1}{\mathfrak{a}(\lambda)}$. Then, the auxiliary function and its dual satisfy the following non-linear integral equations:

$$\begin{aligned}&\log\mathfrak{a}(\lambda)\\&=-\beta e(\lambda)+\frac{h}{T}+\log\frac{\sinh(\lambda+\varphi+s)}{\sinh(\lambda+\varphi-s)}+\int_{\mathcal{C}}\frac{\mathrm{d}w}{2\pi i}K(w-\lambda)\log(1+\mathfrak{a}(w)),\\&\log\overline{\mathfrak{a}}(\lambda)=\\&\beta e(\lambda)-\frac{h}{T}+\log\frac{\sinh(\lambda+\varphi-s)}{\sinh(\lambda+\varphi+s)}-\int_{\mathcal{C}}\frac{\mathrm{d}w}{2\pi i}K(w-\lambda)\log(1+\overline{\mathfrak{a}}(w)),\end{aligned} \tag{3.157}$$

where the driving term in the Trotter limit and the kernel are given by:

$$K(\lambda)=\coth(\lambda+\eta)-\coth(\lambda-\eta),\quad e(\lambda)=\coth(\lambda)-\coth(\lambda+\eta). \tag{3.158}$$

Let us consider the free energy per lattice site in the thermodynamic limit. It can be derived from the largest eigenvalue through the integral over $\mathfrak{a}(\lambda)$ or $\overline{\mathfrak{a}}(\lambda)$:

$$f(T)=-T\lim_{N\to\infty}\log\Lambda(0). \tag{3.159}$$

From the free energy, thermodynamic properties become accessible. In particular, we are interested in the magnetization per unit length at finite magnetic field $h$ and finite temperature $T$, defined as:

$$\begin{aligned}m(h,T)&=-\frac{\partial f(h,T)}{\partial h}=T\frac{\partial\log\Lambda(\lambda)}{\partial h}\Big|_{\lambda=0}\\&=-\frac{1}{2}-\int_{\mathcal{C}}\frac{\mathrm{d}w}{2\pi\mathrm{i}}e(w-\lambda)\frac{\sigma(w)}{1+\overline{\mathfrak{a}}(w)}\Big|_{\lambda=0}.\end{aligned} \tag{3.160}$$

Here, the function $\sigma(w)$ can be calculated from the non-linear integral equation:

$$\sigma(w)=T\partial_h\log\overline{\mathfrak{a}}(w)=1-\int_{\mathcal{C}}\frac{\mathrm{d}\theta}{2\pi\mathrm{i}}K(\theta-w)\frac{\sigma(\theta)}{1+\overline{\mathfrak{a}}(\theta)}. \tag{3.161}$$

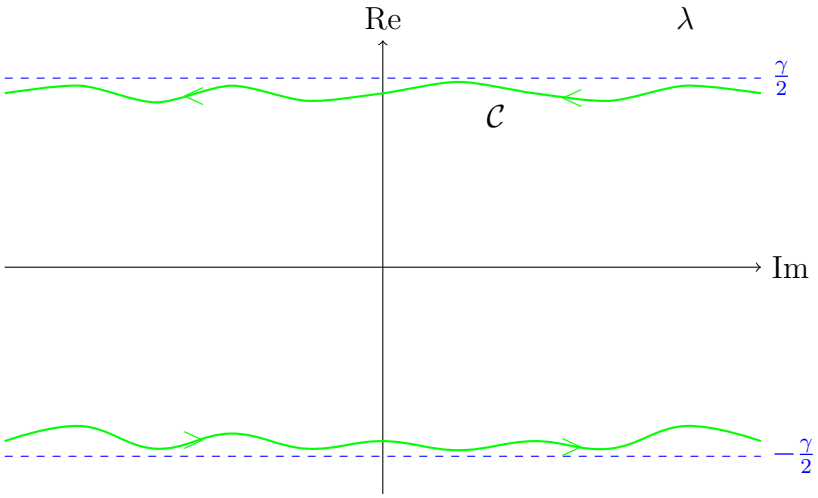



Figure 3.5: The contour $\mathcal{C}$ passes just below $+\frac{\gamma}{2}$ and just above $-\frac{\gamma}{2}$, encircling the real axis in a counterclockwise direction.

We also introduce another function, denoted with $G(w,\lambda)$, which we will use later for the "dressed function trick":

$$\langle (e_2)^1_1 (e_1)^2_2 \rangle_s - \langle (e_1)^1_2 (e_2)^2_1 \rangle_s = -\sinh\eta \int_{\mathcal{C}} \frac{\mathrm{d}w}{2\pi\mathrm{i}} \frac{\partial_\lambda G(w,\lambda)}{1+\mathfrak{a}(w)}\Big|_{\lambda=0}. \tag{3.162}$$

This relation can be derived in accordance with the procedure presented in the paper [36].

The linear integral equation for $G(w,\lambda)$ is given by

$$G(w,\lambda) = e(\lambda - w) - \int_{\mathcal{C}} \frac{\mathrm{d}\theta}{2\pi\mathrm{i}} K(w-\theta) \frac{G(\theta,\lambda)}{1+\mathfrak{a}(\theta)}. \tag{3.163}$$

Now, by using dressed function formalism, it is possible to show

$$\int_{\mathcal{C}} \frac{\mathrm{d}w}{2\pi\mathrm{i}} \partial_\lambda e(\lambda - w) \frac{\sigma(w)}{1+\overline{\mathfrak{a}}(w)}\Big|_{\lambda=0} = \int_{\mathcal{C}} \frac{\mathrm{d}w}{2\pi\mathrm{i}} \frac{\partial_\lambda G(w,\lambda)}{1+\mathfrak{a}(w)}\Big|_{\lambda=0}. \tag{3.164}$$

This leads to:

$$\partial_\lambda m(h,T) = -\int_{\mathcal{C}} \frac{\mathrm{d}w}{2\pi\mathrm{i}} \frac{\partial_\lambda G(w,\lambda)}{1+\mathfrak{a}(w)}\Big|_{\lambda=0} \tag{3.165}$$

and

$$\langle (e_2)^1_1 (e_1)^2_2 \rangle_s - \langle (e_1)^1_2 (e_2)^2_1 \rangle_s = \sinh\eta\, \partial_\lambda m(0,T)|_{\lambda=0}. \tag{3.166}$$

Finally, the scalar product of the spin current and the charge $Q(\varphi)$ can be reconstructed from the derivatives of the magnetization and the modified partition function:

$$\begin{aligned} \langle \mathcal{J}_{\mathfrak{s}} Q(\varphi,s)\rangle\,|_{s=0} &= -4LJ(-\mathrm{i})^{L-1}\sinh\eta\,\partial_s \left( \int_{\mathcal{C}} \frac{\mathrm{d}w}{2\pi\mathrm{i}} \frac{\partial_\lambda G(w,\lambda)}{1+\mathfrak{a}(w)} \frac{Z(\varphi,s)}{Z} \right)\Big|_{\lambda=s=0} \\ &= 4LJ(-\mathrm{i})^{L-1}\sinh\eta\sinh^L\varphi \Big[ \partial_s\partial_\lambda m(0,T) + \partial_\lambda m(0,T)\partial_s \log Z(\varphi,s) \Big]\Big|_{\lambda=s=0}, \end{aligned} \tag{3.167}$$

where $\log Z(\varphi, s) \overset{L\to\infty}{\sim} L \log \Lambda(0)$ and $Z(\varphi, 0)/Z = \sinh^L \varphi$.

For numerical computations, it is more convenient to express the integral over the real line rather than the contour $\mathcal{C}$. This transformation can be achieved by decomposing the contour integral into two separate terms:

$$\begin{aligned}\int_{\mathcal{C}} \frac{\mathrm{d}w}{2\pi\mathrm{i}} K(\lambda - w) \log(1 + \mathfrak{a}(w)) = &- \int_{-\infty}^{\infty} \frac{\mathrm{d}x}{2\pi\mathrm{i}} K(\lambda - x) \log(1 + \mathfrak{a}(x + \frac{\gamma}{2})) \\ &+ \int_{-\infty}^{\infty} \frac{\mathrm{d}x}{2\pi\mathrm{i}} K(\lambda - x + \gamma) \log(1 + \mathfrak{a}(x - \frac{\gamma}{2})).\end{aligned} \tag{3.168}$$

To summarize: the scalar product (3.167) together with the norm (3.59) shows that $\mathfrak{A}_1$ and $\mathfrak{A}_2$ arise from derivatives of the eigenvalues $\Lambda_1$ and $\Lambda_2$, which correspond to the eigenvalue of $\widetilde{T}_1$ for the two cases $t^{1\mathrm{QTM}}$ and $t^{2\mathrm{QTM}}$ with differently defined functions $l(\lambda)$ and $r(\lambda)$, see Section 3.7.

## 3.9 High temperature limit: $T \to \infty$

Now, let us investigate the behavior of the system as the temperature approaches $T \to \infty$. From equation (3.154), we observe that the auxiliary function takes the form:

$$\mathfrak{a}(\lambda) = \frac{\sinh(\lambda + \varphi + s)}{\sinh(\lambda + \varphi - s)}. \tag{3.169}$$

Using this expression and substituting it into the eqution (3.155), find that the eigenvalue $\Lambda(0)$ simplifies to:

$$\Lambda(0) = d(0) \frac{Q(-\eta)}{Q(0)} (1 + \mathfrak{a}(0)) = 2 \sinh\varphi \cosh s. \tag{3.170}$$

Assuming that the partition function scales as $Z(\varphi, s) \sim (\Lambda(0))^L$, we differentiate and evaluate at $s = 0$:

$$\partial_s \log Z(\varphi, s)|_{s=0} = 2L \sinh\varphi \sinh s|_{s=0} = 0. \tag{3.171}$$

Applying the residue theorem to equation (3.163) in the limit $T \to \infty$, we find the following solution:

$$G(w, \lambda) = e(\lambda - w) + \frac{K(w - \lambda)}{1 + \mathfrak{a}(\lambda)}. \tag{3.172}$$

By differentiating with respect to $\lambda$, we obtain:

$$\partial_\lambda G(w, \lambda)|_{\lambda=0} = \frac{\sinh\eta \sinh(2w - \eta)}{\sinh w \sinh(w - \eta)} + \partial_\lambda \frac{K(w - \lambda)}{1 + \mathfrak{a}(\lambda)}\Big|_{\lambda=0}. \tag{3.173}$$

Comparing this result with equation (3.165), we obtain the derivative of the magnetization:

$$\partial_\lambda m(h,T)|_{\lambda=0} = \frac{\tanh s}{2\sinh^2\varphi}. \tag{3.174}$$

Taking an additional derivative with respect to $s$, we get:

$$\partial_s\partial_\lambda m(0,T)|_{\lambda=0} = \frac{1}{\sinh^2\varphi}. \tag{3.175}$$

Finally, we evaluate the scalar product as in equation (3.167) at $T \to \infty$:

$$\langle \mathcal{J}_{\mathfrak{s}} Q(\varphi,s)\rangle\,|_{s=0} = 4LJ(-\mathrm{i})^{L-1}\sinh\eta\sinh^{L-2}\varphi. \tag{3.176}$$

Calculating the squared modulus yields:

$$|\,\langle \mathcal{J}_{\mathfrak{s}} Q(\varphi,s)\rangle\,|^2 = (4LJ)^2|\sinh\eta|^2\sinh^{L-2}\varphi\sinh^{L-2}\overline{\varphi}. \tag{3.177}$$

Extending the scalar product calculation to finite temperature is in principle feasible using the NLIE framework developed in Sections 3.6 and 3.7. The scalar product requires derivatives of the eigenvalues $\Lambda_1$ and $\Lambda_2$, which are obtained from $\widetilde{T}_1(\lambda)$ via the $Y$-functions through the modified NLIEs. At finite $T$, these NLIEs must be solved numerically, and the subsequent differentiation with respect to the parameters $\varphi$ and $s$ adds considerable computational effort. In the high-temperature limit, by contrast, the NLIEs reduce to closed-form expressions, making the derivatives straightforward. A systematic finite-temperature evaluation of the scalar product therefore remains an objective for future work.

# Chapter 4

# Spin Drude Weight

Numerous controversies surround the spin Drude weight for the XXZ chain, with various analytical or numerical studies producing contradictory results. This has motivated us to seek an alternative method for its calculation. Our approach involves combining the thermodynamic Bethe ansatz with the functional relations of the Y-system type, satisfied by the row-to-row transfer matrices. This combination enables us to evaluate the asymptotic behaviour of the spin Drude weight at finite temperatures in relation to the system size.

The Drude weight, in Kohn's formula, is related to the thermal expectation value of the curvature of energy levels. This quantity can be described through the Y-functions and their specific zeros, denoted as $\zeta_j^k$. The main effort in our research is the derivation of suitable non-linear integral equations for the Y-function, which can be solved numerically. We determine the distribution of zeros that describes thermal equilibrium and use them to formulate a set of non-linear integral equations. These zeros can be determined individually or analyzed in terms of their thermodynamic properties. The solution to the non-linear integral equations allows us to determine the spin Drude weight. We will then compare our results with those obtained by Zotos (see (2.96)).

We will provide an overview of the results presented in the paper by Klümper and Sakai [38]. Additionally, we will explore and expand upon the concepts introduced in that paper. In particular, we will consider the case of a Hamiltonian with an anisotropy parameter $\nu$ that is any rational number greater than or equal to 2. Through numerical analysis, it becomes evident that the spin Drude weight exhibits a significant dependence on the system size. We observed that the convergence to the result in the thermodynamic limit is achieved for a significantly large system size.

## 4.1 Introduction

To avoid any confusion in notation, we will revisit the most essential definitions. The Hamiltonian for the Heisenberg spin-1/2 XXZ chain on the periodic lattice, dependent on flux $\phi$, is expressed as follows:

$$H(\phi) = J\sum_{k=1}^{L}\left(e^{\mathrm{i}\phi/L}\sigma_{k+1}^{+}\sigma_{k}^{-} + e^{-\mathrm{i}\phi/L}\sigma_{k}^{+}\sigma_{k+1}^{-} + \frac{\Delta}{2}\sigma_{k}^{z}\sigma_{k+1}^{z}\right), \tag{4.1}$$

where $\Delta = \cos\gamma$, with $\gamma = \frac{\pi}{\nu}$ and $\phi$ taking real values. We are operating in the critical regime where $\gamma$ satisfies $0 \leq \gamma \leq \frac{\pi}{2}$.

The finite-temperature Drude weight is given by Kohn's formula, see Section 2.4. Following [38], we normalise the conductivity as $\mathrm{Re}\,\sigma(\omega) = \pi D\delta(\omega) + \sigma_{reg}(\omega)$, so that $D$ in this chapter is twice the Drude weight defined in (2.59):

$$D = \lim_{L\to\infty} L\sum_{n} p_n \frac{\mathrm{d}^2 E_n(\phi)}{\mathrm{d}\phi^2}\Big|_{\phi=0}, \tag{4.2}$$

where $p_n = \mathrm{e}^{-\beta E_n}/\sum_m \mathrm{e}^{-\beta E_m}$ represents the Boltzmann weight for the energy eigenvalue $E_n$.

To evaluate $D$, we transform the problem of the (1+1)-dimensional quantum system into a two-dimensional classical lattice system. This lattice system, corresponding to the XXZ chain, is the six-vertex model, whose weights are determined by the $R$-matrix $R(v) \in \mathrm{End}(V \otimes V)$, where $V$ is a two-dimensional vector space spanned by the spin-up state $|0\rangle = \binom{1}{0}$ and the spin-down state $|1\rangle = \binom{0}{1}$. The non-zero elements of the $R$-matrix are given by:

$$\begin{aligned} R_{11}^{11}(v) &= R_{22}^{22}(v) = \frac{[v+2]}{[2]}, \\ R_{12}^{12}(v) &= e^{\mathrm{i}\frac{\phi}{L}}\frac{[v]}{[2]}, \\ R_{21}^{21}(v) &= e^{-\mathrm{i}\frac{\phi}{L}}\frac{[v]}{[2]}, \\ R_{12}^{21}(v) &= R_{21}^{12}(v) = 1, \end{aligned} \tag{4.3}$$

with $[v] = \frac{\sin(\gamma v/2)}{\sin\gamma}$.

The $R$-matrix satisfies the Yang-Baxter equations (YBE):

$$R_{23}(v)R_{13}(u)R_{12}(u-v) = R_{12}(u-v)R_{13}(u)R_{23}(v), \tag{4.4}$$

where $R_{jk}(v)$ acts on $V_j \otimes V_k$. The YBE guarantees that the family of row-to-row transfer matrices $T_1(v) \in \mathrm{End}(V^{\otimes L})$,

$$T_1(v) = \mathrm{Tr}_{V_0}\left[R_{0L}(\mathrm{i}(v+\mathrm{i}))R_{0L-1}(\mathrm{i}(v+\mathrm{i}))\cdots R_{01}(\mathrm{i}(v+\mathrm{i}))\right], \tag{4.5}$$

consists of mutually commuting matrices for arbitrary spectral parameters $u$ and $v$:

$$[T_1(u), T_1(v)] = 0. \tag{4.6}$$

The original quantum system (4.1) can be expressed as the logarithmic derivative of $T_1(v)$ with respect to $v$:

$$H(\phi) = \frac{A}{2\pi \mathrm{i}} \frac{\partial}{\partial v} \log T_1(v)\Big|_{v=-\mathrm{i}} - \frac{JL}{2}\Delta, \tag{4.7}$$

where $A = \frac{4\pi J \sin\gamma}{\gamma}$.

The diagonalization of the transfer matrix yields eigenvalues, which can be expressed as follows:

$$T_1(v) = \varphi(v-\mathrm{i})\frac{q(v+2\mathrm{i})}{q(v)}\mathrm{e}^{\mathrm{i}\frac{\phi}{2}} + \varphi(v+\mathrm{i})\frac{q(v-2\mathrm{i})}{q(v)}\mathrm{e}^{-\mathrm{i}\frac{\phi}{2}} \tag{4.8}$$

The transfer matrix $T_1(v)$ is embedded within a larger family of transfer matrices. This allows us to construct functional relations between different $T$- functions that describe the physical system. Let us consider the following definition of $T$-functions:

$$T_{n-1}(v) = \sum_{j=1}^{n} \mathrm{e}^{\frac{\mathrm{i}\phi}{2}(n-2j+1)}\varphi(v+\mathrm{i}(2j-n-1))\frac{q(v+\mathrm{i}n)q(v-\mathrm{i}n)}{q(v+\mathrm{i}(2j-n-2))q(v+\mathrm{i}(2j-n))} \tag{4.9}$$

with

$$\varphi(v) = \Big(\frac{\sinh\frac{\gamma}{2}v}{\sin\gamma}\Big)^L \tag{4.10}$$

and

$$q(v) = \prod_{k=1}^{m} \sinh\frac{\gamma}{2}(v-v_k), \quad m \in \{0,1,2,\ldots,L/2\}. \tag{4.11}$$

A notable property is that $T_{-1}(v) = 0$ and $T_0(v) = \varphi(v)$.

We will exclusively consider the case of the largest eigenvalue of the transfer matrix $T_1(0)$, which corresponds to the number of Bethe roots being $m = L/2$. The parameters $v_k$ are determined by solving the Bethe ansatz equations:

$$\frac{\varphi(v_k+\mathrm{i})}{\varphi(v_k-\mathrm{i})} = \mathrm{e}^{-\mathrm{i}\phi}\frac{q(v_k+2\mathrm{i})}{q(v_k-2\mathrm{i})}. \tag{4.12}$$

As previously mentioned, rather than solving the Bethe ansatz equations directly, we will reformulate the problem in terms of the T- and Y-functions.

In the appendix, we provide the formulas for the T- and Y-system at the root of unity. These will be used later to study the case of $\nu = 5/2$. For now, our focus remains on the case of the "simple root of unity" where $\nu = \nu_1 \in \mathbb{Z} \geq 2$.

## 4.2 T- Y-system at the "simple root of unity"

In this section, we aim to establish a consistent $T$- and $Y$-system, from which we can derive non-linear integral equations that are solvable numerically. An extensive treatment of $T$- and $Y$-systems can be found in [39]. The energy spectrum of the XXZ chain is encoded in the analytical properties of the $T$- and $Y$-functions. We start with defining the following relation for the $T$-system:

$$T_{n-1}(v+\mathrm{i}j)T_{n-1}(v-\mathrm{i}j) = T_{n+j-1}(v)T_{n-j-1}(v) + T_{j-1}(v+\mathrm{i}n)T_{j-1}(v-\mathrm{i}n). \tag{4.13}$$

This relation holds for any complex number $v \in \mathbb{C}$. It can be verified by substituting (4.9) into it. Refer to [40] for more details about functional relations of this type. The following periodicity properties are satisfied:

$$T_{n-1}(v) = T_{n-1}(v+2\nu\mathrm{i}), \quad Q(v) = (-1)^m Q(v+2\mathrm{i}\nu). \tag{4.14}$$

Similarly, we can prove:

$$T_\nu(v) = T_{\nu-2}(v) + 2(-1)^m T_0(v+\mathrm{i}\nu). \tag{4.15}$$

The $Y$-functions are defined in terms of the $T$-functions through the following relations:

$$\begin{aligned} Y_j(v) &= \frac{T_{j-1}(v)T_{j+1}(v)}{T_0(v+\mathrm{i}(j+1))T_0(v-\mathrm{i}(j+1))} \qquad \text{for } 1 \le j \le \nu-2 \\ Y_{\nu-1}(v) &= (-1)^m \mathrm{e}^{-\mathrm{i}\frac{\nu\phi}{2}} \frac{T_{\nu-2}(v)}{T_0(v+\mathrm{i}\nu)} \\ Y_\nu(v) &= (-1)^m \mathrm{e}^{\mathrm{i}\frac{\nu\phi}{2}} \frac{T_{\nu-2}(v)}{T_0(v+\mathrm{i}\nu)}. \end{aligned} \tag{4.16}$$

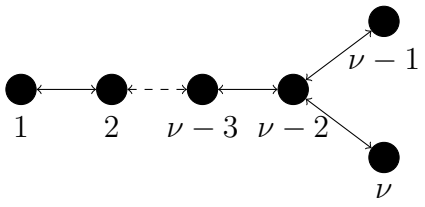
We also set $Y_0(v) = 0$ and $Y_{-1}(v) = \infty$.

In order to establish functional relations between the $Y$-functions, we first note the relations for $1 + Y_n(v)$:

$$\begin{aligned} 1+Y_j(v) &= \frac{T_j(v+\mathrm{i})T_j(v-\mathrm{i})}{T_0(v+\mathrm{i}(j+1))T_0(v-\mathrm{i}(j+1))} \qquad \text{for } 1 \le j \le \nu-2 \\ (1+Y_{\nu-1}(v))(1+Y_\nu(v)) &= \frac{T_{\nu-1}(v+\mathrm{i})T_{\nu-1}(v-\mathrm{i})}{T_0(v+\mathrm{i}\nu)T_0(v-\mathrm{i}\nu)}. \end{aligned} \tag{4.17}$$

Finally, we see that the $Y$-functions satisfy the following functional relations, also known as the $Y$-system:

$$\begin{aligned} &Y_j(v+\mathrm{i})Y_j(v-\mathrm{i}) = (1+Y_{j-1}(v))(1+Y_{j+1}(v)) \qquad \text{for } 1 \le j \le \nu-3, \\ &Y_{\nu-2}(v+\mathrm{i})Y_{\nu-2}(v-\mathrm{i}) = (1+Y_{\nu-3}(v))(1+Y_{\nu-1}(v))(1+Y_\nu(v)) \qquad \text{for } \nu \ge 3, \\ &Y_{\nu-1}(v+\mathrm{i})Y_{\nu-1}(v-\mathrm{i}) = \mathrm{e}^{-i\nu\phi}(1+Y_{\nu-2}(v)), \\ &Y_\nu(v+\mathrm{i})Y_\nu(v-\mathrm{i}) = \mathrm{e}^{i\nu\phi}(1+Y_{\nu-2}(v)). \end{aligned} \tag{4.18}$$




$$A_{jl} = \begin{bmatrix} 0 & 1 & \dots & 0 & 0 & 0 & 0 \\ 1 & 0 & & 0 & 0 & 0 & 0 \\ \vdots & & & 0 & 0 & 0 & 0 \\ 0 & 0 & 0 & 0 & 1 & 0 & 0 \\ 0 & 0 & 0 & 1 & 0 & 1 & 1 \\ 0 & 0 & 0 & 0 & 1 & 0 & 0 \\ 0 & 0 & 0 & 0 & 1 & 0 & 0 \end{bmatrix}_{jl}$$

Figure 4.1: Dynkin diagram of type $D_\nu$ and the corresponding adjacency matrix $A_{jl}$.

Analyzing the properties of the system described by equations (4.18), we derive a set of non-linear integral equations for the $Y_j(v)$ functions. Our approach closely resembles the methods discussed in Section 3.6, and a detailed derivation is available in Appendix A of the paper by Klümper and Sakai. [38]. These integral equations take the form:

$$\log Y_j(v) = p_j(v) + g_j(v) + \sum_{l=1}^{\nu} K_{jl} * \log(1 + Y_l)[v] \quad (1 \le j \le \nu), \tag{4.19}$$

the driving term $p_j(v)$, is defined as:

$$p_j(v) = (\delta_{j1} + \delta_{j2}\delta_{\nu 2})(Lp(v) + s'(v - \mathrm{i})\psi) - \delta_{j\nu-1}\frac{\nu}{2}\phi\mathrm{i} + \delta_{j\nu}\frac{\nu}{2}\phi\mathrm{i}, \tag{4.20}$$

where

$$p(v) = \log\tanh\frac{\pi}{4}v. \tag{4.21}$$

And the kernel is given by

$$K_{jk}(v) = A_{jk}s(v), \quad s(v) = \frac{1}{4\cosh\frac{\pi}{2}v}. \tag{4.22}$$

The variable $\psi$ is set to zero after the calculations. It is important to note that at $\phi = 0$, $Y_{\nu-1}(v) = Y_\nu(v)$.

The driving term $g_j(v)$ encodes information about the excited states. For the ground state, we have $g_j(v) = 0$.

In general, for an excited state, we have:

$$g_j(v) = \sum_{l=1}^{\nu} A_{jl} \sum_{k=1}^{m_l} p(v - \zeta_l^k), \tag{4.23}$$

The parameters $\zeta_l^k$ represent the zeros of the $T$-functions in the physical strip $[-1,1]$. Thus, we have:

$$T_j(\zeta_j^k) = 0 \quad (1 \le j \le \nu - 1), \quad T_{\nu-1}(\zeta_\nu^k) = 0. \tag{4.24}$$

Alternatively, in terms of $Y$-functions:

$$Y_j(\zeta_j^k + \mathrm{i}) = -1 \quad (1 \le k \le m_j \in \mathbb{Z}_{\ge 0};\ 1 \le j \le \nu). \tag{4.25}$$

The driving term $g(v)$ and the parameters $\zeta_j^k$ can be studied through two different approaches. The first approach involves analyzing their thermodynamic properties as their number increases. This method explores the behavior of the system close to the thermodynamic limit for a given temperature. The second approach treats the parameters $\zeta_j^k$ as solutions to Bethe Ansatz (BA)-like equations. This procedure involves examining the counting function, which provides a way to count the number of solutions and understand their distribution. By studying the distribution of the parameters $\zeta_j^k$, we can gain a deeper understanding of the structure and properties of the solutions.

After computing the $Y$-function, we can use Equation (4.17) for $j = 1$ to obtain an equation for $T_1(v)$ (as in Appendix A in [38]):

$$\begin{aligned} \partial_v \log T_1(v) &= \partial_v \log \varphi(v - \mathrm{i}) - 2\pi\mathrm{i} L s * a(v + \mathrm{i}) \\ &+ 2\pi\mathrm{i} \sum_{k=1}^{m_1} s(v + \zeta_1^k) + s' * \log(1 + Y_1)(v). \end{aligned} \tag{4.26}$$

The energy can be evaluated by plugging this result into equation (4.7):

$$E(\phi) = E_{\mathrm{gs}} + A \sum_{j=1}^{\delta_{\nu 2}+1} \left[ \sum_{k=1}^{m_j} s(\zeta_j^k) + \frac{1}{2\pi\mathrm{i}} s' * \log(1 + Y_j)[-\mathrm{i}] \right], \tag{4.27}$$

where the ground state energy is defined as:

$$E_{\mathrm{gs}} = \frac{JL}{2}\Delta - AL \int_{-\infty}^{\infty} a(v) s(v) \mathrm{d}v, \quad a(v) := \frac{\sin\gamma}{2\nu(\cosh\gamma v - \cos\gamma)}. \tag{4.28}$$

Now we can calculate the Drude weight from Equation (4.2):

$$D = \lim_{L\to\infty} \frac{\partial^2}{\partial\phi^2} \sum_{j=1}^{\delta_{\nu 2}+1} \left[ \sum_{k=1}^{m_j} s(\zeta_j^k) + \frac{1}{2\pi\mathrm{i}} s' * \log(1 + Y_j)[-\mathrm{i}] \right]. \tag{4.29}$$

This equation provides an alternative to Zotos' formula for calculating the spin Drude weight for the XXZ spin 1/2 model. The main challenge lies in the determination of the parameters $\zeta_j^k$. When their number is relatively small, they can be determined numerically using Equation (4.25).

## 4.3 Thermodynamic properties of Y's zeros

The number of $\zeta_j^k$ depends on temperature $T$ and the system size $L$. As these parameters increase, the number of $\zeta_j^k$ also grows, making it progressively difficult to extract them directly from the numerical data. Instead, their behaviour can be effectively described through their thermodynamic properties.

Let us consider a system at finite temperature with a large system size, $L \gg 1$. In this limit, the parameters $\zeta_j^k$ condense and can be replaced by densities[1]. We define the density $\rho_j^{\mathrm{h}}(\zeta_j^k)$ in the thermodynamic limit:

$$\rho_j^{\mathrm{h}}(\zeta_j^k) = \lim_{L\to\infty} \frac{1}{L(\zeta_j^{k+1} - \zeta_j^k)} \quad (1 \le j \le \nu). \tag{4.30}$$

Furthermore, we define the total density, which includes both "holes" and "particles":

$$\rho_j^{\mathrm{h}}(\zeta_j^k) + \rho_j(\zeta_j^k) = \lim_{L\to\infty} \frac{I_j^{k+1} - I_j^k}{L(\zeta_j^{k+1} - \zeta_j^k)}. \tag{4.31}$$

We also introduce the ratio of densities:

$$\eta_j(v) = \frac{\rho_j^{\mathrm{h}}(v)}{\rho_j(v)} \quad (1 \le j \le \nu). \tag{4.32}$$

The quantum numbers $I_j^k$ appear when we take the logarithm of (4.25):

$$\log Y_j(\zeta_j^k + \mathrm{i}) = -2\pi\mathrm{i} I_j^k \quad (I_j^k \in \mathbb{Z} + 1/2). \tag{4.33}$$

Now, by combining equations (4.31) and (4.33), we derive:

$$\begin{aligned} \rho_j^{\mathrm{h}}(\zeta_j^k) + \rho_j(\zeta_j^k) &= -\lim_{L\to\infty} \frac{1}{2\pi\mathrm{i}L} \frac{\log Y_j(\zeta_j^{k+1} + \mathrm{i}) - \log Y_j(\zeta_j^k + \mathrm{i})}{\zeta_j^{k+1} - \zeta_j^k} \\ &= -\lim_{L\to\infty} \frac{1}{2\pi\mathrm{i}L} \partial_v \log Y_j(v + \mathrm{i}). \end{aligned} \tag{4.34}$$

From the right-hand side of (4.19), we obtain:

$$\rho_j^{\mathrm{h}}(\zeta_j^k) = -\lim_{L\to\infty} \frac{1}{2\pi\mathrm{i}L} \frac{\log(1 + Y_j(\zeta_j^{k+1} + \mathrm{i})) - \log(1 + Y_j(\zeta_j^k + \mathrm{i}))}{\zeta_j^{k+1} - \zeta_j^k}. \tag{4.35}$$

Additionally, we have:

$$s(v) = -\frac{1}{2\pi\mathrm{i}L} \partial_v p(v). \tag{4.36}$$

[1] In our approach, the objects $\zeta$ are related to so-called "hole solutions" in standard TBA. This is why we call the density functions for $\zeta$ parameters $\rho^h$.

By combining the equations (4.19), (4.34), (4.35), and (4.36), we can formulate linear integral equations for densities as follows:

$$\rho_j^{\mathrm{h}}(v) + \rho_j(v) = s_j(v) + \sum_{l=1}^{\nu} K_{jl} * \rho_l^{\mathrm{h}}[v], \tag{4.37}$$

where

$$s_j(v) = (\delta_{j1} + \delta_{j2}\delta_{\nu 2})s(v). \tag{4.38}$$

The energy eigenvalues per site can be defined as

$$e = e_{\mathrm{gs}} + A\int_{-\infty}^{\infty} s(v)\left\{\rho_1^{\mathrm{h}}(v) + \delta_{\nu 2}\rho_\nu^{\mathrm{h}}(v)\right\}\mathrm{d}v, \tag{4.39}$$

where $e_{\mathrm{gs}}$ denotes the ground state energy per site.

The TBA equations, which characterize the equilibrium state, are derived from the minimization of the free energy $f = e - Ts$ under the constraint of (4.37) [4]. The entropy per site is given by

$$\begin{aligned} s = \sum_{j=1}^{\nu}\int_{-\infty}^{\infty} \big[&(\rho_j(v) + \rho_j^h(v))\log(\rho_j(v) + \rho_j^h(v)) \\ &-\rho_j(v)\log\rho_j(v) - \rho_j^h(v)\log\rho_j^h(v)\big]\,\mathrm{d}v. \end{aligned} \tag{4.40}$$

The resulting TBA equations assume the form:

$$\log\eta_j(v) = -\beta A s_j(v) + \sum_{l=1}^{\nu} K_{jl} * \log(1+\eta_l)[v]. \tag{4.41}$$

The density of holes can be expressed in terms of the $\eta_j(v)$ functions:

$$\rho_j^{\mathrm{h}}(v) = -\frac{1}{A}\partial_\beta \log(1+\eta_j(v)) \quad (1 \le j \le \nu). \tag{4.42}$$

This equation can be verified by substituting it into (4.37).

Note that the asymptotic behaviour of the driving term in (4.61) is $\mathrm{e}^{-\frac{\pi}{2}|v|}$, but the solutions have longer ranged asymptotics. We find for $\log\eta_j(v)$ and for $\rho_j^{\mathrm{h}}(v)$ the asymptotics $\mathrm{e}^{-\frac{\pi}{\nu}|v|}$ with $\nu > 2$.

For a large system size, the non-linear integral equation (NLIE) for $Y_j(v)$ can be replaced by the "thermal" NLIE:

$$\log Y_j^{\mathrm{th}}(v) = p_j(v) + g_j^{\mathrm{th}}(v) + \sum_{l=1}^{\nu} K_{jl} * \log(1+Y_l^{\mathrm{th}})[v], \tag{4.43}$$

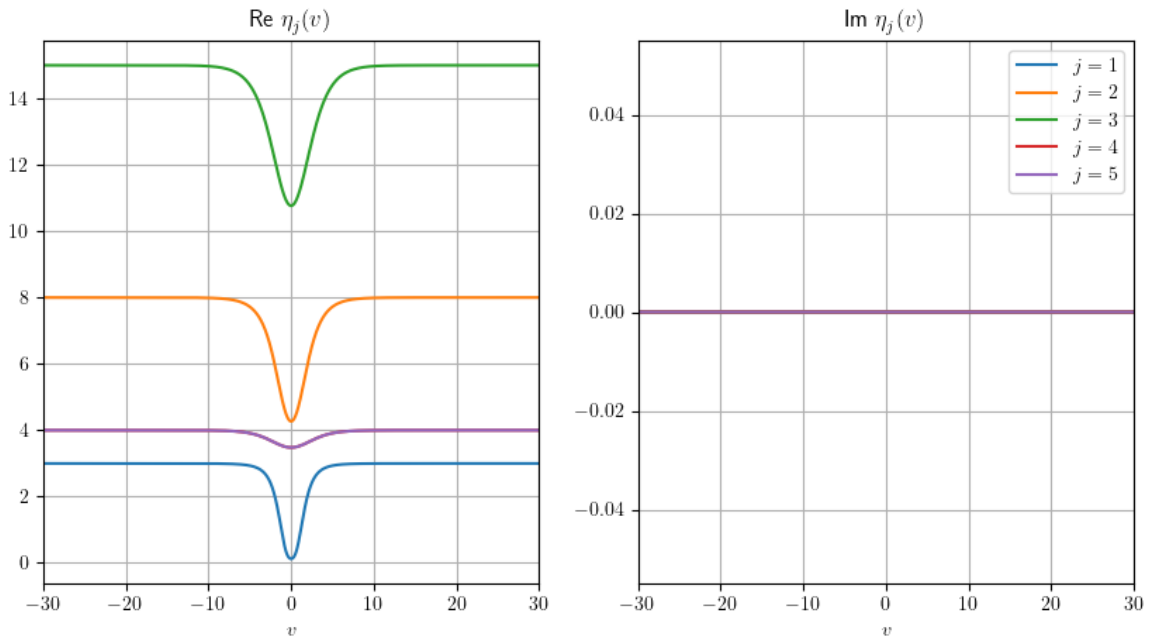



Figure 4.2: Plot of the functions $\eta_j(v)$ for $\nu = 5$. The asymptotic behavior is given by $\eta_j(v) = j(j+1)$ for $j < \nu - 1$, while $\eta_{\nu-1}(v) = \eta_\nu(v) = \nu - 1$.

with

$$g_j^{\rm th}(v) = L \sum_{l=1}^{\nu} A_{jl}\, p * \rho_l^{\rm h}[v]. \tag{4.44}$$

The thermal Y-functions $Y_j^{\rm th}(v)$ represent quantum eigenstates that characterize thermal equilibrium ensembles. Just as the general functions $Y_j(v)$ characterize arbitrary excited states through their discrete zeros and analytic structure, the thermal functions $Y_j^{\rm th}(v)$ play the analogous role for the special class of states that constitute a finite-temperature statistical ensemble. This situation arises in the thermodynamic limit of large system size $L \gg 1$, where discrete quantum states are well approximated by continuous thermal distribution functions. This formulation offers a powerful bridge between exact quantum mechanics and macroscopic thermodynamic behavior, enabling precise computations of finite-temperature transport properties in integrable quantum systems.

To numerically evaluate $Y_j^{\rm th}(v)$, we follow these steps:

1. Solve equation (4.41).
2. Construct the driving term (4.44).
3. Finally, solve the non-linear integral equations (4.43) through numerical iteration.

In some cases, it is more manageable to consider the functions $Y_j^{\rm th}(v)$ and $\eta_j(v)$ at shifted imaginary lines. In our calculations, we often use lines $v \to v \pm \frac{\rm i}{2}$.

It is important to highlight that in our approach, the TBA equations are formulated using only the analytical properties of the Y-system. In contrast, Zotos' approach, as explained in Chapter 2, relies on the string hypothesis.

## 4.4 Calculation of the $g$-function from the zeros of $Y$-functions

Alternatively, the driving term $g_j(v)$ can be computed for small $L$ by numerically finding the zeros of the $Y$-functions. This approach provides a direct computational method that complements the thermodynamic Bethe ansatz formulation. We apply Newton's method to the equation

$$\log Y_j(v + \frac{\rm i}{2})\big|_{\zeta_j^k} + 2\pi {\rm i} I_j^k = 0. \tag{4.45}$$

The parameters $\zeta_j^k$ can be obtained through numerical iterations over $n$ steps:

$$[\zeta_j^k]_{n+1} = [\zeta_j^k]_n + [\Delta\zeta_j^k]_n, \tag{4.46}$$

where $[\zeta_j^k]_0$ is the initial guess, $[\Delta\zeta_j^k]_0 = 0$, and as $n$ becomes large, the approximated solution converges to the true solution, $[\zeta_j^k]_{n\to\infty} = \zeta_j^k$. The iterative process typically

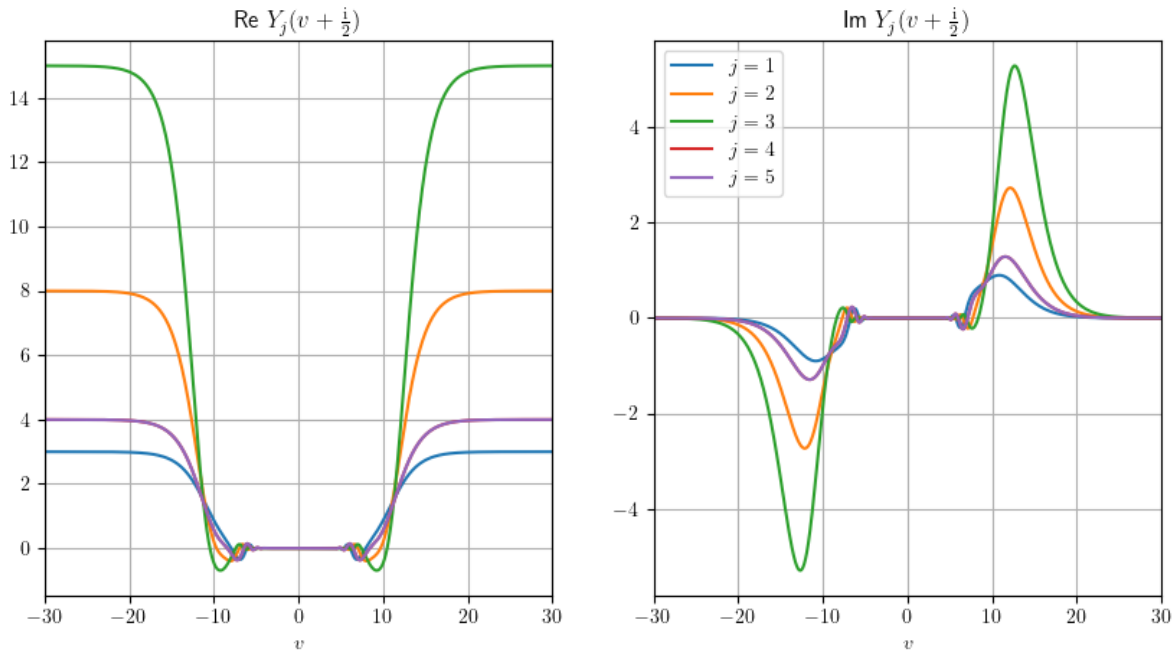



Figure 4.3: Plot of the functions $Y_j^{\text{th}}\left(v+\frac{i}{2}\right)$ for $\nu=5$. Note that they exhibit the same asymptotic behavior as $\eta_j(v)$.

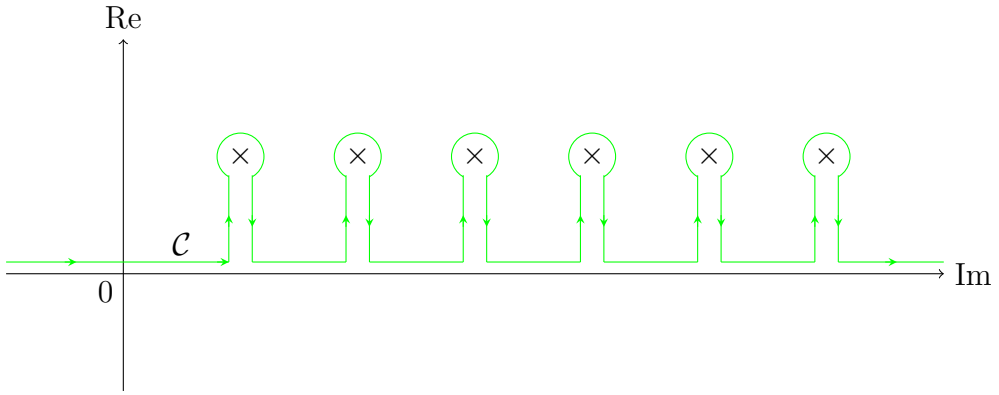



Figure 4.4: An illustration of a modified contour $\mathcal{C}$ encircling $\zeta_j^k + \mathrm{i}$ in a clockwise direction for the function $1 + Y_j(v)$.

converges within a few steps provided the initial guess is reasonably close to the actual zero. The increment is given by

$$[\Delta\zeta_j^k]_n = -\frac{\log Y_j(v+\frac{\mathrm{i}}{2}) + 2\pi\mathrm{i}I_j^k}{\big(\log Y_j(v+\frac{\mathrm{i}}{2})\big)'}\bigg|_{[\zeta_j^k]_n}. \tag{4.47}$$

Let us now consider the case where the number $m_j$ of parameters $\zeta_j^k$ is given by integrating over the densities

$$m_j = L\int_{-\infty}^{\infty}\rho_j(v)\mathrm{d}v, \tag{4.48}$$

the initial guess $[\zeta_j^k]_0$ is chosen such that it satisfies the following equation:

$$\int_{-\infty}^{\zeta_j^k}\rho_j(v)\mathrm{d}v = \frac{1}{L}\left(k-\frac{1}{2}\right) \quad (k=1,2,\ldots,m_j). \tag{4.49}$$

This choice ensures that the initial distribution of zeros approximates the thermal density distribution, providing an optimal starting point for the iterative procedure. The solutions can then be used to construct the $g$-functions as described in equation (4.23) and to evaluate the Drude weight with high numerical precision for finite-size systems.

## 4.5 Drude weight analysis

Another way to express the equation (4.44) is by "hiding" the driving term $g_j(v)$ into a modified contour such, as shown in figure 4.4

$$\log Y_j^{\mathrm{th}}(v) = p_j(v) + \sum_{l=1}^{\nu} K_{jl} \underset{\mathcal{C}_j}{*} \log(1+Y_l^{\mathrm{th}})[v] \tag{4.50}$$

here, the convolution integral is defined over the contour $\mathcal{C}_j$.

On the other hand, the Drude weight can be written as

$$\begin{aligned} D &= \lim_{L\to\infty} \frac{AL}{2\pi \mathrm{i}} \sum_{j=1}^{\nu} \int_{\mathcal{C}_j} \mathrm{d}v\, s'(v-\mathrm{i})\partial_\phi^2 \log(1+\mathrm{Y_j^{th}(v)})\Big|_{\phi=0,\psi=0} \\ &= \lim_{L\to\infty} \frac{AL}{2\pi \mathrm{i}} \sum_{j=1}^{\nu} \int_{\mathcal{C}_j} \mathrm{d}v \frac{(\partial_\phi \log Y_j^{\mathrm{th}}(v))^2 \partial_\psi \log(1+Y_j^{\mathrm{th}}(v))}{1+Y_j^{\mathrm{th}}(v)}\Big|_{\phi=0,\psi=0}. \end{aligned} \tag{4.51}$$

In the passage from the first to the second line, the dressed function formalism has been used. For the detailed calculation, one may consult Appendix B of [38]. The main property for this calculation is the symmetry of the kernel $K_{jl}(v) = K_{lj}(v) = K_{lj}(-v)$. This symmetry allows us to simplify the expression for the Drude weight.

We note that

$$\left(\partial_\phi \log Y_j^{\mathrm{th}}(v)\right)^2\Big|_{\phi=0,\psi=0} = -\frac{\nu^2}{4}(\delta_{j\nu-1} + \delta_{j\nu}) \tag{4.52}$$

and $Y_{\nu-1}^{\mathrm{th}}(v) = Y_\nu^{\mathrm{th}}(v)$. Then the equation for the Drude weight can be written as

$$D = -\frac{AL\nu^2}{4\pi \mathrm{i}} \int_{\mathcal{C}_\nu} \mathrm{d}v \frac{\partial_\psi \log(1+Y_\nu^{\mathrm{th}}(v))}{1+Y_\nu^{\mathrm{th}}(v)}\Big|_{\phi=0,\psi=0}. \tag{4.53}$$

In the following, as already done above, we carry out derivatives with respect to $\phi$ and/or $\psi$ and finally set these parameters to zero. This is sometimes done implicitly by omitting the symbols $\phi = 0$ and $\psi = 0$ for brevity. Modifying the integrand as

$$\frac{\partial_\psi \log(1+Y)}{1+Y} = \frac{Y\partial_\psi \log Y}{(1+Y)^2} = -\frac{\partial_\psi \log Y}{\partial_v \log Y}\partial_v\left(\frac{1}{1+Y}\right) \tag{4.54}$$

and integrating by parts, we find

$$D = \frac{AL\nu^2}{4\pi \mathrm{i}}\left[\frac{\partial_\psi \log Y_\nu^{\mathrm{th}}(v)}{\partial_v \log Y_\nu^{\mathrm{th}}(v)} \frac{1}{1+Y_\nu^{\mathrm{th}}(v)}\Big|_{-\infty}^{\infty} - \int_{\mathcal{L}_\nu} \frac{\mathrm{d}v}{1+Y_\nu^{\mathrm{th}}(v)} \partial_v \left\{\frac{\partial_\psi \log Y_\nu^{\mathrm{th}}(v)}{\partial_v \log Y_\nu^{\mathrm{th}}(v)}\right\}\right]. \tag{4.55}$$

The factor $1/(1+Y_\nu^{\mathrm{th}}(v))$ in the integrand of the above equation has poles at $v = \zeta_\nu^k + \mathrm{i}$ with residues

$$\frac{1}{Y_\nu^{\mathrm{th}\prime}(\zeta_\nu^k + \mathrm{i})} = \frac{1}{Y_\nu^{\mathrm{th}}(\zeta_\nu^k + \mathrm{i})\left[\log Y_\nu^{\mathrm{th}}(\zeta_\nu^k + \mathrm{i})\right]'} = -\frac{1}{\left[\log Y_\nu^{\mathrm{th}}(\zeta_\nu^k + \mathrm{i})\right]'}. \tag{4.56}$$

Using Cauchy's theorem, we modify the integration contour $\mathcal{L}_\nu$ 4.4 to the straight line.

Then performing again an integration by parts, which cancels the surface terms, we obtain

$$\begin{aligned} D =& -\frac{AL\nu^2}{2}\sum_{k=1}^{m_\nu}\frac{1}{\partial_v \log Y_\nu^{\mathrm{th}}(v)}\partial_v\left\{\frac{\partial_\psi \log Y_\nu^{\mathrm{th}}(v)}{\partial_v \log Y_\nu^{\mathrm{th}}(v)}\right\}\Big|_{v=\zeta_\nu^k+\mathrm{i}} \\ &+\frac{AL\nu^2}{4\pi\mathrm{i}}\int_{-\infty}^{\infty}\mathrm{d}v\partial_v\left\{\frac{1}{1+Y_\nu^{\mathrm{th}}(v)}\right\}\frac{\partial_\psi \log Y_\nu^{\mathrm{th}}(v)}{\partial_v \log Y_\nu^{\mathrm{th}}(v)} \\ =& -\frac{AL^2\nu^2}{2}\int_{-\infty}^{\infty}\mathrm{d}v\frac{\rho_\nu^{\mathrm{h}}(v)}{\partial_v \log Y_\nu^{\mathrm{th}}(v+\mathrm{i})}\partial_v\left\{\frac{\partial_\psi \log Y_\nu^{\mathrm{th}}(v+\mathrm{i})}{\partial_v \log Y_\nu^{\mathrm{th}}(v+\mathrm{i})}\right\} \\ &+\frac{AL\nu^2}{4\pi\mathrm{i}}\int_{-\infty}^{\infty}\mathrm{d}v\partial_v\left\{\frac{1}{1+Y_\nu^{\mathrm{th}}(v)}\right\}\frac{\partial_\psi \log Y_\nu^{\mathrm{th}}(v)}{\partial_v \log Y_\nu^{\mathrm{th}}(v)}. \end{aligned} \tag{4.57}$$

Note that we have implicitly taken $\phi \to 0$ and $\psi \to 0$ as explained above. Let us now integrate by parts the first term

$$\begin{aligned} D =& -\frac{AL^2\nu^2}{2}\Bigg(\left[\frac{\rho_\nu^{\mathrm{h}}(v)}{\partial_v \log Y_\nu^{\mathrm{th}}(v+\mathrm{i})}\frac{\partial_\psi \log Y_\nu^{\mathrm{th}}(v+\mathrm{i})}{\partial_v \log Y_\nu^{\mathrm{th}}(v+\mathrm{i})}\right]_{-\infty}^{\infty} \\ &-\int_{-\infty}^{\infty}\mathrm{d}v\partial_v\left\{\frac{\rho_\nu^{\mathrm{h}}(v)}{\partial_v \log Y_\nu^{\mathrm{th}}(v+\mathrm{i})}\right\}\frac{\partial_\psi \log Y_\nu^{\mathrm{th}}(v+\mathrm{i})}{\partial_v \log Y_\nu^{\mathrm{th}}(v+\mathrm{i})}\Bigg) \\ &+\frac{AL\nu^2}{4\pi\mathrm{i}}\Bigg(\frac{\partial_\psi \log Y_\nu^{\mathrm{th}}(\infty)}{\partial_v \log Y_\nu^{\mathrm{th}}(\infty)}\int_0^{\infty}\mathrm{d}v\partial_v\left\{\frac{1}{1+Y_\nu^{\mathrm{th}}(v)}\right\} \\ &+\frac{\partial_\psi \log Y_\nu^{\mathrm{th}}(-\infty)}{\partial_v \log Y_\nu^{\mathrm{th}}(-\infty)}\int_{-\infty}^{0}\mathrm{d}v\partial_v\left\{\frac{1}{1+Y_\nu^{\mathrm{th}}(v)}\right\}\Bigg). \end{aligned} \tag{4.58}$$

In the third and fourth lines of (4.58), we have factored out the ratio of the derivatives, as it remains constant outside the central region, where the other term vanishes. We will analyze this behavior in more detail in the final part of this section. Furthermore, we have used (4.34) and the definition of $\eta_j(v)$ to express the equation in terms of $\eta_j(v)$. The symmetry properties of the derivatives of $\log Y_\nu(v)$ allow us to further simplify the equation.

$$\begin{aligned} D =& \frac{AL\nu^2}{4\pi\mathrm{i}}\Bigg(\left[\frac{\eta_\nu(v)}{1+\eta_\nu(v)}\frac{\partial_\psi \log Y_\nu^{\mathrm{th}}(v+\mathrm{i})}{\partial_v \log Y_\nu^{\mathrm{th}}(v+\mathrm{i})}\right]_{-\infty}^{\infty} \\ &-\int_{-\infty}^{\infty}\mathrm{d}v\partial_v\left\{\frac{\eta_\nu(v)}{1+\eta_\nu(v)}\right\}\frac{\partial_\psi \log Y_\nu^{\mathrm{th}}(v+\mathrm{i})}{\partial_v \log Y_\nu^{\mathrm{th}}(v+\mathrm{i})} \\ &+2\frac{\partial_\psi \log Y_\nu^{\mathrm{th}}(\infty)}{\partial_v \log Y_\nu^{\mathrm{th}}(\infty)}\int_0^{\infty}\mathrm{d}v\partial_v\left\{\frac{1}{1+Y_\nu^{\mathrm{th}}(v)}\right\}\Bigg). \end{aligned} \tag{4.59}$$

Taking into account the asymptotic values of $\eta_\nu(v)$ and $Y_\nu^{\mathrm{th}}(v)$, the first and the third

terms will cancel each other. Thus, we obtain

$$\begin{aligned} D = \frac{AL\nu^2}{4\pi\mathrm{i}}\Bigg(2\frac{\nu-1}{\nu}\frac{\partial_\psi \log Y_\nu^{\mathrm{th}}(\infty)}{\partial_v \log Y_\nu^{\mathrm{th}}(\infty)} - 2\frac{\partial_\psi \log Y_\nu^{\mathrm{th}}(\infty)}{\partial_v \log Y_\nu^{\mathrm{th}}(\infty)}\frac{\nu-1}{\nu} \\ - \int_{-\infty}^{\infty}\mathrm{d}v\partial_v\left\{\frac{\eta_\nu(v)}{1+\eta_\nu(v)}\right\}\frac{\partial_\psi \log Y_\nu^{\mathrm{th}}(v+\mathrm{i})}{\partial_v \log Y_\nu^{\mathrm{th}}(v+\mathrm{i})}\Bigg) \\ = -\frac{AL\pi}{4\beta^2\mathrm{i}}\int_{-\infty}^{\infty}\mathrm{d}v\frac{\eta_\nu(v)\partial_v\log\eta_\nu(v)}{(1+\eta_\nu(v))^2}\frac{\partial_\psi \log Y_\nu^{\mathrm{th}}(v+\mathrm{i})}{\partial_v \log Y_\nu^{\mathrm{th}}(v+\mathrm{i})}. \end{aligned} \tag{4.60}$$

If we perform the substitution (valid for large $L$, see the discussion after (4.69))

$$\frac{\partial_v \log\eta_\nu(v)}{\partial_\beta \log\eta_\nu(v)} \backsimeq -2\pi\mathrm{i}L\beta\frac{\partial_\psi \log Y_\nu^{\mathrm{th}}(v+\mathrm{i})}{\partial_v \log Y_\nu^{\mathrm{th}}(v+\mathrm{i})} \tag{4.61}$$

we will get the Drude weight formula derived by Zotos

$$D = -\frac{A}{8\gamma^2\beta}\int_{-\infty}^{\infty}\mathrm{d}v\frac{\eta_\nu(v)}{(1+\eta_\nu(v))^2}\frac{(\partial_v\log\eta_\nu(v))^2}{\partial_\beta\log\eta_\nu(v)}. \tag{4.62}$$

This shows that our approach is consistent with the results obtained by Zotos, provided that (4.61) holds. We have both numerical and analytical arguments supporting its validity. In Figure 4.5, we plotted its right-hand side, which exhibits a formidable overlap with the left-hand side. The difference between the two sides, given by $\mathrm{LHS}-\mathrm{RHS} \sim \alpha e^{-cL}$ for some positive constants $\alpha$ and $c$, becomes exponentially small as the system size increases, confirming the validity of the relation in the thermodynamic limit.

In order to provide an analytical justification for (4.61), let us analyze our system in two distinct regions: the asymptotic region ($v > v_l$) and the central region ($v < v_l$). Here, $v_l$ denotes the transition point, which we assume to be $v_l \approx \frac{\nu}{\pi}\log L$ for our calculations (see note after (4.42)). In both regions, the following equation holds:

$$\begin{aligned} \partial_v \log Y_j^{\mathrm{th}}(v+\mathrm{i}) = \partial_v p_j(v+\mathrm{i}) - 2\pi\mathrm{i}L\sum_{l=1}^{\nu}\int_{-\infty}^{\infty}\mathrm{d}x K_{jl}(v-x)\rho_l^h(x) \\ + \sum_{l=1}^{\nu}\int_{-\infty}^{\infty}\mathrm{d}x K_{jl}(v-x)\frac{Y_l^{\mathrm{th}}(x+\mathrm{i})}{1+Y_l^{\mathrm{th}}(x+\mathrm{i})}\partial_v\log Y_l^{\mathrm{th}}(x+\mathrm{i}) \end{aligned} \tag{4.63}$$

In the central region ($v < v_l$), the last integral becomes negligible. Consequently, we can simplify the equation as follows:

$$\begin{aligned} \partial_v \log Y_j^{\mathrm{th}}(v+\mathrm{i}) = 2\pi\mathrm{i}s(v) + \frac{2\pi\mathrm{i}L}{A}\sum_{l=1}^{\nu}\int_{-\infty}^{\infty}\mathrm{d}x K_{jl}(v-x)\partial_\beta\log(1+\eta_j(v)) \\ = \frac{2\pi\mathrm{i}L}{A}\partial_\beta\log\eta_j(v). \end{aligned} \tag{4.64}$$

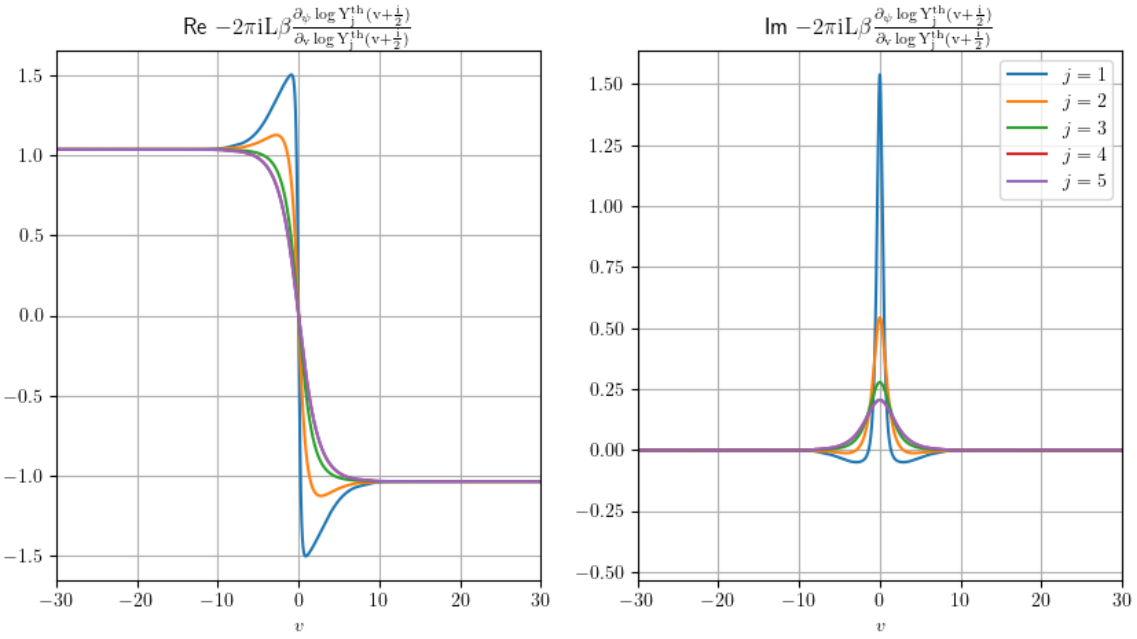



Figure 4.5: Right hand side of the (4.61) for $\nu = 5$.

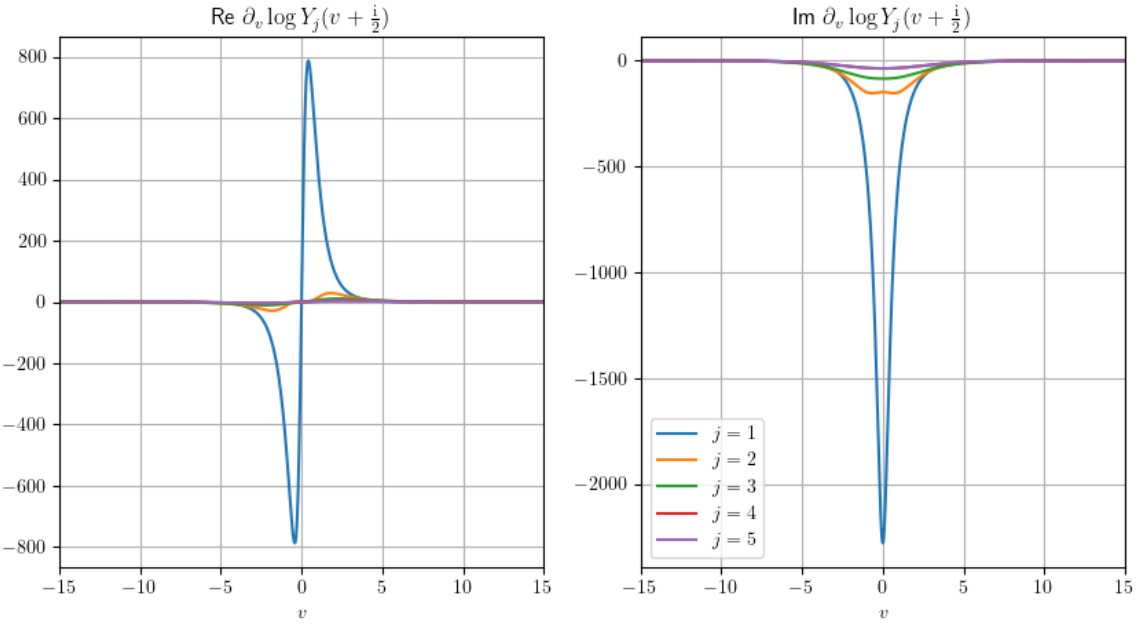



Figure 4.6: $v$-derivatives $Y$-functions.

For the $\psi$-derivatives, we have

$$\begin{aligned}\partial_\psi \log Y_j^{\rm th}(v+\mathrm{i}) &= s'(v)\\ &+\sum_{l=1}^{\nu}\int_{-\infty}^{\infty}\mathrm{d}x K_{jl}(v-x)\Big(\frac{-2\pi\mathrm{i}L\rho_l^h(x)}{\partial_v \log Y_l^{\rm th}(x+\mathrm{i})}+\frac{Y_l^{\rm th}(x+\mathrm{i})}{1+Y_l^{\rm th}(x+\mathrm{i})}\Big)\partial_\psi \log Y_l^{\rm th}(x+\mathrm{i})\end{aligned} \tag{4.65}$$

Here, the first term in the summation arises from the contributions of the zeros $\zeta_j^k$. For $v<v_l$ we can again neglect the second term in the second line and use

$$\frac{-2\pi\mathrm{i}L\rho_l^h(v)}{\partial_v \log Y_j^{\rm th}(v+\mathrm{i})}=\frac{\eta_j(v)}{1+\eta_j(v)} \tag{4.66}$$

then

$$\partial_\psi \log Y_j^{\rm th}(v+\mathrm{i}) = s'(v)+\sum_{l=1}^{\nu}\int_{-\infty}^{\infty}\mathrm{d}x K_{jl}(v-x)\frac{\eta_j(v)}{1+\eta_j(v)}\partial_\psi \log Y_l^{\rm th}(x+\mathrm{i}) \tag{4.67}$$

from which follows

$$\partial_\psi \log Y_j^{\rm th}(v+\mathrm{i}) = -\frac{1}{\beta A}\partial_v \log \eta_j(v) \tag{4.68}$$

as both functions satisfy the same linear integral equation. Now (4.64) combined with (4.68) can be used to show that the equation in (4.61) holds in the central region.

We now turn to the asymptotic region and provide arguments that (4.61) also holds there. Assuming that the integral equations (4.63) and (4.65) admit a unique solution, we demonstrate that imposing (4.61) leads to the expected solution for $\partial_\psi \log Y_j^{\rm th}(v)$ in terms of $\partial_v \log Y_j^{\rm th}(v)$. We rewrite (4.61) as

$$\frac{\partial_\psi \log Y_j^{\rm th}(v+\mathrm{i})}{\partial_v \log Y_j^{\rm th}(v+\mathrm{i})}=\frac{\mathrm{i}}{2\pi L\beta}\frac{\partial_v \log \eta_j(v)}{\partial_\beta \log \eta_j(v)}\,, \tag{4.69}$$

where the asymptotics of the rhs is a number $R$ independent of the index $j$. Next, we use (4.63) for all arguments $v$ and check whether the integral equations (4.63) and (4.65) are satisfied. In fact, for $|v|<v_l$ this has already been done. We now look at (4.65) for $|v|>v_l$. In (4.63) and (4.65) we may drop the driving term, see the note after (4.42). The rhs of (4.65) consists of integrals with a quickly decaying kernel; this requires that not only $v$ but also $x$ be large. Hence, the ratio of $\psi$- and $v$-derivatives of $\log Y^{\rm th}$ can be replaced by $R$:

$$\begin{aligned}\partial_\psi \log Y_j^{\rm th}(v+\mathrm{i}) = R\Big[&-2\pi\mathrm{i}L\sum_{l=1}^{\nu}\int_{-\infty}^{\infty}\mathrm{d}x\, K_{jl}(v-x)\,\rho_l^h(x)\\ &+\sum_{l=1}^{\nu}\int_{-\infty}^{\infty}\mathrm{d}x\, K_{jl}(v-x)\,\frac{Y_l^{\rm th}(x+\mathrm{i})}{1+Y_l^{\rm th}(x+\mathrm{i})}\,\partial_v \log Y_l^{\rm th}(x+\mathrm{i})\Big]\,,\end{aligned} \tag{4.70}$$

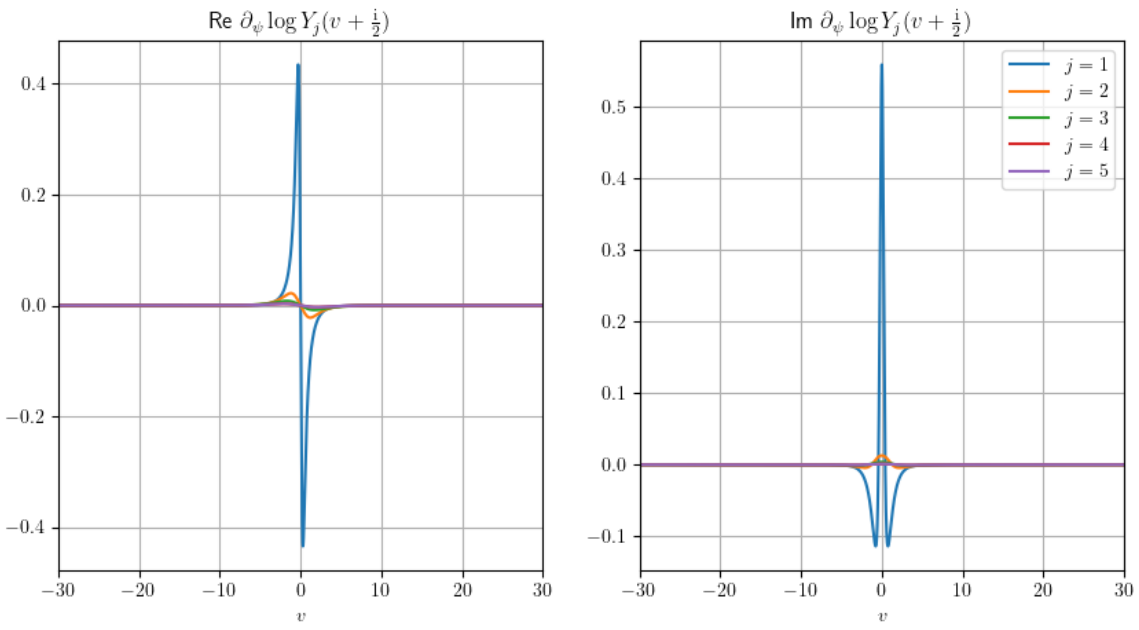



Figure 4.7: $\psi$-derivatives $Y$-functions.

and this is $R$ times the rhs of (4.63) without the driving term. We therefore see that $\partial_\psi \log Y_j^{\text{th}}$ from (4.69) satisfies the integral equation (4.65) if $\partial_v \log Y_j^{\text{th}}$ satisfies (4.63).

These considerations demonstrate that (4.61) holds consistently in both the central and asymptotic regions, thereby providing analytical support for the numerical results.

## 4.6 $T$- $Y$-system at root of unity

To further reinforce the validity of the relation given in (4.61), we will study the $T$- and $Y$-systems at the root of unity for the more intricate case of $\nu_1 = 2$, $\nu_2 = 2$. Following this, we will compute the Drude weight for this specific scenario and compare it with Zotos' result.

In their work [34], Kuniba, Sakai, and Suzuki derived non-linear integral equations for the $T$- and $Y$-functions for the anisotropy of the form $\Delta = \cos\frac{\pi}{\nu}$, where $\nu$ is a rational number not smaller than 2, as defined in (3.108).

In this section we will present the fundamental formulas for the general case of the $T$- and $Y$-systems, with $\pi/\gamma = [\nu_1, \ldots, \nu_\alpha]$, before progressing to the specific example of $\pi/\gamma = [\nu_1 = 2, \nu_2 = 2]$, which will be discussed in detail in the subsequent section.

The $T$-functions, as defined in (4.9), satisfy the relation

$$T_{y_\alpha + y_{\alpha-1}-1}(v) = T_{y_\alpha - y_{\alpha-1}-1}(v) + 2(-1)^{mz_\alpha} T_{y_{\alpha-1}-1}(v + iy_\alpha) \tag{4.71}$$

valid for $1 \leq j \leq m_\alpha - 1$ and $m$ is the number of BAE roots. The $Y$-functions can be expressed in terms of the $T$-functions as

$$\begin{aligned}
Y_j(v) &= \frac{T_{\tilde{n}_{j+1}+y_r-1}(v+iw_j\nu)T_{\tilde{n}_{j+1}-y_r-1}(v+iw_j\nu)}{T_{y_r-1}(v+i\tilde{n}_{j+1}+iw_j\nu)T_{y_r-1}(v-i\tilde{n}_{j+1}+iw_j\nu)}, \\
1+Y_j(v) &= \frac{T_{\tilde{n}_{j+1}-1}(v+iy_r+iw_j\nu)T_{\tilde{n}_{j+1}-1}(v-iy_r+iw_j\nu)}{T_{y_r-1}(v+i\tilde{n}_{j+1}+iw_j\nu)T_{y_r-1}(v-i\tilde{n}_{j+1}+iw_j\nu)}, \\
K(v) &= \frac{(-1)^{mz_\alpha}T_{y_\alpha-y_{\alpha-1}-1}(v+i(z_\alpha-z_{\alpha-1}-1)\nu)}{T_{y_{\alpha-1}-1}(v+iy_\alpha+i(z_\alpha-z_{\alpha-1}-1)\nu)}.
\end{aligned} \tag{4.72}$$

To derive the non-linear integral equations for the $Y$-functions, it is essential to establish the functional equations between $Y_j$ and $1+Y_j$. These are given for $m_{r-1} \leq j \leq m_r-2$ ($1 \leq r \leq \alpha$) by

$$Y_j(v+ip_r)Y_j(v-ip_r) = (1+Y_{j-1}(v))^{1-2\delta_{jm_{r-1}}}(1+Y_{j+1}(v)) \tag{4.73}$$

and for $j = m_r - 1$ ($1 \leq r \leq \alpha - 1$) the functional equations become more intricate:

$$\begin{aligned}
&Y_j(v+ip_r+ip_{r+1})Y_j(v-ip_r-ip_{r+1})Y_j(v-ip_r+ip_{r+1})Y_j(v+ip_r-ip_{r+1}) \\
&= \{(1+Y_{j-1}(v+ip_{r+1}))(1+Y_{j-1}(v-ip_{r+1}))\}^{1-2\delta_{1r}}\,(1+Y_{j+1}(v+ip_r)) \\
&\times (1+Y_{j+1}(v-ip_r))(1+Y_j(v+ip_r+ip_{r+1}))(1+Y_j(v-ip_r+ip_{r+1})), \\
&1+Y_{m_\alpha-1}(v) = (1+K(v))^2, \\
&K(v+ip_\alpha)K(v-ip_\alpha) = 1+Y_{m_\alpha-2}(v).
\end{aligned} \tag{4.74}$$

The equations in (4.71), (4.72), (4.73) and (4.74) are based on Takahashi-Suzuki (TS) numbers, denoted by $n_j$ and $\tilde{n}_j$, which are derived from the sequences $m_j$, $y_j$, $z_j$, $p_j$, and $w_j$. They are constructed from continued fraction expansions. The definitions of these numbers are given in figure 4.8.

## 4.7 NLIE derivation for $\nu_1 = 2$, $\nu_2 = 2$

To compute the Drude weight later, we introduce the flux $\phi$ into the system. This is achieved by incorporating a phase into the relations for the $Y$-functions. We focus on the specific case where $\nu_1 = 2$ and $\nu_2 = 2$. The anisotropy is expressed as:

$$\nu = \nu_1 + \frac{1}{\nu_2} = \frac{5}{2}, \quad \gamma = \frac{\pi}{\nu}. \tag{4.75}$$

The Takahashi-Suzuki numbers and other sequences needed to derive our equations are summarized in Table 4.9.

| **Term** | **Definition** |
|---|---|
| $m_j$ | $m_j = \nu_1 + \nu_2 + \cdots + \nu_j$, $0 \leq j \leq \alpha$<br>$m_0 = 0$, $m_{\alpha+1} = \infty$ |
| $y_j$ | $y_j = y_{j-2} + \nu_j y_{j-1}, \quad 1 \leq j \leq \alpha,$<br>$y_{-1} = 0$, $y_0 = 1$, $y_1 = \nu_1$, $y_2 = 1 + \nu_1\nu_2$, |
| $z_j$ | $z_j = z_{j-2} + \nu_j z_{j-1}, \quad 1 \leq j \leq \alpha,$<br>$z_{-1} = 1$, $z_0 = 0$, $z_1 = 1$, $z_2 = \nu_2$, |
| $p_j$ | $p_j = p_{j-2} - \nu_{j-1}p_{j-1}$, $2 \leq j \leq \alpha + 1$<br>$p_0 = \nu, p_1 = 1$, $p_2 = p_0 - \nu_1$, $p_{\alpha+1} = 0$, |
| $n_j$ | $n_j = y_{r-1} + (j - m_r)y_r, \quad m_r \leq j < m_{r+1},$ |
| $\tilde{n}_j$ | $\tilde{n}_j = y_{r-1} + (j - m_r)y_r, \quad m_r < j \leq m_{r+1},$ |
| $w_j$ | $w_j = z_{r-1} + (j - m_r)z_r - 1, \quad m_r \leq j < m_{r+1}.$ |

Figure 4.8: Definition of the TS-numbers. These numbers are associated with the admissible lengths of string solutions of the BAE. For a detailed physical interpretation, see Appendix A of [34] or [25].

| **Term** | **Definition** |
|---|---|
| $m_j$ | $m_0 = 0$, $m_1 = 2$, $m_2 = 4$ $m_{\alpha+1} = \infty$, |
| $y_j$ | $y_{-1} = 0$, $y_0 = 1$, $y_1 = 2$, $y_2 = 5$, |
| $z_j$ | $z_{-1} = 1$, $z_0 = 0$, $z_1 = 1$, $z_2 = 2$, |
| $p_j$ | $p_1 = 1$, $p_2 = \frac{1}{2}$, $p_3 = 0$, |
| $n_j$ | $n_1 = 1$, $n_2 = 1$ |
| $\tilde{n}_j$ | $\tilde{n}_1 = 1$, $\tilde{n}_2 = 2$, $\tilde{n}_3 = 3$, |
| $w_j$ | $w_1 = 0$, $w_2 = -1$. |

Figure 4.9: TS-numbers for constructing the functional relations of the Y- and T-systems in the case $\nu_1 = 2$, $\nu_2 = 2$.

Following the equation (4.72), the $Y$-functions are defined in terms of the $T$-functions as follows:

$$\begin{aligned} Y_1(v) &= \frac{T_2(v)T_0(v)}{T_0(v+2\mathrm{i})T_0(v-2\mathrm{i})}, \\ Y_2(v) &= \frac{T_4(v-\frac{5}{2}\mathrm{i})T_0(v-\frac{5}{2}\mathrm{i})}{T_1(v+\frac{\mathrm{i}}{2})T_1(v-\frac{\mathrm{i}}{2})}, \\ Y_3(v) &= \mathrm{e}^{-\frac{5}{2}\phi\mathrm{i}}\frac{T_2(v)}{T_1(v)}, \\ Y_4(v) &= \mathrm{e}^{\frac{5}{2}\phi\mathrm{i}}\frac{T_2(v)}{T_1(v)} \end{aligned} \tag{4.76}$$

and the relations for $1+Y$ in terms of the $T$-functions are given by:

$$\begin{aligned} 1+Y_1(v) &= \frac{T_1(v+\mathrm{i})T_1(v-\mathrm{i})}{T_0(v+2\mathrm{i})T_0(v-2\mathrm{i})}, \\ 1+Y_2(v) &= \frac{T_2(v+\frac{\mathrm{i}}{2})T_2(v-\frac{\mathrm{i}}{2})}{T_1(v+\frac{\mathrm{i}}{2})T_1(v-\frac{\mathrm{i}}{2})}, \\ (1+Y_3(v))(1+Y_4(v)) &= \frac{T_4(v+2\mathrm{i})T_4(v-2\mathrm{i})}{T_1(v)T_1(v)}. \end{aligned} \tag{4.77}$$

The functional equations for the $Y$-functions are derived using equations (4.73) and (4.74), and are given by:

$$\begin{aligned} &Y_1\Big(v+\frac{3}{2}\mathrm{i}\Big)Y_1\Big(v-\frac{3}{2}\mathrm{i}\Big)Y_1\Big(v+\frac{\mathrm{i}}{2}\Big)Y_1\Big(v-\frac{\mathrm{i}}{2}\Big) = \\ &\Big(1+Y_2(v+\mathrm{i})\Big)(1+Y_2(v-\mathrm{i}))\Big(1+Y_1(v+\frac{\mathrm{i}}{2})\Big)\Big(1+Y_1(v-\frac{\mathrm{i}}{2})\Big), \\ &Y_2\Big(v+\frac{\mathrm{i}}{2}\Big)Y_2\Big(v-\frac{\mathrm{i}}{2}\Big) = \Big(1+Y_1(v)\Big)^{-1}\Big(1+Y_3(v)\Big)\Big(1+Y_4(v)\Big), \\ &Y_3\Big(v+\frac{\mathrm{i}}{2}\Big)Y_3\Big(v-\frac{\mathrm{i}}{2}\Big) = \mathrm{e}^{-5\phi\mathrm{i}}\Big(1+Y_2(v)\Big), \\ &Y_4\Big(v+\frac{\mathrm{i}}{2}\Big)Y_4\Big(v-\frac{\mathrm{i}}{2}\Big) = \mathrm{e}^{5\phi\mathrm{i}}\Big(1+Y_2(v)\Big). \end{aligned} \tag{4.78}$$

The following relations hold and have been used to formulate the previous equations:

$$\begin{aligned} T_6(v) &= T_2(v) + 2\cos\left(\frac{5}{2}\phi\right)T_1(v), \\ T_n(v) &= T_n(v+5\mathrm{i}), \\ Q(v) &= Q(v+10\mathrm{i}). \end{aligned} \tag{4.79}$$

As with the simple root of unity, the thermodynamics of the zeros of the $Y$-functions can also, in this case, be described in terms of the density of particles $\rho_j(v)$ and the density of holes $\rho_j^h(v)$. These quantities are defined as:

$$\begin{aligned}
\rho_1^h(v) + \rho_1(v) &= -\lim_{L\to\infty} \frac{1}{2\pi \mathrm{i} L} \partial_v \log Y_1(v+\mathrm{i}), \\
\rho_2^h(v) + \rho_2(v) &= \lim_{L\to\infty} \frac{1}{2\pi \mathrm{i} L} \partial_v \log Y_2(v+\mathrm{i}), \\
\rho_3^h(v) + \rho_3(v) &= \lim_{L\to\infty} \frac{1}{2\pi \mathrm{i} L} \partial_v \log Y_3(v+\mathrm{i}) \\
\rho_4^h(v) + \rho_4(v) &= \lim_{L\to\infty} \frac{1}{2\pi \mathrm{i} L} \partial_v \log Y_4(v+\mathrm{i}).
\end{aligned} \tag{4.80}$$

Please note that the densities with index 3 are identical to those with index 4. However, we keep them separate to reflect their relationship with the $Y$-functions, where $Y_3(v)$ differs from $Y_4(v)$ due to the flux $\phi$.

The densities of particles and holes are further related by linear integral equations:

$$\begin{aligned}
\rho_1(v) + \rho_1^h(v) &= s_1(v) + s_1 * \rho_1^h[v] - s_2 * \rho_2^h[v], \\
\rho_2(v) + \rho_2^h(v) &= s_2 * (\rho_1^h + \rho_3^h + \rho_4^h)[v], \\
\rho_3(v) + \rho_3^h(v) &= s_2 * \rho_2^h[v], \\
\rho_4(v) + \rho_4^h(v) &= s_2 * \rho_2^h[v],
\end{aligned} \tag{4.81}$$

where the driving terms are defined as:

$$s_1(v) = \frac{1}{4\cosh(\frac{\pi}{2}v)}, \quad s_2(v) = \frac{1}{2\cosh(\pi v)}. \tag{4.82}$$

By minimizing the free energy $f = e - Ts$, under the constraint of linear integral equations (4.81), we derive TBA equations for $\eta_j(v) = \rho_j^h(v)/\rho_j(v)$:

$$\begin{aligned}
\log \eta_1(v) &= -\beta A s_1(v) + s_1 * \log(1+\eta_1)[v] + s_2 * \log(1+\eta_2)[v], \\
\log \eta_2(v) &= -s_2 * \log(1+\eta_1)[v] + s_2 * \log(1+\eta_3)[v] + s_2 * \log(1+\eta_4)[v], \\
\log \eta_3(v) &= s_2 * \log(1+\eta_2)[v], \\
\log \eta_4(v) &= s_2 * \log(1+\eta_2)[v].
\end{aligned} \tag{4.83}$$

This system of equations can be solved numerically, and the results are shown in Figure 4.10. A relation between the densities of holes and the quantites $\eta_j(v)$ can be estab-

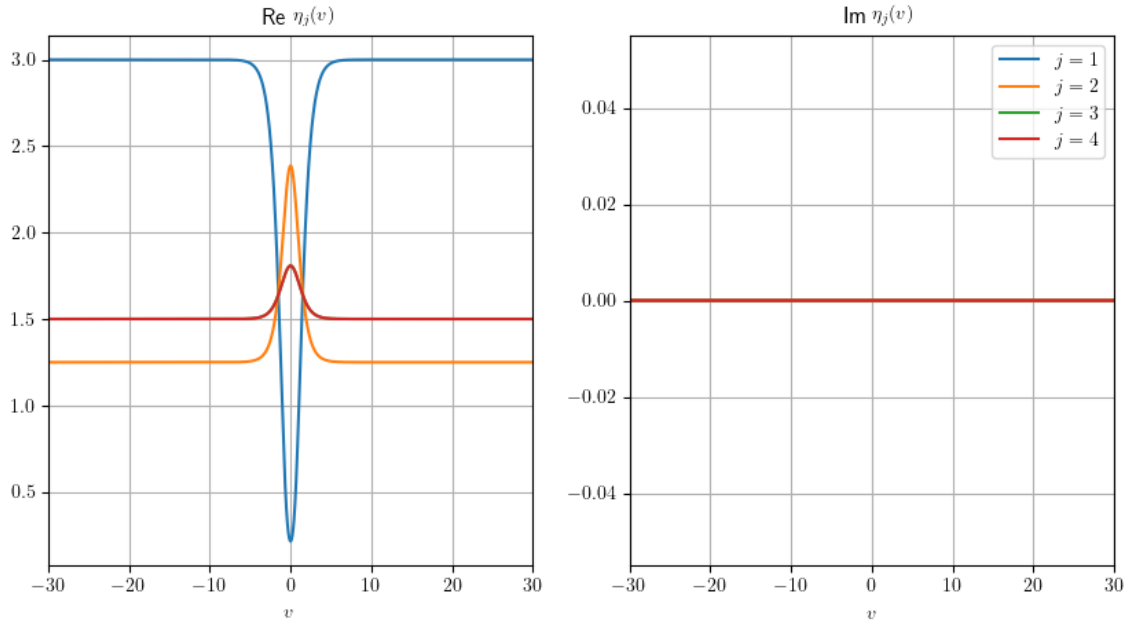



Figure 4.10: Plot of the functions $\eta_j(v)$, solutions of Eq. (4.83), for parameters $\nu_1 = 2$, $\nu_2 = 2$, and inverse temperature $\beta = 1$.

lished by the following equations:

$$\begin{aligned}
\rho_1^h(v) &= -\frac{1}{A}\partial_\beta \log(1+\eta_1(v)),\\
\rho_2^h(v) &= \frac{1}{A}\partial_\beta \log(1+\eta_2(v)),\\
\rho_3^h(v) &= \frac{1}{A}\partial_\beta \log(1+\eta_3(v)),\\
\rho_4^h(v) &= \frac{1}{A}\partial_\beta \log(1+\eta_4(v)),
\end{aligned} \tag{4.84}$$

where the sign can be also understood by looking at the plot of $\eta_j(v)$ in Figure 4.10.

The functional relations (4.78) can be used to derive the NLIEs for the $Y$-functions:

$$\begin{aligned}
\log Y_1^{\mathrm{th}}(v) &= g_1(v) + s_1 * \log(1+Y_1^{\mathrm{th}})[v] + s_2 * \log(1+Y_2^{\mathrm{th}})[v],\\
\log Y_2^{\mathrm{th}}(v) &= g_2(v) + s_2 * (-\log(1+Y_1^{\mathrm{th}}) + \log(1+Y_3^{\mathrm{th}}) + \log(1+Y_4^{\mathrm{th}}))[v],\\
\log Y_3^{\mathrm{th}}(v) &= g_3(v) + s_2 * \log(1+Y_2^{\mathrm{th}})[v],\\
\log Y_4^{\mathrm{th}}(v) &= g_4(v) + s_2 * \log(1+Y_2^{\mathrm{th}})[v],
\end{aligned} \tag{4.85}$$

where the driving terms are given by:

$$\begin{aligned} g_1(v) &= g_1^{\text{th}}(v) + Lp(v) + s'(v-\mathrm{i})\psi, \\ g_2(v) &= g_2^{\text{th}}(v), \\ g_3(v) &= g_3^{\text{th}}(v) - \frac{5}{2}\phi\mathrm{i}, \\ g_4(v) &= g_4^{\text{th}}(v) + \frac{5}{2}\phi\mathrm{i}. \end{aligned} \tag{4.86}$$

We also introduce the fictitious parameter $\psi$, which is necessary for the calculation of the Drude weight and will be set to zero at the end of the calculation.

The driving terms for the excited states, generated by the densities of holes in the $Y$-functions, can be determined from the following conditions:

$$\begin{aligned} \partial_v \log Y_1(v+\mathrm{i}) &= -2\pi\mathrm{i}L\rho_1^T(v), \\ \partial_v \log Y_2(v+\mathrm{i}) &= 2\pi\mathrm{i}L\rho_2^T(v), \\ \partial_v \log Y_3(v+\mathrm{i}) &= 2\pi\mathrm{i}L\rho_3^T(v), \\ \partial_v \log Y_4(v+\mathrm{i}) &= 2\pi\mathrm{i}L\rho_4^T(v) \end{aligned} \tag{4.87}$$

where the $\rho_j^T(v) = \rho_j^h(v) + \rho_j(v)$ are total densities, and

$$\begin{aligned} \partial_v \log(1+Y_1(v+\mathrm{i})) &\approx 0, \\ \partial_v \log(1+Y_2(v+\mathrm{i})) &\approx \partial_v \log Y_2(v+\mathrm{i}), \\ \partial_v \log(1+Y_3(v+\mathrm{i})) &\approx \partial_v \log Y_3(v+\mathrm{i}), \\ \partial_v \log(1+Y_4(v+\mathrm{i})) &\approx \partial_v \log Y_4(v+\mathrm{i}). \end{aligned} \tag{4.88}$$

Now we use the difinition of $\rho_i^T(v)$, (4.87), (4.88), and apply them to the $v$-derivative of (4.85). This produces the following equations:

$$\begin{aligned} \partial_v g_1^{\text{th}}(v+\mathrm{i}) &= -2\pi\mathrm{i}L\big(s_1 * \rho_1^h[v] + s_2 * \rho_2[v]\big), \\ \partial_v g_2^{\text{th}}(v+\mathrm{i}) &= -2\pi\mathrm{i}L\big(s_2 * (-\rho_1^h + \rho_3 + \rho_4)[v]\big), \\ \partial_v g_3^{\text{th}}(v+\mathrm{i}) &= -2\pi\mathrm{i}L\big(s_2 * \rho_2[v]\big), \\ \partial_v g_4^{\text{th}}(v+\mathrm{i}) &= -2\pi\mathrm{i}L\big(s_2 * \rho_2[v]\big) \end{aligned} \tag{4.89}$$

from which we get:

$$\begin{aligned} g_1^{\text{th}}(v) &= Lp_1 * \rho_1^h[v] + Lp_2 * \rho_2[v], \\ g_2^{\text{th}}(v) &= Lp_2 * (-\rho_1^h + \rho_3 + \rho_4)[v], \\ g_3^{\text{th}}(v) &= Lp_2 * \rho_2[v], \\ g_4^{\text{th}}(v) &= Lp_2 * \rho_2[v]. \end{aligned} \tag{4.90}$$

We define the function $p_1(v)$ and $p_2(v)$ as:

$$p_1(v) = p(v) = \log\tanh\frac{\pi}{4}v, \quad p_2(v) = \log\tanh\frac{\pi}{2}(v+\frac{\mathrm{i}}{2}). \tag{4.91}$$

which are related to the driving terms $s_1(v)$ and $s_2(v)$ by:

$$s_1(v) = \frac{-1}{2\pi\mathrm{i}}\partial_v p_1(v+\mathrm{i}), \quad s_2(v) = \frac{-1}{2\pi\mathrm{i}}\partial_v p_2(v+\mathrm{i}). \tag{4.92}$$

## 4.8 Numerical analysis of NLIE for $\nu_1 = 2$, $\nu_2 = 2$

The non-linear equations (4.85) are difficult to treat numerically, as they present a strong oscillatory behavior. In order to avoid this, we introduce the following transformation:

$$\begin{aligned}
\log Y_2(v) &= -\log\frac{1}{Y_2(v)} = -\log\tilde{Y}_2(v),\\
\log Y_3(v) &= -\log\frac{1}{Y_3(v)} = -\log\tilde{Y}_3(v),\\
\log Y_4(v) &= -\log\frac{1}{Y_4(v)} = -\log\tilde{Y}_4(v)
\end{aligned} \tag{4.93}$$

and from this follow the relations:

$$\begin{aligned}
\log(1+Y_2(v)) &= -\log\tilde{Y}_2(v) + \log(1+\tilde{Y}_2(v)),\\
\log(1+Y_3(v)) &= -\log\tilde{Y}_3(v) + \log(1+\tilde{Y}_3(v)),\\
\log(1+Y_4(v)) &= -\log\tilde{Y}_4(v) + \log(1+\tilde{Y}_4(v)).
\end{aligned} \tag{4.94}$$

In momentum space, we solve the following system of equations:

$$\begin{aligned}
\mathcal{F}[\log Y_1](k) &= \mathcal{F}[g_1](k) + \mathcal{F}[s_1](k)\,\mathcal{F}[\log(1+Y_1)](k)\\
&\quad + \mathcal{F}[s_2](k)\,\mathcal{F}\left[\log\left(\frac{1+\tilde{Y}_2}{\tilde{Y}_2}\right)\right](k),\\
\mathcal{F}[\log\tilde{Y}_2](k) &= -\mathcal{F}[g_2](k) + \mathcal{F}[s_2](k)\,\mathcal{F}[\log(1+Y_1)](k)\\
&\quad - \mathcal{F}[s_2](k)\left(\mathcal{F}\left[\log\left(\frac{1+\tilde{Y}_3}{\tilde{Y}_3}\right)\right](k) + \mathcal{F}\left[\log\left(\frac{1+\tilde{Y}_4}{\tilde{Y}_4}\right)\right](k)\right),\\
\mathcal{F}[\log\tilde{Y}_3](k) &= -\mathcal{F}[g_3](k) - \mathcal{F}[s_2](k)\,\mathcal{F}\left[\log\left(\frac{1+\tilde{Y}_2}{\tilde{Y}_2}\right)\right](k),\\
\mathcal{F}[\log\tilde{Y}_4](k) &= -\mathcal{F}[g_4](k) - \mathcal{F}[s_2](k)\,\mathcal{F}\left[\log\left(\frac{1+\tilde{Y}_2}{\tilde{Y}_2}\right)\right](k).
\end{aligned} \tag{4.95}$$

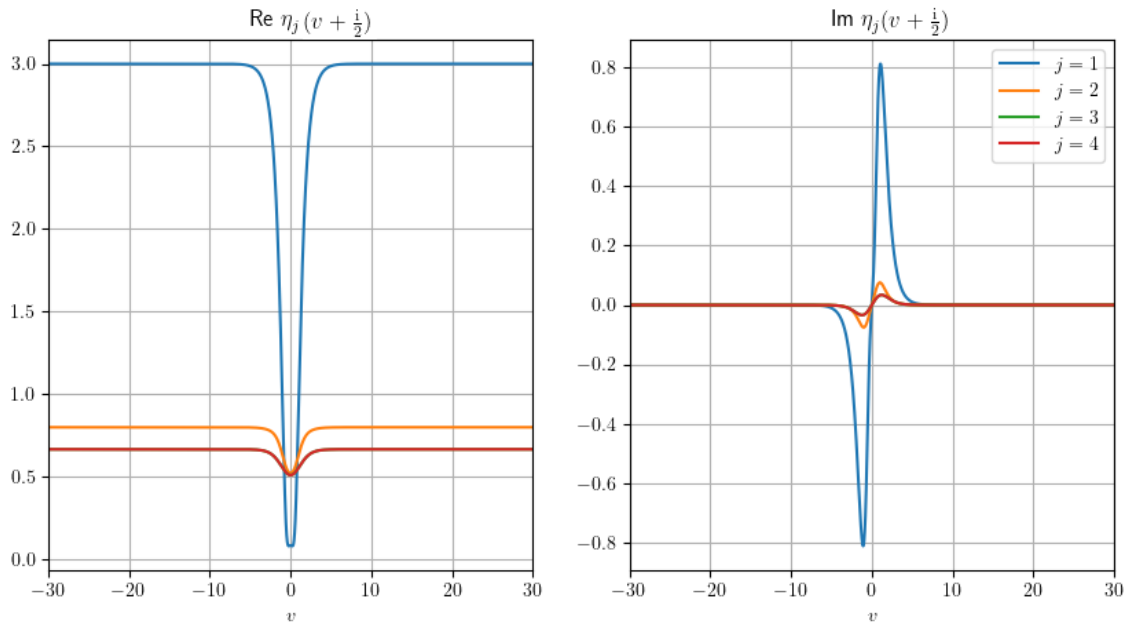



Figure 4.11: Plot of the functions $\eta_j(v+\frac{i}{2})$, solutions of Eq. (4.100), for parameters $\nu_1 = 2$, $\nu_2 = 2$, and inverse temperature $\beta = 1$.

which lead to the following NLIE's:

$$\begin{aligned}
\log Y_1(v) =& h_1(v) + s_3 * \log(1+\tilde{Y}_2)[v] + s_1 * \log(1+\tilde{Y}_3)[v] + s_1 * \log(1+\tilde{Y}_4)[v],\\
\log \tilde{Y}_2(v) =& h_2(v) + s_3 * \log(1+Y_1)[v] - 2s_1 * \log(1+\tilde{Y}_2)[v]\\
&- s_3 * \log(1+\tilde{Y}_3)[v] - s_3 * \log(1+\tilde{Y}_4)[v],\\
\log \tilde{Y}_3(v) =& h_3(v) + s_1 * \log(1+Y_1)[v] - s_3 * \log(1+\tilde{Y}_2)[v]\\
&- s_1 * \log(1+\tilde{Y}_3)[v] - s_1 * \log(1+\tilde{Y}_4)[v],\\
\log \tilde{Y}_4(v) =& h_4(v) + s_1 * \log(1+Y_1)[v] - s_3 * \log(1+\tilde{Y}_2)[v]\\
&- s_1 * \log(1+\tilde{Y}_3)[v] - s_1 * \log(1+\tilde{Y}_4)[v].
\end{aligned} \tag{4.96}$$

Where the driving terms are defined as:

$$\begin{aligned}
h_1(v) &= g_1(v) + s_3 * g_2[v] + s_1 * g_3[v] + s_1 * g_4[v],\\
h_2(v) &= -g_2(v) - 2s_1 * g_2[v] - s_3 * g_3[v] - s_3 * g_4[v],\\
h_3(v) &= -g_3(v) - s_3 * g_2[v] - s_1 * g_3[v] - s_1 * g_4[v],\\
h_4(v) &= -g_4(v) - s_3 * g_2[v] - s_1 * g_3[v] - s_1 * g_4[v]
\end{aligned} \tag{4.97}$$

and its $v$-derivative can be written as:

$$\begin{aligned}
\partial_v h_1(v+i) &= -2\pi i L\Big(s_1(v) + s_3 * \rho_2[v] + s_1 * \rho_3[v] + s_1 * \rho_4[v]\Big),\\
\partial_v h_2(v+i) &= -2\pi i L\Big(s_3 * \rho_1^h[v] - 2s_1 * \rho_2[v] - s_3 * \rho_3[v] - s_3 * \rho_4[v]\Big),\\
\partial_v h_3(v+i) &= -2\pi i L\Big(s_1 * \rho_1^h[v] - s_3 * \rho_2[v] - s_1 * \rho_3[v] - s_1 * \rho_4[v]\Big),\\
\partial_v h_4(v+i) &= -2\pi i L\Big(s_1 * \rho_1^h[v] - s_3 * \rho_2[v] - s_1 * \rho_3[v] - s_1 * \rho_4[v]\Big),
\end{aligned} \tag{4.98}$$

where

$$s_3(k) = \frac{s_1(k)}{s_2(k)} = s_2(k)(1 + 2s_1(k)) = \frac{\cosh\frac{k}{2}}{\cosh k}. \tag{4.99}$$

By introducing these transformations and definitions, we can simplify the numerical treatment of the non-linear equations and make the problem more manageable. The NLIE in (4.96) is, in fact, numerically solvable, and the result can be used to compute the Drude weight. This "partial particle-hole transformation" can also be applied to the densities in

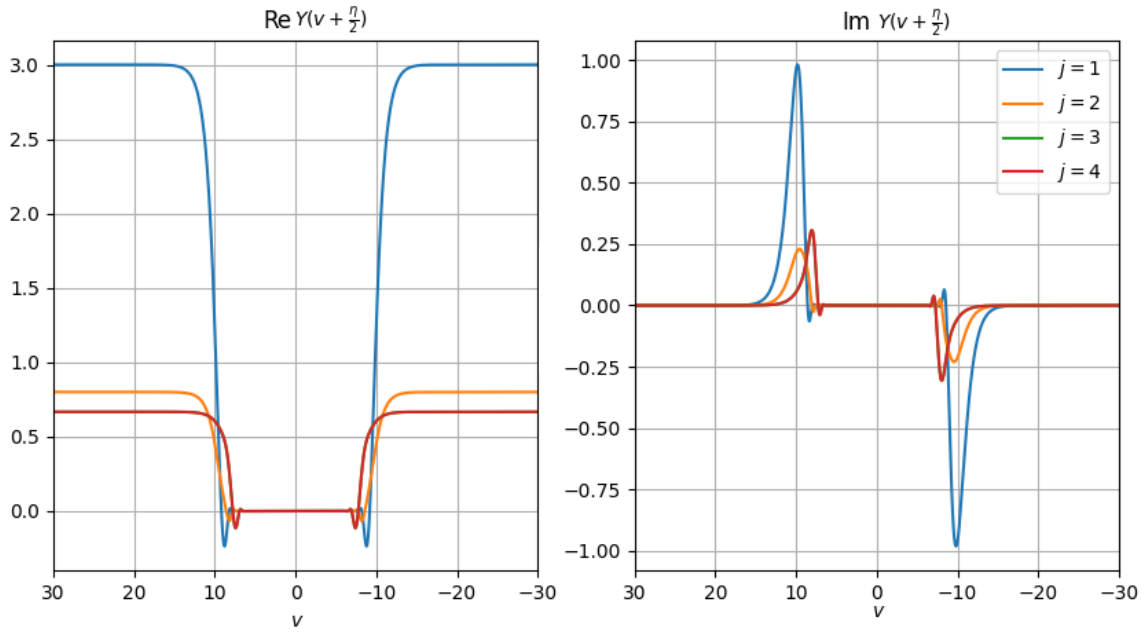



Figure 4.12: Plot of the $Y$-functions for $\nu_1 = 5$, $\nu_2 = 2$ at $\beta = 1$ and $L = 10^5$.

the TBA equations, resulting in the following equations:

$$\begin{aligned}
\log \eta_1(v) &= -\beta A s_1(v) + s_3 * \log(1+\eta_2)[v] + s_1 * \Big( \log(1+\eta_3[v]) + \log(1+\eta_4[v]) \Big), \\
\log \eta_2(v) &= s_3 * \log(1+\eta_1)[v] - 2 s_1 * \log(1+\eta_2)[v] \\
&\quad - s_3 * \Big( \log(1+\eta_3[v]) + \log(1+\eta_4[v]) \Big), \\
\log \eta_3(v) &= s_1 * \log(1+\eta_1)[v] - s_3 * \log(1+\eta_2)[v] \\
&\quad - s_1 * \Big( \log(1+\eta_3[v]) + \log(1+\eta_4[v]) \Big), \\
\log \eta_4(v) &= s_1 * \log(1+\eta_1)[v] - s_3 * \log(1+\eta_2)[v] \\
&\quad - s_1 * \Big( \log(1+\eta_3[v]) + \log(1+\eta_4[v]) \Big).
\end{aligned} \tag{4.100}$$

The numerical solution is represented in Figure 4.11.

The $v$-derivative of the driving term of the $Y$-functions can then be recast in the form:

$$\begin{aligned}
\partial_v h_1(v+i) &= -2\pi i L \Big( s_1(v) + s_3 * \rho_2^h[v] + s_1 * \rho_3^h[v] + s_1 * \rho_4^h[v] \Big), \\
\partial_v h_2(v+i) &= -2\pi i L \Big( s_3 * \rho_1^h[v] - 2 s_1 * \rho_2^h[v] - s_3 * \rho_3^h[v] - s_3 * \rho_4^h[v] \Big), \\
\partial_v h_3(v+i) &= -2\pi i L \Big( s_1 * \rho_1^h[v] - s_3 * \rho_2^h[v] - s_1 * \rho_3^h[v] - s_1 * \rho_4^h[v] \Big), \\
\partial_v h_4(v+i) &= -2\pi i L \Big( s_1 * \rho_1^h[v] - s_3 * \rho_2^h[v] - s_1 * \rho_3^h[v] - s_1 * \rho_4^h[v] \Big).
\end{aligned} \tag{4.101}$$

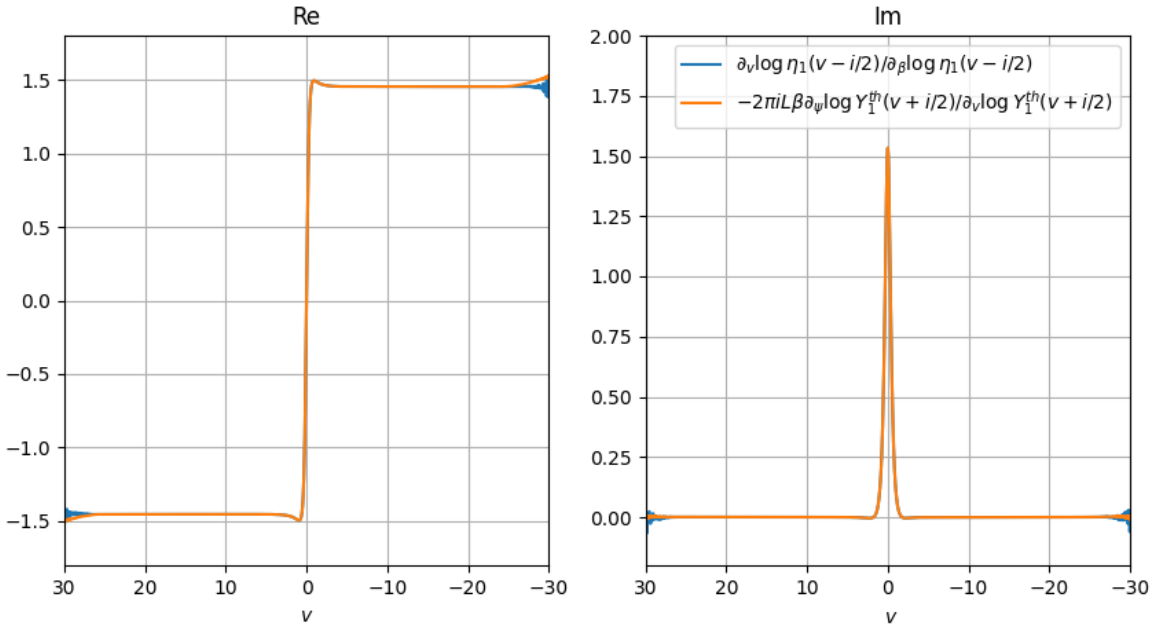



Figure 4.13: Plot of the functions of the right hand side and of the left hand side of (4.61) for index $j = 1$. An almost perfect overlap is observed.

We are now finally able to solve the NLIEs for the $Y$-functions. The results are shown in Figures 4.12.

As for the simple root of unity, we compute the derivatives of the $Y$-functions to determine the Drude weight and verify the ratio in (4.61). Our findings confirm that the ratio holds: the derivatives of the $Y$-functions align perfectly with the corresponding ratios of the derivatives of the $\eta$-functions. The numerical results illustrating this agreement are presented in Figure 4.13.

The proof of Zotos' formula based on the $T$-$Y$-system for thermodynamic states as treated in Sections 4.5 and 4.8 for anisotropies corresponding to simple and next-simple roots of unity should hold for all roots of unity. Taking the validity of Zotos' formula for arbitrary temperature and root of unity as granted, A. Urichuk et al. [41] presented already numerical results for the low-temperature spin Drude weight of the Heisenberg spin-1/2 quantum chain.

# Chapter 5

# Conclusions

## 5.1 Conclusion

In this thesis, we have investigated the transport properties of the spin-1/2 XXZ Heisenberg model, with a particular focus on the spin Drude weight. Using analytical techniques such as the thermodynamic Bethe Ansatz (TBA) and the functional relations of the Y-system, we derived and analyzed non-linear integral equations (NLIEs) to access the Drude weight. While most research in this direction has focused on the high-temperature regime, we have built a framework that allows us to compute the Drude weight at finite temperatures.

We began in Chapter 2 with an overview of fundamental transport phenomena in integrable systems. First, we presented linear response theory, and then we applied it to the specific case of spin transport in the spin-1/2 XXZ Heisenberg model. We discussed the Kubo formula, which relates transport coefficients to equilibrium correlation functions; the Mazur inequality, which provides a lower bound on the Drude weight; and Kohn's formula, which connects the Drude weight to the curvature of the ground-state energy. These tools form the basis for the subsequent work on computing the spin Drude weight.

In Chapter 3, we focused on the Mazur inequality and its application to the computation of the Drude weight. We examined the contribution of quasi-local conserved charges, which exhibit a non-trivial overlap with the spin current operator. These charges were shown to play a crucial role in sustaining ballistic transport in the XXZ model. Our results underscored the importance of identifying and characterizing such conserved quantities to gain a comprehensive understanding of the transport behavior in integrable systems. Our primary achievement in this chapter was the development of a framework that enables the computation of the lower bound of the Drude weight at finite temperatures. To achieve this, we introduced a mixed method based on the quantum transfer matrix, utilizing both non-linear integral equations (NLIEs) for "root of unity" cases and NLIEs for auxiliary functions. This approach allowed us to compute all contributions to

the spin Drude weight. While the inclusion of finite temperature increases the complexity of the NLIEs, they remain numerically tractable.

In Chapter 4, the derivation of the spin Drude weight is based on Kohn's formula, which relates the Drude weight to the thermal average of the energy level curvatures with respect to the flux. Unlike Chapter 3, where the column-to-column formalism was used, here we employed the row-to-row transfer matrix. We derived the NLIEs such that the excitations due to temperature and system size are encoded in a driving term. This driving term is then computed from the TBA-like equations. First, we focused on the case where the anisotropy parameter can be expressed as a "simple root of unity", and then we derived the NLIEs for the specific case of $\nu_1 = 2$ and $\nu_2 = 2$. The Takahashi-Suzuki numbers and related sequences were instrumental in constructing the functional relations for the $Y$- and $T$-systems. These relations allowed us to reformulate the problem in terms of non-linear integral equations, which were solved numerically to obtain the Drude weight at finite temperatures. We also compared our results with Zotos' findings, validating our approach and highlighting the robustness of the derived equations in capturing the transport properties of the XXZ model.

## 5.2 Future directions

While this work has addressed several key aspects of spin transport in the XXZ model, there remain many open questions and opportunities for future research. Below, we outline specific directions for each chapter:

### Chapter 3: Mazur inequality and quasi-local conserved charges

- Our framework allowes to compute the lower bound of the Drude weight at finite temperatures, but the numerical implementation is still very challenging. The structure of NLIEs depend on the anisotropy and numerically treatable cases are not many. Future work could focus on developing more efficient numerical techniques to solve the NLIEs for larger system sizes and higher temperatures. One possible way is to reformulate the problem in terms of NLIEs for auxiliary functions, which are not sensitive to the anisotropy parameter.

- In our calculations we used the quasi-local conserved charges which depend on a parameter $\varphi$. Our formulation is focused on the case where $\varphi$ maximizes the Mazur bound. However, in order to obtain stronger bound, the integration over $\varphi$ should be performed. This would require a more detailed analysis of the dependence of the Drude weight on the parameter $\varphi$.

- In our work we used quasi-local conserved charges identified by T. Prosen in [33]. However, there might be other conserved quasi-local charges which present a non

trivial overlap with the spin current operator. Future work could focus on identifying and characterizing these charges, and analyzing their contributions to the Drude weight.

## Chapter 4: Non-linear integral equations and numerical analysis

- We formulated NLIEs that are related to the continued fraction expansion of the anisotropy. Extending the NLIE framework to encompass more general values of the anisotropy parameter, and investigating the behavior of the Drude weight across different regimes, including both the massive and critical phases, would be a valuable direction for future research.

- In this work, we focused on the case where the twist angle at the boundary is $\phi = 0$. Future studies could explore the effects of varying the twist angle and its influence on the Drude weight. This would likely require more sophisticated numerical methods, as for $\phi = 0$ the Drude weight depends only on the function $Y_\nu^{\mathrm{th}}$, whereas for $\phi \neq 0$ it may depend on all $Y^{\mathrm{th}}$-functions.

- A more rigorous mathematical derivation of Zotos' formula from our results would be valuable. This could involve a deeper analysis of the underlying functional relations and their consequences for the transport properties of the system.

The nature of the discontinuous behavior of the Drude weight with respect to the anisotropy parameter is still not fully understood. Further research could focus on understanding the underlying mechanisms that lead to this behavior and its implications for the transport properties of the system. Additionally, it would be interesting to connect the presented results to experimental observations by comparing theoretical predictions with experimental data.

# Bibliography


[1] W. Heisenberg. "Zur Theorie des Ferromagnetismus". In: *Zeitschrift für Physik* 49 (1928), pp. 619–636. DOI: https://doi.org/10.1007/BF01328601.

[2] H. Bethe. "Zur Theorie der Metalle". In: *Zeitschrift für Physik* 71 (1931), pp. 205–226. DOI: https://doi.org/10.1007/BF01341708.

[3] C. N. Yang and C. P. Yang. "One-Dimensional Chain of Anisotropic Spin-Spin Interactions. I. Proof of Bethe's Hypothesis for Ground State in a Finite System". In: *Phys. Rev.* 150 (1 1966), pp. 321–327. DOI: 10.1103/PhysRev.150.321.

[4] C. N. Yang and C. P. Yang. "One-Dimensional Chain of Anisotropic Spin-Spin Interactions. II. Properties of the Ground-State Energy Per Lattice Site for an Infinite System". In: *Phys. Rev.* 150 (1 1966), pp. 327–339. DOI: 10.1103/PhysRev.150.327.

[5] C. N. Yang and C. P. Yang. "One-Dimensional Chain of Anisotropic Spin-Spin Interactions. III. Applications". In: *Phys. Rev.* 151 (1 1966), pp. 258–264. DOI: 10.1103/PhysRev.151.258.

[6] Ryogo Kubo. "Statistical-Mechanical Theory of Irreversible Processes. I. General Theory and Simple Applications to Magnetic and Conduction Problems". In: *Journal of the Physical Society of Japan* 12.6 (1957), pp. 570–586. DOI: 10.1143/JPSJ.12.570.

[7] J. Sirker. "Transport in one-dimensional integrable quantum systems". In: (2020). DOI: 10.21468/scipostphyslectnotes.17.

[8] A. Klümper and K. Sakai. "The thermal conductivity of the spin-$\frac{1}{2}$ XXZ chain at arbitrary temperature". In: *Journal of Physics A: Mathematical and General* 35.9 (2002), pp. 2173–2182. DOI: 10.1088/0305-4470/35/9/307.

[9] X. Zotos, F. Naef, and P. Prelovsek. "Transport and conservation laws". In: *Phys. Rev. B* 55 (17 May 1997), pp. 11029–11032. DOI: 10.1103/PhysRevB.55.11029. URL: https://link.aps.org/doi/10.1103/PhysRevB.55.11029.

[10] G. D. Mahan. "Many-particle physics". In: (2000).

[11] Frank Göhmann et al. “Spin conductivity of the XXZ chain in the antiferromagnetic massive regime”. In: *SciPost Physics* 12.5 (2022). DOI: 10.21468/scipostphys.12.5.158. URL: https://doi.org/10.21468%2Fscipostphys.12.5.158.

[12] Fabian H. L. Essler et al. *The One-Dimensional Hubbard Model*. Cambridge University Press, 2005. DOI: 10.1017/CBO9780511534843.

[13] Thierry Giamarchi and B. Sriram Shastry. “Persistent currents in a one-dimensional ring for a disordered Hubbard model”. In: *Phys. Rev. B* 51 (16 1995), pp. 10915–10922. DOI: 10.1103/PhysRevB.51.10915.

[14] H. Castella, X. Zotos, and P. Prelovš ek. “Integrability and Ideal Conductance at Finite Temperatures”. In: *Physical Review Letters* 74.6 (1995), pp. 972–975. DOI: 10.1103/physrevlett.74.972.

[15] Walter Kohn. “Theory of the Insulating State”. In: *Phys. Rev.* 133 (1A Jan. 1964), A171–A181. DOI: 10.1103/PhysRev.133.A171. URL: https://link.aps.org/doi/10.1103/PhysRev.133.A171.

[16] P. Mazur. “Non-ergodicity of phase functions in certain systems”. In: *Physica* 43.4 (1969), pp. 533–545. ISSN: 0031-8914. DOI: https://doi.org/10.1016/0031-8914(69)90185-2.

[17] M. Suzuki. “Ergodicity, constants of motion, and bounds for susceptibilities”. In: *Physica* 51.2 (1971), pp. 277–291. ISSN: 0031-8914. DOI: https://doi.org/10.1016/0031-8914(71)90226-6.

[18] A. Dhar, A. Kundu, and K. Saito. “Revisiting the Mazur bound and the Suzuki equality”. In: *Chaos, Solitons and Fractals* 144 (2021), p. 110618. ISSN: 0960-0779. DOI: https://doi.org/10.1016/j.chaos.2020.110618.

[19] X. Zotos, F. Naef, and P. Prelovsek. *Finite temperature transport in integrable quantum many body systems*. 1999. arXiv: cond-mat/9906441 [cond-mat].

[20] B. Bertini et al. “Finite-temperature transport in one-dimensional quantum lattice models”. In: *Rev. Mod. Phys.* 93 (2 May 2021), p. 025003. DOI: 10.1103/RevModPhys.93.025003.

[21] Michael Karbach and Gerhard Muller. *Introduction to the Bethe ansatz I*. 1998. arXiv: cond-mat/9809162 [cond-mat.stat-mech].

[22] Michael Karbach, Kun Hu, and Gerhard Müller. “Introduction to the Bethe Ansatz II”. In: *Computers in Physics* 12.6 (1998), pp. 565–573. DOI: 10.1063/1.168740.

[23] X. Zotos. “Finite Temperature Drude Weight of the One-Dimensional Spin- 1/2 Heisenberg Model”. In: *Phys. Rev. Lett.* 82 (8 1999), pp. 1764–1767. DOI: 10.1103/PhysRevLett.82.1764.

[24] M. Takahashi. “One-Dimensional Anisotropic Heisenberg Chain. II. Thermodynamics”. In: *Progress of Theoretical Physics* 46.2 (1971), pp. 401–413.

[25] Minoru Takahashi and Masuo Suzuki. "One-Dimensional Anisotropic Heisenberg Model at Finite Temperatures". In: *Progress of Theoretical Physics* 48.6 (Dec. 1972), pp. 2187–2209. DOI: 10.1143/PTP.48.2187. eprint: https://academic.oup.com/ptp/article-pdf/48/6/2187/5255323/48-6-2187.pdf. URL: https://doi.org/10.1143/PTP.48.2187.

[26] M. Gaudin. *La Fonction d'Onde de Bethe*. Paris: Masson, 1983.

[27] J. Benz et al. "On the Finite Temperature Drude Weight of the An- isotropic Heisenberg Chain". In: *Journal of the Physical Society of Japan* 74 (2005), pp. 181–190. DOI: 10.1143/jpsjs.74s.181.

[28] R. G. Pereira et al. "Exactly conserved quasilocal operators for the XXZ spin chain". In: *Journal of Statistical Mechanics: Theory and Experiment* 2014.9 (2014), P09037. DOI: 10.1088/1742-5468/2014/09/p09037.

[29] Masuo Suzuki. "Transfer-matrix method and Monte Carlo simulation in quantum spin systems". In: *Phys. Rev. B* 31 (5 Mar. 1985), pp. 2957–2965. DOI: 10.1103/PhysRevB.31.2957. URL: https://link.aps.org/doi/10.1103/PhysRevB.31.2957.

[30] Junji Suzuki, Yasuhiro Akutsu, and Miki Wadati. "A New Approach to Quantum Spin Chains at Finite Temperature". In: *Journal of the Physical Society of Japan* 59.8 (Aug. 1990), p. 2667. DOI: 10.1143/JPSJ.59.2667.

[31] A. Klümper. "Thermodynamics of the anisotropic spin-1/2 Heisenberg chain and related quantum chains." In: *Z. Physik B - Condensed Matter* 91 (1993), pp. 507–519. DOI: 10.1007/BF01316831.

[32] R.J. Baxter. *Exactly Solved Models in Statistical Mechanics*. Academic Press, 1982.

[33] T. Prosen. "Open $XXZ$ Spin Chain: Nonequilibrium Steady State and a Strict Bound on Ballistic Transport". In: *Phys. Rev. Lett.* 106 (21 2011), p. 217206. DOI: 10.1103/PhysRevLett.106.217206.

[34] A. Kuniba, K. Sakai, and J. Suzuki. "Continued fraction TBA and functional relations in XXZ model at root of unity". In: *Nuclear Physics B* 525.3 (1998), pp. 597–626. DOI: 10.1016/s0550-3213(98)00300-9.

[35] A. Klümper. "Free energy and correlation lengths of quantum chains related to restricted solid-on-solid lattice models". In: *Annalen der Physik* 504.7 (1992), pp. 540–553. DOI: https://doi.org/10.1002/andp.19925040707.

[36] Frank Göhmann, Nils P Hasenclever, and Alexander Seel. "The finite temperature density matrix and two-point correlations in the antiferromagnetic XXZ chain". In: *Journal of Statistical Mechanics: Theory and Experiment* 2005.10 (2005), P10015. DOI: 10.1088/1742-5468/2005/10/P10015.

[37] Frank Göhmann, Andreas Klümper, and Alexander Seel. "Integral representations for correlation functions of the XXZ chain at finite temperature". In: *Journal of Physics A: Mathematical and General* 37.31 (2004), p. 7625. DOI: 10.1088/0305-4470/37/31/001. URL: https://dx.doi.org/10.1088/0305-4470/37/31/001.

[38] A. Klümper and K. Sakai. *The spin Drude weight of the spin-1/2 XXZ chain: An analytic finite size study* . 2019. arXiv: 1904.11253 [cond-mat.stat-mech].

[39] Atsuo Kuniba, Tomoki Nakanishi, and Junji Suzuki. "T-systems andY-systems in integrable systems". In: *Journal of Physics A: Mathematical and Theoretical* 44.10 (Feb. 2011), p. 103001. ISSN: 1751-8121. DOI: 10.1088/1751-8113/44/10/103001. URL: http://dx.doi.org/10.1088/1751-8113/44/10/103001.

[40] A. Kuniba, T. Nakanishi, and J. Suzuki. "Functional Relations in Solvable Lattice Models I: Functional Relations and Representation Theory". In: *International Journal of Modern Physics A* 09.30 (Dec. 1994), pp. 5215–5266. ISSN: 1793-656X. DOI: 10.1142/s0217751x94002119. URL: http://dx.doi.org/10.1142/S0217751X94002119.

[41] Andrew Urichuk, Jesko Sirker, and Andreas Klümper. "Analytical results for the low-temperature Drude weight of the XXZ spin chain". In: *Phys. Rev. B* 103 (24 June 2021), p. 245108. DOI: 10.1103/PhysRevB.103.245108. URL: https://link.aps.org/doi/10.1103/PhysRevB.103.245108.